



---

All Theses and Dissertations

---

2009-02-13

# A New Model for Aqueous Electrolyte Solutions Near the Critical Point of Water Incorporating Aqueous Reaction Equilibria

Craig J. Peterson

*Brigham Young University - Provo*

Follow this and additional works at: <https://scholarsarchive.byu.edu/etd>



Part of the [Chemical Engineering Commons](#)

---

## BYU ScholarsArchive Citation

Peterson, Craig J., "A New Model for Aqueous Electrolyte Solutions Near the Critical Point of Water Incorporating Aqueous Reaction Equilibria" (2009). *All Theses and Dissertations*. 1779.

<https://scholarsarchive.byu.edu/etd/1779>

This Dissertation is brought to you for free and open access by BYU ScholarsArchive. It has been accepted for inclusion in All Theses and Dissertations by an authorized administrator of BYU ScholarsArchive. For more information, please contact [scholarsarchive@byu.edu](mailto:scholarsarchive@byu.edu), [ellen\\_amatangelo@byu.edu](mailto:ellen_amatangelo@byu.edu).

A NEW MODEL FOR AQUEOUS ELECTROLYTE SOLUTIONS NEAR  
THE CRITICAL POINT OF WATER INCORPORATING  
AQUEOUS REACTION EQUILIBRIA

by  
Craig J. Peterson

A dissertation submitted to the faculty of  
Brigham Young University  
in partial fulfillment of the requirements for the degree of  
Doctor of Philosophy

Department of Chemical Engineering  
Brigham Young University

April 2009



BRIGHAM YOUNG UNIVERSITY

GRADUATE COMMITTEE APPROVAL

of a dissertation submitted by

Craig J. Peterson

This dissertation has been read by each member of the following graduate committee and by majority vote has been found to be satisfactory.

\_\_\_\_\_  
Date

\_\_\_\_\_  
John L. Oscarson, Chair

\_\_\_\_\_  
Date

\_\_\_\_\_  
Richard L. Rowley

\_\_\_\_\_  
Date

\_\_\_\_\_  
W. Vincent Wilding

\_\_\_\_\_  
Date

\_\_\_\_\_  
William G. Pitt

\_\_\_\_\_  
Date

\_\_\_\_\_  
Randy S. Lewis



BRIGHAM YOUNG UNIVERSITY

As chair of the candidate's graduate committee, I have read the dissertation of Craig J. Peterson in its final form and have found that (1) its format, citations, and bibliographical style are consistent and acceptable and fulfill university and department style requirements; (2) its illustrative materials including figures, tables, and charts are in place; and (3) the final manuscript is satisfactory to the graduate committee and is ready for submission to the university library.

---

Date

---

John L. Oscarson  
Chair, Graduate Committee

Accepted for the Department

---

Larry L. Baxter  
Graduate Coordinator

Accepted for the College

---

Alan R. Parkinson  
Dean, Ira A. Fulton College of Engineering  
and Technology



## ABSTRACT

# A NEW MODEL FOR AQUEOUS ELECTROLYTE SOLUTIONS NEAR THE CRITICAL POINT OF WATER INCORPORATING AQUEOUS REACTION EQUILIBRIA

Craig J. Peterson

Department of Chemical Engineering

Doctor of Philosophy

Aqueous electrolyte solutions at temperature and pressure conditions near the critical point of water are difficult to describe using traditional equations of state based upon the excess Gibbs energy. Models based upon the residual Helmholtz energy have proven more effective. Anderko and Pitzer<sup>1</sup> developed a residual Helmholtz energy model (AP) for aqueous electrolyte solutions in which the electrolyte is assumed to be fully associated. The model has been effectively used in describing densities and vapor-liquid equilibria for simple electrolyte systems. The model is less effective for describing enthalpic properties such as heats of dilution.

Oscarson and coworkers<sup>2,3</sup> modified the AP model for NaCl solutions by adding a term accounting for the change in Helmholtz energy as a result of aqueous dissociation



reactions. This new model, called the RI model, is more accurate than the AP model at conditions where the NaCl dissociates more fully into ions.

Liu et. al<sup>4,5</sup> modified the RI model by adding a term to describe interactions between ions in solution and by regressing new model parameter values. This new model, called the RIII model, is more accurate than both the AP model and the RI model and may be used to predict species concentrations in solution as a result of aqueous phase reactions. The RIII model has substantial thermodynamic inconsistencies, however, and is poorly suited for describing mixed solute solutions.

This dissertation presents the RIV model which is an electrolyte solution model for solutions in the ranges of 350 °C to 400 °C and 18 MPa to 40 MPa. The RIV model has been applied to aqueous NaCl solutions and aqueous LiCl solutions. The RIV model is a modification of the AP model and includes aqueous phase reactions implicitly through fundamental species interactions. The RIV model is thermodynamically consistent. It is capable of describing densities and heats of dilution. Density predictions from the RIV model are less accurate than the AP model predictions (6.66 % error vs. 3.51 % error) but are reasonable. The heats of dilution predictions from the RIV model are much more accurate than those from the AP model (25.16 % error vs. 78.78 % error). Predictions of the ionic species concentration from the RIV model are likely to be poor as indicated by the poor agreement between experimental values and calculated values of equilibrium constants valid at infinite dilution.

In order to provide the necessary data from which to regress the parameters of the RIV model, experimental heat of dilution values were determined using flow calorimetry techniques. These values are also reported in this dissertation.



## ACKNOWLEDGEMENTS

First, I thank my wife, children, and parents for their continual support.

I wish to thank my advisor Dr. John L. Oscarson for his support and mentoring. I also wish to thank Dr. Reed M. Izatt for his constant encouragement and advice. I express gratitude for the advice of Dr. Richard L. Rowley and Dr. Douglas J. Henderson.

Dr. Jaime Cardenas Garcia was invaluable for his assistance while I was performing the experimental portion of my research.

I would like to acknowledge the financial support of the Army Research Office throughout my studies.



# TABLE OF CONTENTS

TABLE OF CONTENTS.....	vii
Glossary of Terms.....	xi
LIST OF TABLES.....	xv
LIST OF FIGURES.....	xvii
1 Introduction.....	1
2 Literature Review.....	7
2.1 The Global Critical Region.....	7
2.2 Approaches for Modeling Fundamental Interactions.....	9
2.2.1 Perturbation Methods.....	10
2.2.2 Integral Equation Methods.....	11
2.2.3 Comparison Between Perturbation and MSA Approaches and Primitive and Non-Primitive Approaches.....	13
2.3 Previous Models.....	15
2.3.1 Gibbs Excess Models.....	15
2.3.2 The Helmholtz Energy Models.....	16
2.3.2.1 Anderko-Pitzer Model.....	17
2.3.2.2 The RI Model.....	19
2.3.2.3 The RIII Model.....	20
2.4 Literature Data.....	23
2.4.1 VLE and Volumetric Data.....	23

2.4.1.1	NaCl-H <sub>2</sub> O.....	23
2.4.1.2	LiCl-H <sub>2</sub> O.....	24
2.4.2	Enthalpy Data.....	24
2.4.2.1	NaCl-H <sub>2</sub> O.....	24
2.4.2.2	LiCl – H <sub>2</sub> O.....	24
2.4.3	Equilibrium Constants.....	24
2.4.3.1	NaCl-H <sub>2</sub> O.....	24
2.4.3.2	LiCl-H <sub>2</sub> O.....	25
2.5	Isothermal Flow Calorimetry.....	25
3	Objectives and Approach.....	27
4	Development of the Model.....	29
4.1	Development of the Model Concept.....	29
4.2	The Hard-sphere Repulsion Term.....	32
4.3	The Non-primitive Mean Spherical Approximation.....	33
4.4	The AP Perturbation Term.....	38
4.5	Water Ligand Term.....	40
4.6	Determination of Ionic Speciation.....	41
4.7	Calculation of Volumes.....	42
4.8	Calculation of $\Delta_{dil}H$ Values.....	43
4.9	Calculation of Heat Capacities.....	46
4.10	log K <sub>o</sub> Calculation.....	47
5	Application of the RIV Model.....	49
5.1	The Application of the RIV Model to Water.....	50

5.2	Application of the RIV Model to Aqueous NaCl and LiCl Solutions .....	53
5.2.1	The Hard-Sphere Diameters .....	54
5.2.2	The Perturbation Term Parameters .....	56
5.2.3	Water Ligand Term Parameters .....	58
5.3	The Ideal Gas Term .....	58
6	Model Results and Discussion .....	63
6.1	The Water Model .....	63
6.2	The NaCl Solution and LiCl Solution Models.....	65
6.2.1	Results for Molar Volume .....	65
6.2.2	Results for $\Delta_{dil}H$ .....	77
6.2.3	Fraction of the Solute Dissociated .....	82
6.2.4	$\log K$ Predictions Valid at Infinite Dilution .....	85
7	Experimental Work .....	87
7.1	Recent Improvements Made to the Calorimeter .....	87
7.2	Methodology .....	88
7.3	Experimental Conditions .....	90
7.4	Comparison to Literature Data .....	92
8	Conclusions and Recommendations .....	95
8.1	Development of the RIV Model .....	95
8.2	Results Using the RIV Model .....	97
8.3	Contributions this Work Makes to the Body of Knowledge .....	98
8.4	Recommendations .....	100
9	References .....	103

Appendix A Measured Molar Volumes and Those Predicted Using the RIV Model for NaCl Solutions .....	115
Appendix B Measured Molar Volumes and Those Predicted Using the RIV Model for LiCl Solutions .....	123
Appendix C Measured $\Delta_{dil}H$ values and Those Predicted Using the RIV Model for NaCl Solutions .....	129
Appendix D Measured $\Delta_{dil}H$ values and Those Predicted Using the RIV Model for LiCl Solutions .....	135
Appendix E Measured $\Delta_{dil}H$ values for Sodium Acetate Solutions.....	137
Appendix F RIV Model Fortran Code .....	141

## Glossary of Terms

$A$	molar Helmholtz energy
$A$	parameter in NPMSA equation
$A_{dip}$	molar Helmholtz energy of the dipole contribution
$A_{diss}$	molar Helmholtz energy of the dissociation term
$A_{HS}$	molar Helmholtz energy of the hard-sphere contribution
$A_{IG}$	molar Helmholtz energy of the ideal gas
$A_{IGmix}$	molar Helmholtz energy of ideal gas mixture
$A_{lig}$	molar Helmholtz energy of the water ligand contribution
$A_{lig^*}$	parameter in water ligand term
$A_{MSA}$	molar Helmholtz energy of the primitive MSA contribution
$A_{NPMSA}$	molar Helmholtz energy of NPMSA contribution
AP	Anderko and Pitzer model <sup>1</sup>
$A_{per}$	molar Helmholtz energy of the perturbation contribution
$A_{ref}$	molar Helmholtz energy of the reference system
$A_{rep}$	molar Helmholtz energy of the hard-sphere contribution in the AP model
$A_o$	ideal gas standard state molar Helmholtz energy
$a$	total Helmholtz energy
$a$	parameter in the perturbation term
$ac, ad, ae$	parameters in the perturbation term
$acb, adb, aeb$	parameters in the perturbation term
$a_{cp}$	DIPPR ideal gas correlation constant
$a_{H_2O}, a_{H_2O1}, a_{H_2O2}, a_{H_2O3}, a_{H_2O4}$	pure water parameters in perturbation term
$a_{ij}, (ac)_{ijk}, (ad)_{ijkl}, (ae)_{ijklm}$	parameters in perturbation term
$a_1, a_2$	parameters in NPMSA equations
$a_{1-7}$	pure solute perturbation term parameters
$b$	van der Waals co-volume
$b_{cp}$	DIPPR ideal gas correlation constant
$b_{ij}, b_{ijk}, b_{ijkl}, b_{ijklm}$	parameters in perturbation term

$b_0, b_1, b_2$	NPMSA parameters relating to ion-ion, ion-dipole, and dipole-dipole interactions, respectively
$C_p$	constant pressure heat capacity
$C_p^{IG}$	ideal gas constant pressure heat capacity
$C_v$	constant volume heat capacity
$c$	parameter in the perturbation term
$c_{cp}$	DIPPR ideal gas correlation constant
$c_{H_2O}, c_{H_2O1}, c_{H_2O2}, c_{H_2O3}, c_{H_2O4}$	pure water parameters in perturbation term
$D$	parameter in hard-sphere term
DFT	Density Functional Theory
$D_f$	parameter in NPMSA equation
$d$	parameter in the perturbation term
$d_{cp}$	DIPPR ideal gas correlation constant
$d_{H_2O}, d_{H_2O1}, d_{H_2O2}, d_{H_2O3}, d_{H_2O4}$	pure water parameters in perturbation term
$d_0, d_2$	parameters in NPMSA equations
$E$	parameter in hard-sphere term
Error	total model error (as compared to experiment) and regression objective function for minimization
$Error_V, Error_{\Delta_{dil}H}$	contributions to regression objective function from volume predictions and heat of dilution predictions, respectively
$e_{cp}$	DIPPR ideal gas correlation constant
$F$	parameter in hard-sphere term
$F_{diss}$	Fraction of solute dissociated into ions in solution
$G$	molar Gibbs energy
$G_{ex}$	molar excess Gibbs energy
$G^*$	molar standard state Gibbs energy (hypothetical, infinitely dilute, 1 m solution)
$g$	total Gibbs energy
$H$	molar enthalpy
$H_i, H_f, H_{H_2O}$	molar enthalpies in heat of dilution calculation
$I$	Ionic Strength
IAPWS	Referring to the IAPWS water model <sup>6</sup>
$h$	total enthalpy
$J'$	quantity in NPMSA equations
$K$	reaction equilibrium constant
$K_m$	molal reaction equilibrium constant
$K_{m_o}$	infinite dilution molal equilibrium constant
$K_o$	infinite dilution reaction equilibrium constant
$k$	Boltzmann's constant ( $1.38066 \times 10^{-23}$ J/K)
MSA	mean spherical approximation

$m$	molality
$N_A$	Avogadro's number ( $6.02214 \times 10^{23} \text{ mol}^{-1}$ )
$N_V, N_{\Delta_{dil}H}$	number of volume data and number of heat of dilution data in regression, respectively
NPMSA	non-primitive mean spherical approximation
$n$	number of moles of water in heat of dilution calculation
$P$	pressure
$P_c$	critical pressure
$P_{NPMSA}$	pressure of NPMSA contribution
$Q$	dissociation species ratio
$q, q_{var}$	parameters in perturbation term
$q_e$	charge of electron ( $1.602177 \times 10^{-19} \text{ C}$ )
$R$	ideal gas constant ( $8.314471 \text{ (J/mol-K)}$ )
RI	referring to the RI model <sup>2,3</sup>
RIII	referring to the RIII model <sup>4,5</sup>
RIV	referring to the RIV model (present work)
$S$	molar entropy
SAFT	Statistical Associating Fluid Theory <sup>7</sup>
$S_o$	molar ideal gas standard state entropy
$s$	total entropy
$T$	temperature
$T_c$	critical temperature
$T_r$	reduced temperature
$T_{ref}$	reference temperature in hard-sphere diameter calculation
$T_o$	ideal gas standard state temperature
$U$	molar internal energy
$U_{IGmix}$	molar internal energy of ideal gas mixture
$U_{NPMSA}$	molar internal energy of NPMSA contribution
$U_o$	molar ideal gas standard state internal energy
$u$	total internal energy
$V$	molar volume
$V_{dat_i}, V_{RIV_i}$	molar volumes from literature and RIV predictions, respectively
$V_o$	molar ideal gas standard state volume
$v$	total volume
$x$	mole fraction
$x_c$	critical composition (mole fraction)
$x_{NaCl_i}^o, x_{NaCl_f}^o$	initial and final mole fractions of NaCl in heat of dilution calculation, respectively
$y_l$	parameter in NPMSA equation
$Z$	compressibility
$Z_{HS}$	compressibility of the hard-sphere contribution

$Z_{NPMSA}$	compressibility of NPMSA contribution
$Z_{per}$	compressibility of the perturbation term
$Z_{rep}$	compressibility of the hard-sphere contribution
$z$	species charge

## Greek Letters

$\alpha_{ij}, \alpha_{12}, \alpha_{1-7}$	parameters in perturbation term
$\beta_3, \beta_6, \beta_{12}, \beta_{24},$	parameters in NPMSA equations
$\delta_{1112}, \delta_{1122}, \delta_{1222}, \delta_{1-6}, \delta_{ijkl}$	parameters in perturbation term
$\Delta_{dil}H$	heat of dilution
$\Delta_{dil}H_{dat_i}, \Delta_{dil}H_{RIV_i}$	heats of dilution from literature and RIV predictions, respectively
$\Delta$	parameter in NPMSA equations
$\epsilon, \epsilon_{ijklm}$	parameters in perturbation term
$\epsilon_{NaCl}$	extent of reaction of NaCl dissociation reaction
$\epsilon_0$	permittivity of vacuum [8.85419e10 <sup>-12</sup> C <sup>2</sup> /(N-m <sup>2</sup> )]
$\epsilon_1, \epsilon_2$	extents of reaction in heat of dilution calculations as defined in Figure 3
$\gamma_{112}, \gamma_{122}, \gamma_{1-11}, \gamma_{ijk}$	parameters in perturbation term
$\eta$	reduced density
$\Lambda$	parameter in NPMSA equation
$\mu$	dipole moment
$\pi$	mathematical constant
$\theta$	perturbation term parameter ( $T/100$ K)
$\rho$	density
$\rho_c$	critical density
$\sigma$	hard-sphere diameter
$\sigma$	NPMSA diameter
$\tau, \tau_{1-9}$	parameters in perturbation term

## Miscellaneous

$\infty$	infinity
----------	----------

## LIST OF TABLES

Table 1: Range of acceptable values <sup>70</sup> for the solution of equations (16)-(18). .....	36
Table 2: Sources for literature data used in the regression of parameters in the RIV model for the NaCl and LiCl solutions. ....	50
Table 3: Regressed parameters for water in the perturbation term. ....	52
Table 4: Hard-sphere diameters in the water NPMSA and hard-sphere terms. ....	53
Table 5: Dipole moments of NaCl and LiCl in the RIV model, AP Model, and from the literature. <sup>129</sup> The AP model has never been applied to LiCl solutions. ....	54
Table 6: Hard-sphere diameter function terms for the NaCl solution model. ....	55
Table 7: Hard-sphere diameter function terms for the LiCl solution model. ....	55
Table 8: Pure NaCl parameter values. ....	56
Table 9: Pure LiCl parameter values. ....	56
Table 10: Mixing parameter values for NaCl and LiCl solutions. ....	57
Table 11: The values for $A_{lig}^*$ for the aqueous NaCl and LiCl solutions. ....	58
Table 12: Ideal Gas Standard State values (273.15 K, 1 m <sup>3</sup> /mol) from DFT calculations. ....	59
Table 13: Parameters for ideal gas $C_p$ model for LiCl. ....	60
Table 14: Summary of $\Delta_{dil}H$ experiments conducted for NaCl solutions. ....	91
Table 15: Summary of $\Delta_{dil}H$ experiments conducted for sodium acetate solutions. ....	92
Table 16: The average percent difference between calculated values and literature values of molar volume and $\Delta_{dil}H$ from the AP model, the RIII model, and the RIV model. ....	98
Table 17: A comparison of the characteristics between the RI, RIII, AP, and RIV Models. ....	99



## LIST OF FIGURES

Figure 1: The $a$ of a system versus the extent of the dissociation reaction. The minimum in $a$ coincides with the reaction equilibrium. The constants $\kappa$ and $\zeta$ are equal to 1273956.39196637 and -0.0853234, respectively, and are added to the plotted values to make the plot easier to read. ....	42
Figure 2: Algorithm used to determine molar volume from temperature, pressure, and composition.....	43
Figure 3: The $\Delta_{dil}H$ process.....	45
Figure 4: Plot of $\log Q$ values predicted using the RIV model versus the square root of ionic strength. A quadratic function was fitted to the predictions and extrapolated to zero ionic strength to determine a $\log K_{mo}$ value of about -11.4. As the solution becomes more dilute, numerical instability makes it difficult to calculate concentrations precisely.....	48
Figure 5: Pure water $C_V$ predictions from both the AP model and the IAPWS model versus pressure.....	51
Figure 6: Plot of LiCl $C_p^{IG}$ versus temperature as predicted from DFT calculations and the DIPPR correlation (Equation 90).....	61
Figure 7: Plot of vapor pressure versus temperature. Vapor pressure predictions from the AP and RIV models are compared with IAPWS model <sup>6</sup> predictions. The AP model predictions are closer to IAPWS model values, but RIV model predictions are reasonable. ....	64
Figure 8: Plot of calculated molar volumes versus literature values of molar volume. Calculated values of molar volume of NaCl solutions from the RIV model and the AP model are compared to literature values. ....	66
Figure 9: Plot of calculated molar volumes from the RIV model versus literature values of molar volume. Calculated values of the molar volume of LiCl solutions from the RIV model are compared to literature values. ....	67
Figure 10: Plot of molar volume versus literature values of molar volume. Predictions from the RIV model for NaCl solution molar volume are compared to literature	

values that were not used to regress model parameters. Agreement between model predictions and literature values are similar to those in Figure 8. ....	67
Figure 11: Plot of molar volumes versus literature values of molar volume. Predictions from the RIV model for LiCl solution molar volume are compared to literature values that were not used to regress model parameters. Agreement between model predictions and literature values are similar to those in Figure 9. ....	68
Figure 12: Plot of molar volumes versus mole fraction of NaCl as predicted using the AP model and the RIV model compared with literature molar volumes at 350 °C and pressure between 13.5 and 16.8 MPa.....	69
Figure 13: Plot of molar volumes versus mole fraction of LiCl. Results from the RIV model are compared to literature values for the LiCl solution at 400 °C and 28 MPa. ..	70
Figure 14: Plot of the percent difference between experimental values and model values of molar volume versus mole fraction of NaCl. The percent differences for both the AP model and the RIV model are shown.....	71
Figure 15: Plot of molar volumes for the NaCl solution at 400 °C and $7.16 \times 10^{-2}$ mole fraction of NaCl versus pressure. Predictions from the RIV model and AP model are compared to literature values. ....	72
Figure 16: Plot of molar volumes versus pressure for the LiCl solutions at 604 K and $8.66 \times 10^{-5}$ mole fraction LiCl. Literature values are compared with RIV predictions. ....	73
Figure 17: Plot of the percent difference between model predictions and literature values of molar volume for NaCl solutions as a function of pressure. The percent differences for both the RIV and the AP models are shown.....	74
Figure 18: Plot of molar volumes versus temperature at 28 MPa and $4.51 \times 10^{-5}$ mole fraction NaCl. The RIV model predictions and the AP model predictions are compared to literature values. ....	75
Figure 19: Plot of molar volumes of LiCl solutions at 28 MPa and $4.44 \times 10^{-4}$ mole fraction LiCl as a function of temperature. The RIV model predictions are compared to literature values.....	75
Figure 20: Plot of the percent difference between model predictions and literature values of molar volume versus temperature. The percent differences for both the RIV and the AP models are shown.....	76
Figure 21: Plot of $\Delta_{dil}H$ values versus literature values of $\Delta_{dil}H$ . Predictions from the AP model and the RIV model for the NaCl solution are compared to literature values.....	77

Figure 22: Plot of $\Delta_{dil}H$ values versus literature values of $\Delta_{dil}H$ for NaCl solutions. RIV model predictions are compared to literature values that were not used to regress model parameters. Generally, the agreement between literature values and model predictions are similar to those in Figure 21.....	78
Figure 23: Plot of $\Delta_{dil}H$ values for LiCl solutions at 350 °C and 17.6 MPa as a function of final solute concentration. The initial mole fraction of LiCl is $4.48 \times 10^{-3}$ . RIV predictions are compared with literature values. ....	79
Figure 24: Plot of $\Delta_{dil}H$ values for LiCl solutions at 350 °C and 17.6 MPa as a function of final solute concentration. The initial mole fraction of LiCl is $8.93 \times 10^{-3}$ . RIV predictions are compared with literature values. ....	80
Figure 25: Plot of the percent difference between predictions from the RIV model and literature values of $\Delta_{dil}H$ as a function of temperature for NaCl solutions. ....	80
Figure 26: Plot of the percent difference between predictions from the RIV model and literature values of $\Delta_{dil}H$ as a function of pressure.....	81
Figure 27: Plot of the percent difference between predictions from the RIV model and literature values of $\Delta_{dil}H$ as a function of the mole fraction of NaCl.....	81
Figure 28: Plot of the fraction dissociated of NaCl versus $x_{NaCl}$ as predicted using the RIV model at 350 °C and 40 MPa. ....	82
Figure 29: Plot of the fraction dissociated of NaCl versus the $x_{NaCl}$ as predicted using the RIV model at 350 °C and different pressures. ....	83
Figure 30: Plot of the fraction dissociated of NaCl versus the mole fraction of NaCl as predicted using the RIV model at 40 MPa and varying temperatures. ....	84
Figure 31: Plot of $\log K_{mo}$ values versus temperature at 28 MPa. $\log K_{mo}$ values are taken from the literature and compared to those calculated using the RIV model. ....	84
Figure 32: Plot of heater output from the calorimeter versus time. This shows a series of baselines and reaction lines obtained from the calorimeter in our laboratory for two reaction conditions. The lines near 1350 on the y-axis are base lines and are obtained when there is no reaction occurring. The lines near 750 and near 1000 are reaction lines and are obtained when a reaction is occurring. The differences between the reaction lines and baselines, combined with a calibration constant, yield enthalpy changes for the reaction. ....	89
Figure 33: Plot of $\Delta_{dil}H$ values versus final NaCl molality. This compares results from three previous studies reported in the literature to those from this study. The conditions are at 350 °C and 17.5 MPa for this study and 17.6 MPa for the three literature studies. ....	92



# 1 Introduction

In recent years, aqueous electrolyte solutions near the critical point of water (373.946 °C, 22.0640 MPa) have attracted a great deal of attention. These systems are encountered in a variety of geothermal environments as well as industrial applications such as wastewater treatment, extraction, desalinization, and distillation.

One industrial application, Supercritical Water Oxidation (SCWO), is a promising technology that may be used to dispose of sewages,<sup>8</sup> sludges,<sup>9, 10</sup> polychlorinated biphenyls,<sup>11</sup> hazardous chemicals,<sup>12-17</sup> and aqueous organics.<sup>8, 9, 18, 19</sup> The properties of supercritical water are ideal for dissolution of organic compounds and oxygen, and these properties allow extremely effective mixing during an oxidation reaction.<sup>20</sup> The effective mixing and high densities are favorable to rapid kinetics as well as destruction efficiencies that are frequently greater than 99.99% for small residence times.<sup>20</sup> Additionally, operating temperatures are significantly lower for SCWO (400 to 650 °C) than are those for traditional incineration (1000 to 2000 °C). Also, the high densities of the fluids allow more efficient use of space. A major advantage of SCWO over traditional incineration is the lack of nitrogen oxides in the product under typical operating conditions.<sup>13, 20</sup>

In the SCWO process, or any other process involving solutions near the critical point of water, a proper understanding of reactions involving inorganic salts and neutral species is vital. A proper understanding of those reactions helps to predict the exothermicity of the reactions. In addition, corrosion, which is closely tied to aqueous reactions, has been

recognized<sup>21-23</sup> as a major issue in the design of processes under these temperature and pressure conditions.

Conducting experiments to describe thermodynamic behavior near the critical point of water is costly and time consuming. It is also difficult to obtain accurate data at conditions in this region. A thermodynamic equation of state for aqueous, electrolyte solutions, therefore, is essential in order to effectively design processes involving aqueous solutions near the critical point of water. Use of a thermodynamic equation of state could provide volumetric properties, enthalpic changes, and reaction equilibria.

Many models have been proposed to describe the behavior of electrolyte solutions. For solutions at conditions far below the critical point of water, excess molar Gibbs energy,  $G_{ex}$ , models have proven to be successful. The Pitzer ion-interaction model<sup>24</sup> is a notable example. At conditions near the critical point of water, however, excess Gibbs energy models are ineffective<sup>25-27</sup> as a result of the critically divergent behavior of the infinite dilution standard state which differs markedly from the smooth behavior of the finite dilution solution.

There are several challenges in modeling electrolyte solutions near the critical point of water. One obstacle is the significant decrease in the dielectric constant of water as the critical point is approached which alters the interactions of electrolytes in solution. This change causes many electrolytes that are strong at lower temperatures to become weak. As a result, there are significant changes in species concentrations with changes in temperature and pressure which have a marked effect on solution properties.

There are three principal methods for modeling solutions that include aqueous reactions:

- 1) treating the electrolyte as fully dissociated,
- 2) treating the electrolyte as fully associated, and
- 3) including chemical reactions as part of the model.

Anderko and Pitzer<sup>1, 28</sup> employed the second method in modeling aqueous solutions of NaCl and KCl. They developed a model based on the molar residual Helmholtz energy,  $A_{res}$ , that can be used to accurately describe densities and phase equilibria. However, because the model assumes the electrolyte is associated into neutral species, it cannot be used to determine ionic species concentrations and does a poor job of predicting enthalpic properties such as heat of dilution,  $\Delta_{dil}H$ , values.

Clearly, a more realistic model using the third method that is capable of incorporating the effects of chemical reactions in solution is desirable because such a model would allow for prediction of species concentrations and therefore more accurate molar enthalpy values. In order to model the effects of chemical speciation on the thermodynamic properties of a solution, a means of describing the extent of the reaction and the species concentrations is necessary.

Using the Anderko and Pitzer (AP) model as a basis, Palmer and coworkers<sup>2, 3</sup> developed the RI model, based upon the third method, by adding chemical speciation. The NaCl dissociation constant model proposed by Gruszkiewicz and Wood<sup>29</sup> was modified and added to the AP model. The resulting RI model is more accurate for enthalpy change predictions than the AP model.

Liu and coworkers<sup>4, 5</sup> developed the RIII model by incorporating a term into the RI model to describe concentration effects of the ions in solution. The RIII model is more

accurate than either the AP model or the RI model for describing the densities and enthalpy changes of NaCl solutions and is also capable of predicting ionic speciation in solution.

The terms in the RIII model, however, are thermodynamically inconsistent with each other. For example, the speciation term in the model is only valid when the ions are at infinite dilution. The speciation term, however, is used to describe the reaction of NaCl molecules at finite dilution. Also, the ionic speciation term is valid at the dielectric constant of water at a given temperature and pressure but is used to describe speciation in solutions with finite concentrations of electrolytes and, therefore, with different dielectric constants. While predictions from the RIII model are close to the literature values from which the RIII model parameters were regressed, the theoretical inconsistencies make predictions at other conditions suspect.

An electrolyte solution model is presented here, the RIV model, which allows for aqueous reactions but avoids the difficulties of the RIII model. The RIV model can be used to predict  $\log K$  values for aqueous reactions in solutions at infinite dilution. It can also be used to predict ionic species concentrations in regions of finite concentration without the thermodynamic inconsistencies of the RIII model. No other such electrolyte solution model exists for solvents near their critical point.

A broad range of experimental heat of dilution values was vital for regressing the parameters in the RIV model. An important part of the development of the RIV model, therefore, was the determination of experimental heat of dilution values using flow calorimetry techniques. This experimental work is reported here as well.

In this dissertation, a literature review of applicable topics will first be presented followed by a description of the objectives of this study and the approach adopted. Next, the

application of the model to real systems will be discussed followed by a discussion of the results. Following this, the experimental portion of the research will be described. The dissertation will be concluded with a summary and recommendations for future efforts.



## 2 Literature Review

### 2.1 *The Global Critical Region*

The development of useful thermodynamic equations of state represents a great stride forward in thermodynamics theory. The van der Waals model was impressive when it was first published, in part, because the model could be used to predict a critical point. In time, however, experiments and developing theoretical understanding indicated that classical models, such as the van der Waals model and other engineering equations of state, can be used to qualitatively predict chemical behavior in the critical region, but they cannot be used to provide quantitatively accurate predictions.<sup>30,31</sup> These models are called, in general, mean field models because they replace the interactions of individual solvent molecules with an overall field effect. As a result, local effects, such as fluctuations in the density of the solution, are averaged out over the whole system. Short-ranged intermolecular interactions become the defining effects. Because the correlation lengths, and therefore the range of fluctuations, are large near the critical point, these models do not work well at conditions near the critical point.

In the range of conditions where fluctuations dominate, certain properties of the fluid are of greater predictive importance. For example, the difference between the density of the fluid and the critical density ( $\rho - \rho_c$ ), called the order parameter, is a measure of the criticality (or critical-like behavior) of a fluid.<sup>30</sup> Fluid mixtures have additional order parameters

defined by the difference between the compositions of the species and the critical compositions of the species,  $x-x_c$ . The order parameter goes to zero as the critical point is reached. Theory and experiment show that fluctuations of the order parameter dominate in the critical region.<sup>31</sup> Accordingly, changes with respect to the order parameter ( $\partial/\partial\rho$ ) are extremely important near the critical point.

The response function is another useful measure of criticality and is related to changes in the order parameter. The response function for fluids is  $(\partial\rho/\partial P)_{T,x}$ . Near the critical point, the response function diverges indicating an increasingly large change in density with a small change in pressure. Other properties also diverge at the critical point. The isobaric and isochoric heat capacities,  $C_p$  and  $C_v$ , respectively, as well as the compressibility,  $Z$ , are examples.

The correlation length, the response function, and  $Z$  all start to change significantly as  $T \rightarrow T_c$  and approach their asymptotic limits. Thus, there is a temperature /pressure region surrounding the critical point where the fluid behaves non-classically and must be treated differently than the fluid at conditions far away from the critical point. This region surrounding the critical point has been called the “global critical region”.<sup>32</sup>

Electrolyte solutions in the global critical region present further challenges. The coulombic interactions that are present in these solutions are both stronger and longer-ranged than the intermolecular interactions found in non-electrolyte solutions. Because the interactions are longer ranged, it may at first seem that the correlation length would not be longer than the range of the intermolecular interactions. It might be tempting, therefore, to assume a classical behavior for the electrolyte solution. It should be noted<sup>27</sup>, however, that at the critical point of a solution, the correlation length will still go to infinity. Coulombic

forces are inversely proportional to the square of the distance between point charges and therefore become significantly smaller as distance increases. In addition, because ions attract spheres of oppositely charged ions around themselves, they become “screened” and are therefore not as long-ranged as bare ions. The coulombic interactions become effectively short-ranged. Thus, the critical behavior of electrolyte solutions remains non-classical.

In the global critical region for aqueous solutions, there is a decrease in electrolyte dissociation for many salts, even for those salts that at room temperature are considered 100% dissociated. Experimental measurements<sup>29, 33, 34</sup> as well as molecular simulations<sup>35-37</sup> have demonstrated this. The reason for an increase in association is the decrease in the dielectric constant as the critical point is approached. Ionic charges have a stronger effect as a result, and this stronger coulombic effect leads to ions associating in the solution.

## ***2.2 Approaches for Modeling Fundamental Interactions***

The interactions between molecules and ions in an electrolyte solution are complex. They can be dealt with more easily if only pairwise interactions between molecules are considered. Pairwise interactions may then be further decoupled into several types of intermolecular interactions such as ion-ion, ion-dipole, dipole-dipole, and dispersion interactions. One may also consider other interactions (quadrupole, octapole, ion-induced dipole, etc.) though they may not be as significant. There are two main statistical mechanical methods for quantifying these interactions: perturbation methods and integral equation methods.

## 2.2.1 Perturbation Methods

Perturbation methods have been reviewed by Boublík<sup>38</sup> and Li.<sup>39</sup> The methods consist of defining some reference system, such as an ideal gas or hard-sphere mixture, and basing some property of a system, such as pressure or molar Helmholtz energy, upon that reference system using a mathematical expansion. Higher ordered terms are dropped from the expansion typically leaving an equation correct to first or second order. The perturbation approach is successful if these higher-order terms are of little or of monotonically decreasing significance. If the higher-order terms are not significant, then the expansion converges quickly, and the perturbation approach will be effective in representing the idealized system.

Simple polar fluids have been described using perturbation theory by Stell et al.<sup>40, 41</sup>, Rushbrooke et al.<sup>42</sup>, and Barker and Henderson.<sup>43</sup> These authors have developed a simple closed-form expression for the molar Helmholtz energy of a dipolar hard-sphere mixture. More complicated perturbation methods for dipolar mixtures include the perturbed anisotropic chain theory<sup>44, 45</sup>, statistical associating fluid theory<sup>7</sup> (SAFT), and statistical associating fluid theory–variable range (SAFT-variable range).<sup>46</sup> All of these theories have been successfully used in various applications.

Mixtures of ions and dipoles have been described with perturbation theory using both primitive and non-primitive approaches. The primitive approach is to treat the dipoles as a dielectric continuum rather than as individual molecules. This approach requires a dielectric constant as a function of composition. The ions are then treated discretely. Henderson<sup>47</sup> developed a primitive electrolyte perturbation method with equal diameter hard spheres as the reference system. Jin and Donohue<sup>48-50</sup> combined Henderson's perturbation term for ion-

ion interactions with perturbed anisotropic chain theory to create equations of state for electrolyte solutions.

Non-primitive approaches treat both the ions and the dipoles discretely in the solution. The dielectric constant between the species, therefore, is the vacuum dielectric constant. This is an advantage because the solution dielectric constant is often not known. Larsen et al.<sup>51</sup> developed a non-primitive approach to electrolyte systems that worked well for 1:1 electrolytes but poorly for 2:2 electrolytes. Henderson et al.<sup>52</sup> developed a non-primitive perturbation approach to electrolyte solutions. In this approach, equal diameter hard spheres are the reference system, ions are modeled as charged hard spheres, and the solvent molecules are modeled as dipolar hard spheres. The difficulty encountered in the Henderson et al. perturbation approach is that the ion-ion terms are divergent and are not very accurate when compared with Monte Carlo simulation results.<sup>53</sup> Chan<sup>54</sup> combined the Henderson et al. results<sup>52</sup> of the ion-ion term with a solvent primitive model and applied the theory to simple electrolyte solutions with poor results.

### **2.2.2 Integral Equation Methods**

The integral equation methods are all based upon the Ornstein-Zernike equation<sup>55</sup>. There are three main approaches to solving the Ornstein-Zernike equation: the Percus-Yevick, the Hypernetted Chain, and the Mean Spherical Approximation (MSA). While less accurate than the Percus-Yevick and Hypernetted Chain approach, the MSA is more practical for routine calculations because it provides a simple analytic solution.

An MSA solution for dipolar hard spheres was obtained by Wertheim.<sup>56</sup> For electrolyte solutions, just as with perturbation methods, the MSA has both primitive and non-

primitive solutions. The primitive MSA solution was derived by Waisman and Lebowitz<sup>57, 58</sup> and by Blum.<sup>59</sup> As with primitive perturbation models, it is a simpler approach but still requires knowledge of the solution dielectric constant as a function of temperature and composition. This approach yields an ion-ion interaction but does not provide dipole-dipole and ion-dipole interactions because they are treated as part of the mean field effect.

Non-primitive solutions to the MSA are significantly more complicated than the primitive solution because they determine ion-ion, ion-dipole, and dipole-dipole interactions. These interactions are linked, respectively, to three parameters:  $b_0$ ,  $b_1$ , and  $b_2$ . In order to obtain these parameters, a simultaneous system of nonlinear equations must be solved. With the exception of the most general case of the non-primitive MSA, three of these equations must be solved.

The non-primitive MSA has been solved for dipoles and ions of equal size by Blum et al.<sup>60</sup> and Adelman and Deutch.<sup>61</sup> Further refinements were made by Vericat and Blum<sup>62</sup> and by Perezhernandez and Blum.<sup>63</sup> These solutions are valid for one solvent and one electrolyte.

A non-primitive MSA solution was obtained by Blum<sup>64</sup> for a single solvent and an arbitrary mixture of ions with varying charges and diameters. Further refinements to this solution were later obtained.<sup>65-67</sup> A study with this non-primitive MSA solution in a region near the critical point of the solvent was conducted by Wei and Blum.<sup>68</sup>

Finally, a completely general non-primitive MSA solution was obtained by Protsykevich<sup>69</sup>. This solution allows for any number of dipoles with different dipole moments and different diameters as well as any number of ions with different charges and different diameters. While flexible, this solution is prohibitively complicated for engineering calculations since it requires the solution to eight simultaneous nonlinear equations.

Lvov and Wood<sup>70</sup> used the non-primitive MSA to develop an equation of state for aqueous NaCl solutions at temperatures from 273 to 973 K with good results. They developed expressions for the MSA diameters as a function of temperature and concentration. Liu et al.<sup>71, 72</sup> combined the non-primitive MSA with statistical associating fluid theory to correlate the mean ionic activity coefficients for a wide range of 1:1 electrolytes at low temperature with good results. Gao et al.<sup>73</sup> predicted high pressure solubilities of various gases in an aqueous electrolyte solution using the non-primitive MSA with good results. Lotfikian and Modarress<sup>74</sup> applied the non-primitive MSA to simple electrolytes while modifying the diameters in the MSA to be a function of concentration. They did not compare their results to experimental data.

### **2.2.3 Comparison Between Perturbation and MSA Approaches and Primitive and Non-Primitive Approaches**

According to Li,<sup>39</sup> non-primitive approaches are less accurate than primitive approaches, and perturbation approaches are more accurate than MSA approaches as indicated by the comparative accuracy of a series of equations of state based upon these models and compared to experiment. Li acknowledges that the non-primitive perturbation approaches have terms that do not converge.

Li et al.<sup>75</sup> indicate that the non-primitive MSA can be used effectively to describe ion-ion interactions, but the predictions for ion-dipole interactions are underestimated when compared to molecular simulations. Liu et al.<sup>76</sup> also compared the individual interactions within the perturbation and MSA approaches to those determined using Monte Carlo data and found that both the primitive and non-primitive MSA approaches give good agreement with Monte Carlo data while the perturbation theory approaches do not. Results from the

MSA approach were less accurate than those obtained using perturbation methods for the ion-dipole term. The MSA approach was found to underestimate ion-dipole molar internal energy,  $U$ , values while the perturbation technique was found to overestimate ion-dipole internal energies. Liu et al. found the MSA approach to be more accurate than the perturbation approach for dipole-dipole interactions.

Lotfikian and Modarress<sup>74</sup> applied the primitive MSA and the non-primitive MSA to simple aqueous electrolyte solutions. The authors concluded that the non-primitive MSA yields more correct predictions because it takes into account solvent effects due to dipole moments.

It appears that the non-primitive MSA approach is valid for describing electrolyte solutions while the non-primitive perturbation approach does not perform as well because of the difficulty in dealing with the long-range ion-ion term. The primary advantage of the non-primitive approach versus the primitive approach is that you do not need solution dielectric constants. Further, because solvent effects are explicitly accounted for in non-primitive MSA and perturbation approaches, the models seem to be more accurate when compared to molecular simulation data. The lone publication that disagrees with this analysis is the paper by Li<sup>39</sup> which compared a variety of different equations of state using the perturbation and MSA approaches. The other studies mentioned above that specifically compare the individual interactions with molecular simulation data and provide more insight into the strengths of the approaches.

## 2.3 Previous Models

### 2.3.1 Gibbs Excess Models

Aqueous, electrolyte solutions have been described in the past using several models. Most of these models describe the excess Gibbs energy of the solution as a function of temperature, pressure, and concentration, usually molality,  $m$ . The excess Gibbs energy term accounts for the difference between the standard state mixture (hypothetical, infinitely dilute, 1 molal solution) and the real solution as:

$$G(T,P,m) = G^*(T,P) + G_{ex}(T,P,m) \quad (1)$$

where  $G^*$  refers to the standard state molar Gibbs Energy for the solution and  $G$  refers to the molar Gibbs Energy of the real solution. These excess Gibbs energy models are effective in describing low  $Z$  solutions and are well adapted to providing equilibrium ratios.

Models based upon excess Gibbs energy, however, are only effective up to about 300 °C and are entirely unacceptable at temperature values a little above 300 °C, as shown by Pitzer<sup>25,26</sup> and Sengers et al.<sup>27</sup> The infinitely dilute standard state in a excess Gibbs energy model is the root of the problem. Near the critical point of the solvent, many standard state properties will diverge strongly and tend towards infinity. For example, small deviations in pressure can cause large changes in density at standard state conditions. The solution density, however, differs from the standard state density because the critical point of the solution may be very different from that at the standard state by virtue of the concentrated solute interactions. The critical point of a solution containing even a small amount of solute is very different from the critical point of the infinitely dilute standard state solution. The

infinitely dilute standard state solution has the same critical point as water. For example, the critical point of an aqueous NaCl solution with only 0.01 mole fraction,  $x$ , of NaCl is 32 °C higher than the critical point of pure water.<sup>77</sup> As a result, the excess Gibbs energy term must make up the difference between a standard state solution that is going to infinity and the solution that has not begun to approach the critical point divergence yet. This requires activity coefficients that are very far from unity for even very small solute concentrations, and excess Gibbs energy models cannot be used to predict these activity coefficients accurately.

### 2.3.2 The Helmholtz Energy Models

A better approach<sup>25-27</sup> for describing aqueous electrolyte solutions near the critical point of water is to use residual Helmholtz energy as the modeled parameter. The residual Helmholtz energy is effective as the modeled parameter for two reasons.

First, this approach avoids the difficulties with standard states that excess Gibbs energy models encounter because the standard state for residual Helmholtz energy is the ideal gas. The residual Helmholtz energy is defined as

$$A_{res} = A - A_{IG} \quad (2)$$

where  $A$  is the molar Helmholtz energy of the real solution and  $A_{IG}$  is the molar Helmholtz energy of the ideal gas, which may be calculated from standard thermodynamic relationships. The ideal gas model does not have divergent properties because an ideal gas has no critical point. Thus, the reference behavior is continuous and smooth in the critical region.

Second, in the residual Helmholtz energy approach, density replaces pressure as an independent variable. This replacement is better because density is the independent variable in the order parameter, and fluctuations of the order parameter dominate in the global critical region. In excess Gibbs energy models, the order parameter is described using pressure as an independent variable. The derivative  $(\partial\rho/\partial P)_{T,x}$ , however, is the response function and diverges in the critical region. This means that small changes in the independent variable, pressure, lead to drastic changes in the dependent variable, density, in the global critical region when using excess Gibbs energy models. By using the order parameter as the independent variable in residual Helmholtz energy models, changes in the dependent variables are more manageable, and critical behavior is much more easily described. Because of these two advantages, residual Helmholtz energy models are the preferred choice for use in the global critical region.

### 2.3.2.1 Anderko-Pitzer Model

Anderko and Pitzer developed a model<sup>1</sup>, the AP Model, that can be used to successfully describe aqueous NaCl solutions in near-critical and supercritical solutions. The AP model is a residual Helmholtz energy model and therefore has an ideal gas standard state. It assumes that no dissociation of NaCl occurs, and therefore all coulombic interactions in the solution are ignored. All interactions are treated as hard-sphere and dipole-dipole interactions. This is an effective approximation at high solute  $m$  values and at high temperature and low pressure values where the fraction of the solute dissociated,  $F_{diss}$ , is small.

In the AP model, residual Helmholtz energy is described as the sum of contributions from a reference state, defined as a mixture of dipolar hard spheres, and a perturbation contribution:

$$A_{res} = A_{ref} + A_{per} \quad (3)$$

where  $A_{ref}$  is the reference state contribution, and  $A_{per}$  is the perturbation contribution. The perturbation contribution is used to account for those effects that are not included in a description of dipolar hard spheres. It is based upon the attractive portion of the equation of state from Anderko and Pitzer<sup>78</sup> for non-polar or slightly-polar fluids. It is a truncated virial expansion of a van der Waals attractive term with parameters determined by regression from volumetric and phase equilibria data. Because the polar interactions are accounted for explicitly in  $A_{ref}$ , the perturbation term is only included to account for those interactions that would exist in a non-polar fluid. The perturbation term is well suited for this task.

The reference state describes both the ion pairs and solvent molecules as hard spheres with dipole moments, though the ion pairs have much stronger dipoles than the solvent molecules. Thus, there are three pair-wise interactions: ion pair-ion pair, ion pair-solvent, and solvent-solvent.

These three pair-wise interactions have two common components of interaction. First there is a hard-sphere repulsion between the species represented as  $A_{rep}$ . The second interaction is due to dipolar attractive interactions and is represented by  $A_{dip}$ . Thus the  $A_{ref}$  contribution is described by

$$A_{ref} = A_{rep} + A_{dip}. \quad (4)$$

The AP model is effective in describing the volumetric properties and phase equilibria near the critical point of water at conditions where  $F_{diss}$  is small. While it is a great advance from the excess Gibbs energy models, it still has shortcomings because it assumes all the solute is fully associated. For example, because it assumes the solute is associated, it cannot describe ionic speciation in the solution. Knowledge of the speciation is necessary in order to predict corrosion potential and other important behaviors. In addition, the AP Model cannot predict enthalpy changes effectively. It does not include any speciation, a major contributor to changes in enthalpy, and it was not fitted to any enthalpy change data. Finally, it fails to predict any behavior accurately at conditions where speciation is significant such as at low concentrations and high pressure values.

### 2.3.2.2 The RI Model

Use of the RI model, developed by Oscarson and his coworkers<sup>2,3</sup>, offers considerable improvement in accuracy over the AP model at the cost of a small computational increase. These workers made use of the fully associated framework of the AP model and added speciation effects. Using the correlation for the standard state molal equilibrium constant,  $K_{mo}$ , developed by Gruskiewicz and Wood<sup>29</sup>, the Palmer model added a contribution to the Helmholtz energy due to dissociation of the NaCl ion pairs,  $A_{diss}$ . The equation for the residual Helmholtz energy is written as

$$A_{res} = A_{ref} + A_{per} + A_{diss}. \quad (5)$$

The RI model performs significantly better than the AP model does when the fraction of the solute dissociated is significant which occurs at low concentrations of NaCl. The AP model performs better when the fraction of the solute dissociated is small.

Additionally, the RI model is strikingly better than the AP model at predicting  $\Delta_{dil}H$  values. The RI model did not change any of the regressed parameters in the perturbation term of the AP model. This means that the RI model is not fit to enthalpy data. Rather, because the change in enthalpy is so significant when the ions move from a high energy associated state to a lower energy state with water ligands, adding a term for this effect significantly improves the  $\Delta_{dil}H$  predictions.

### 2.3.2.3 The RIII Model

Because the  $\log K_m$  term used in the RI model is valid for the infinitely dilute standard state, effects from ion-ion interactions are not accounted for in the RI model. In an attempt to account for these interactions, Liu et al.<sup>4,5</sup> developed a revised model, the RIII model, which contains ion-ion interactions. Liu incorporated the altered primitive MSA used by Myers et al.<sup>79</sup> into the RIII model in order to account for the electrostatic interactions that would arise from the speciation of NaCl into ions and to better represent solutions of a finite concentration. In addition, Liu re-regressed the parameters in the  $A_{per}$  term of the AP model so that the parameters were no longer implicitly accounting for dissociation and concentration effects. The form for the RIII model may be written as

$$A_{res} = A_{ref} + A_{per} + A_{diss} + A_{MSA}. \quad (6)$$

Liu used the pure water dielectric constant equation of Archer and Wang<sup>80</sup> to obtain dielectric constants needed for the MSA term for the RIII model. The Archer and Wang equation, however, is not designed to predict the dielectric constant of the solution containing water and ion pairs as is required by the MSA term. Liu used the Archer and Wang equation as an approximation, and, rather than using water density as an independent variable, the solution density was used. This helped to empirically remove some of the difference between model predictions and experimental values. In addition, the fitted terms in the RIII model also helped to offset the difference.

Further, Liu observed that use of the  $\log K_m$  equation developed by Gruszkiewicz and Wood<sup>29</sup> and used in the RI model failed to give reasonable  $\log K_m$  predictions at lower temperature and density values. The primary reason for this is the limited range of conditions over which the equation was fitted to experimental data. Also, the equation was not fitted to properties requiring a derivative of the Helmholtz energy such as enthalpy changes and molar volumes. Liu proposed a different  $\log K$  equation fitted to a broader data set including molar volume and enthalpy change data.

Use of the RIII model provides better predictions of both molar volume and enthalpic behavior of the solution than use of either the RI or AP model. The RIII model may be used to predict speciation as well. It is the most versatile and accurate model for describing aqueous sodium chloride solutions near the critical point of water.

The RIII model, however, has some disadvantages. First, it has only been used to describe aqueous solutions containing a single solute, NaCl. In practice, solutions will almost always be multi-component. While the RIII model could easily be extended to other similar species, such as KCl, it does not have the capability to be used with compounds that

lead to multiple significant association/dissociation reactions in solution. Finally, the RIII model was never used to predict  $\log K$  values valid at infinite dilution. As a result, the aqueous phase reactions were not compared to experiment, and speciation predictions from using the model are unsubstantiated.

In addition, there are thermodynamic as well as model inconsistencies in the RIII model. While the model can be used to accurately reproduce literature values from which it was regressed, extrapolation to other temperature,  $P$ , and concentration conditions is risky when the theoretical underpinnings of the model are not sound. The inconsistencies are reviewed below:

- 1) The standard state for the  $A_{diss}$  term is not consistent with the standard state for the rest of the model. The standard state for the  $A_{diss}$  term is the infinitely dilute one molal solution while the other terms in the model reference the ideal gas standard state.
- 2) The  $A_{MSA}$  term standard state refers to a dielectric continuum which is dependant upon the concentration of the non-ionic species in solution. Whenever those concentrations change, therefore, the standard state must change. This is especially a problem with more than one solute.
- 3) The  $A_{MSA}$  term uses a dielectric continuum for the non-ionic species while all other terms treat the non-ionic species discretely.
- 4) The  $A_{diss}$  term is a valid representation of the change in the Helmholtz energy with reaction when the solute species are at infinite dilution. At finite solute concentrations, however, it is not valid because the reaction is occurring in an environment with a very different dielectric constant. Thus,

while this term is used in the RIII model to describe reaction at finite concentrations, the  $A_{diss}$  term is not valid for this use.

These inconsistencies are compensated for by adding additional regressible parameters into the RIII model.

Although species including  $\text{Na}^+$ ,  $\text{Cl}^-$ ,  $\text{HCl}$ ,  $\text{NaOH}$  and polynuclear clusters of  $\text{NaCl}$  could form in aqueous  $\text{NaCl}$  solutions,<sup>81</sup> the RIII model makes the reasonable assumption that the  $\text{Na}^+ + \text{Cl}^- \leftrightarrow \text{NaCl}$  reaction is the only significant reaction in solution. The assumption that there is only one significant reaction may not be reasonable for solutes other than  $\text{NaCl}$ . For example, sodium acetate has several significant reactions including the hydrolysis of sodium acetate into acetic acid and the release of  $\text{H}^+$  by acetic acid. The RIII model has also never been extended to aqueous solutions containing a non-polar solute such as  $\text{CO}_2$ ,  $\text{NH}_3$ , or  $\text{SO}_2$ .

## **2.4 Literature Data**

Data useful in developing an equation of state include molar volume, enthalpy, and equilibrium constant,  $K$ , values. Pure-component data for  $\text{H}_2\text{O}$  can be satisfactorily calculated using the equation of state developed by Wagner and Pruss<sup>6</sup> which has been shown to be accurate.

### **2.4.1 VLE and Volumetric Data**

#### **2.4.1.1 NaCl-H<sub>2</sub>O**

The  $\text{NaCl-H}_2\text{O}$  system has been well characterized experimentally. Khaibullin and Borosov<sup>82-85</sup> measured vapor-liquid equilibria as well as densities between 300 and 430 °C.

Relations for  $P$ - $V$ - $T$ - $x$  quantities were investigated by Bodnar<sup>86</sup>, and both Urusova<sup>87</sup> and Bodnar<sup>88</sup> measured single-phase densities near the critical point of water.

#### **2.4.1.2 LiCl-H<sub>2</sub>O**

The LiCl-H<sub>2</sub>O system has not been characterized as well as the NaCl-H<sub>2</sub>O system. Majer et al.<sup>89</sup> determined densities for 0.0025 to 3.0  $m$  solutions from 604.4 K to 725.5 K, and from 18.5 MPa to 38 MPa using a vibrating tube densimeter. Pepinov et al.<sup>90</sup> determined densities of aqueous LiCl solutions at 20 MPa and 30 MPa at 350 °C.

### **2.4.2 Enthalpy Data**

#### **2.4.2.1 NaCl-H<sub>2</sub>O**

$\Delta_{dil}H$  values for the H<sub>2</sub>O-NaCl system have been reported by Busey and coworkers<sup>91</sup> at temperature values up to 400 °C. Chen et al.<sup>92</sup>, Fuangswasdi et al.<sup>93</sup>, and Oscarson et al.<sup>2</sup> all reported  $\Delta_{dil}H$  values up to 350 °C.

#### **2.4.2.2 LiCl – H<sub>2</sub>O**

Gillespie et al.<sup>94</sup> determined  $\Delta_{dil}H$  data for LiCl from 300 °C to 350 °C and from 11.0 MPa to 17.6 MPa.

### **2.4.3 Equilibrium Constants**

#### **2.4.3.1 NaCl-H<sub>2</sub>O**

Values of  $K$  for the NaCl dissociation reaction are available from several studies. Gruszkiewicz and Wood<sup>29</sup> used conductance measurements to determine values of the logarithm of equilibrium constants valid at infinite dilution,  $\log K_o$ , from 603 K to 674 K and

at pressures from 15 MPa to 28 MPa. Franck<sup>95</sup> determined  $\log K_o$  values using conductance measurements at 550 °C from 0.3 to 0.7 g/cm<sup>3</sup>. Ho et al.<sup>96</sup> determined  $\log K_o$  values from conductance measurements between 350 °C and 600 °C and densities between 0.3 g/cm<sup>3</sup> and 0.75 g/cm<sup>3</sup>. Zimmerman et al.<sup>34</sup> used conductance methods to determine  $\log K_o$  values between 580 °C and 677 °C and from 9.8 MPa to 28 MPa. Ho et al.<sup>33</sup> used conductance measurements to determine  $\log K_o$  values between 250 °C and 403 °C and from 10 MPa to 33 MPa. Oelkers and Helgeson<sup>97</sup> determined  $K$  values from conductance data from 400 °C to 800 °C and from 500 bar to 4000 bar.

#### **2.4.3.2 LiCl-H<sub>2</sub>O**

Gruskiewicz and Wood<sup>29</sup> determined  $\log K_o$  through conductance measurements for aqueous LiCl solutions for solutions from 603.32 K to 658.07 K and from 15 MPa to 24 MPa. Zimmerman et al.<sup>34</sup> used conductance techniques to determine  $\log K_o$  values from 604.58 K to 672.89 K and from 22 MPa to 28 MPa. Ho et al.<sup>33</sup> also used conductance measurements to determine  $\log K_o$  values for temperatures up to 678.15 K and pressures up to 30 MPa. Ho and Palmer<sup>98</sup> determined  $\log K_o$  values from 400 to 600 °C and from 0.3 g/cm<sup>3</sup> to 0.8 g/cm<sup>3</sup>. Gillespie et al.<sup>94</sup> calculated  $\log K_o$  values from  $\Delta_{dil}H$  data for LiCl from 300 °C to 350 °C and from 11.0 MPa to 17.6 MPa. Oelkers and Helgeson<sup>97</sup> calculated  $K$  values using conductance data from 400 °C to 800 °C and from 500 bar to 4000 bar.

### **2.5 Isothermal Flow Calorimetry**

Isothermal flow calorimetry has proven to be a valuable technique for investigating electrolyte solutions. The method consists of measuring the energy change required to

maintain a constant temperature within a system during a reaction from the mixing of two continuously flowing streams.

Several different isothermal flow calorimeters have been developed in the past<sup>99-104</sup>. Recently, a new calorimeter was designed<sup>93</sup> that improved upon previous designs for calorimeters of this type by improving temperature control, ease of maintenance, and the ability to make accurate measurements above 350 °C. Methodologies for determining heats of reaction (including  $\Delta_{dil}H$  values),  $K$  values,<sup>105-111</sup> heats of mixing,<sup>112</sup> and vapor-liquid equilibrium<sup>113-115</sup> have all been reported.

Additionally,  $\log K_o$  values can be obtained from calorimetric data. Following the method used by Chen et al.,<sup>107</sup> the measured enthalpy changes may be attributed to several contributions. These contributions include heats of aqueous phase reactions,  $\Delta_{dil}H$  values, heats of phase change, and heats of non-ideal vapor phase interactions between molecules. By subtracting contributions other than those of the reactions in the aqueous phase, enthalpy changes due to reactions may be obtained.  $\log K$  values may then be fitted to these enthalpy changes.

Methods are available<sup>107</sup> for calculating the contributions to calorimetric measurements. An activity coefficient model may be used to calculate  $\Delta_{dil}H$  values and also to extrapolate the  $\log K$  values from the experimental conditions to their infinite dilution standard state values. An equation of state is used to calculate fugacity coefficients for the gaseous species as well as the enthalpy changes due to non-ideal gas interactions. Heats of vaporization for water are commonly available and can be used to subtract the H<sub>2</sub>O phase change enthalpy values.

### 3 Objectives and Approach

The objective of this research is to develop a thermodynamic equation of state, the RIV model, for aqueous electrolyte solutions at conditions near the critical point of water (350-400 °C, 18-40 MPa) with the following properties:

- 1) thermodynamic consistency between the individual terms,
- 2) capability of modeling aqueous reactions,
- 3) generality in form enabling direct application to other electrolyte solutions, and
- 4) rigor based on a holistic approach that relies upon fundamental relationships between interacting particles to describe aqueous reactions rather than empirical  $\log K$  equations.

Use of the RIV model should allow accurate prediction of densities and  $\Delta_{dil}H$  values. If these capabilities can be realized, some confidence may be had in the usefulness of the RIV model in predicting ionic species concentrations at finite dilutions. No other model extant has these properties.

In order to develop a model capable with these properties and capabilities, it was necessary to have a broad range of experimental  $\Delta_{dil}H$  values from which to regress the model parameters. A vital portion of this research effort, therefore, was the determination of experimental  $\Delta_{dil}H$  values using flow calorimetry techniques.

The approach used in the development of the AP model by Anderko and Pitzer<sup>1</sup> was used in the development of the RIV model. They developed the AP model by first identifying the interactions between species in the solution and then including terms in their model that describe those interactions. The RIV model allows a significantly more complex situation than the AP model because it allows for ions to be present in solution. The approach, however, is the same – that of examining the interactions between species in solution and including terms that model those interactions. Aqueous reactions are a result of the modeled interactions and basic thermodynamic relationships rather than being directly included as an empirical  $\log K$  equation.

This approach is different from the approach taken in developing the RI and RIII models. In the RI and RIII models, aqueous reactions were included by adding a separate reaction term in the models. The approach taken for the AP model and the RIV model is more fundamental and is thermodynamically consistent.

## 4 Development of the Model

In this chapter the reasoning for the form of the RIV model as well as the development of the individual terms will be discussed. The model is composed of two separate theoretical contributions and one semi-empirical contribution. The two theoretical contributions describe, respectively, hard-sphere repulsion effects and the ion and dipole interactions. The semi-empirical contribution describes interactions that would be present in a non-polar system. In addition, the method for calculating the thermodynamic properties will be discussed.

### 4.1 *Development of the Model Concept*

The AP model makes the simplifying assumption that the electrolyte is fully associated and identifies key molecular interactions. Because there are no ions, the interactions are fewer and can mostly be described using a hard-sphere repulsion term and a dipole-dipole interaction term. The perturbation term is added to the AP model to account for dispersion effects and other interactions that are not specifically accounted for in the model.

In order to extend the AP approach so that it is closer to reality, the dissociation of the solute into ions is permitted in the RIV model. This theoretical extension also introduces ion-ion and ion-dipole interactions. There are relatively few models that describe interactions when ions are involved and even fewer that are useful for engineering

calculations. Based upon studies summarized in the literature review, the non-primitive MSA, NPMSA, was chosen because, of all the non-primitive approaches, it alone includes an ion-ion interaction term that converges. Additionally, the NPMSA does not require a temperature and concentration dependent dielectric constant as do primitive approaches. Finally, a discrete approach, as opposed to a mean-field approach, is more consistent with the hard-sphere term.

Though the AP model already includes a dipole-dipole interaction term from perturbation theory, this was discarded in favor of the dipole-dipole interaction described by the NPMSA. The reasons for this are: 1) while the separate internal energy contributions from the three interactions (dipole-dipole, ion-dipole, and ion-ion) can be decoupled, the Helmholtz energy contributions cannot, and 2) it seems more consistent to use the same model for all three contributions.

The perturbation term used in the AP model is also used in the RIV model since it is well-suited for describing the remaining interactions such as dispersion interactions and quadrupole interactions. The form is derived from a van der Waals type attraction term and may, therefore, be considered a mean field term. Thus, the perturbation term may also be considered inconsistent with the other terms in the model which are not mean field terms. Because the parameters in the term are regressed as part of the model as a whole, however, it is more a perturbation term than a theoretical mean field term. The model is, in that respect, fully consistent in its approach.

As in the AP model, the perturbation term is only used to describe the remaining interactions of the dipolar water and dipolar NaCl molecules. Ions, which are included in the RIV model, possess these same interactions. However, because the ion interactions are so

fully dominated by the coulombic effects already described in the NPMSA, it is assumed that the non-coulombic interactions are negligible for the ions.

Finally, a simple water ligand term is included to account for changes in the Helmholtz energy resulting from the interaction of water ligands with the species involved in aqueous phase reactions.

What emerges from this approach is a model that is as consistent thermodynamically as the AP model but more general in that it allows ionic species. All the terms have consistent standard states, and discrete models are not mixed with non-discrete models. In equation (7), this model is given as

$$A_{res} = A_{HS} + A_{NPMSA} + A_{per} + A_{lig} \quad (7)$$

where  $A_{HS}$  is the hard-sphere repulsive contribution,  $A_{NPMSA}$  is the non-primitive MSA contribution,  $A_{per}$  is the perturbation contribution, and  $A_{lig}$  is the water ligand term. The  $Z$  is described as

$$Z = Z_{HS} + Z_{NPMSA} + Z_{per} \cdot \quad (8)$$

The difference between the RIV equation of state and others<sup>3, 5</sup> that are designed to predict speciation, is that the thermodynamic contributions from aqueous reactions are not represented in the RIV model using a separate equilibrium constant model. Instead, the speciation is a result of the theoretical interactions themselves. That is, speciation occurs as a

result of the minimization of the total Helmholtz energy,  $a$ , at a constant temperature and density as a function of the extent of the speciation of the neutral species into ions.

## 4.2 The Hard-sphere Repulsion Term

The hard-sphere term is identical to that used in the AP model given by Boublik<sup>116</sup> and Mansoori et al.<sup>117</sup> It is based upon the single-component equation developed by Carnahan and Starling<sup>118</sup> and generalized for multi-component mixtures. The residual Helmholtz energy of a hard-sphere mixture,  $A_{HS}$ , with an ideal-gas reference state is given by

$$\frac{A_{HS}}{RT} = \frac{3DE}{F} \frac{\eta - \frac{E^3}{F^2}}{1 - \eta} + \frac{\frac{E^3}{F^2}}{(1 - \eta)^2} + \left( \frac{E^3}{F^2} - 1 \right) \ln(1 - \eta) \quad (9)$$

where

$$D = \sum_{i=1}^n x_i \sigma_i \quad (10)$$

$$E = \sum_{i=1}^n x_i \sigma_i^2 \quad (11)$$

$$F = \sum_{i=1}^n x_i \sigma_i^3 \quad (12)$$

and where  $x_i$  and  $\sigma_i$  are the mole fraction and hard-sphere diameter of species  $i$ , respectively.

The reduced density  $\eta$  is defined as

$$\eta = b/4V \quad (13)$$

where  $V$  is the molar volume, and  $b$  is the van der Waals co-volume parameter which is defined as

$$b = 2/3\pi N_A F \quad (14)$$

where  $\pi$  is the numerical constant pi and  $N_A$  is Avogadro's Number. The  $Z$  of the hard-sphere mixture including the ideal gas contribution,  $Z_{HS}$ , is obtained from the thermodynamic

identity  $Z = -\frac{V}{RT} \left( \frac{\partial A}{\partial V} \right)_{T,P,x}$  and can be shown to be

$$Z_{HS} = \frac{1 + \left( \frac{3DE}{F} - 2 \right) \eta + \left( \frac{3E^3}{F^2} - \frac{3DE}{F} + 1 \right) \eta^2 - \frac{E^3}{F^2} \eta^3}{(1 - \eta)^3}. \quad (15)$$

### 4.3 The Non-primitive Mean Spherical Approximation

The formulation used for the NPMSA is taken from the work of Blum<sup>60</sup>. In this derivation, there is one diameter for all species in solution. The solution to the NPMSA requires solving three simultaneous nonlinear equations in order to determine the values of  $b_o$ ,  $b_l$ , and  $b_2$  which relate to the ion-ion, ion-dipole, and dipole-dipole interactions, respectively. These equations are given as

$$a_1^2 + a_2^2 = d_o^2 \quad (16)$$

$$\frac{a_1 b_1}{2} + a_2 \beta_3 = d_o \Delta A \quad (17)$$

$$\frac{b_1^2}{4} + \beta_3^2 = \Delta^2 (y_1^2 + A^2) \quad (18)$$

where

$$A = d_2 - \frac{d_o b_1 \Lambda}{2\Delta} \quad (19)$$

$$a_1 = \frac{\Delta - 2\beta_6 D_f}{2D_f^2} \quad (20)$$

$$a_2 = \frac{b_1 \left( \frac{\Delta}{2} + D_f \beta_3 \right)}{2D_f^2 \beta_6} \quad (21)$$

with

$$\Delta = \frac{b_1^2}{4} + \beta_6^2 \quad (22)$$

$$D_f = \frac{1}{2} \left[ \beta_6 (1 + b_o) - \frac{b_1^2}{12} \right] \quad (23)$$

$$\Lambda = \frac{1}{2} (1 + b_o) + \frac{\beta_6}{6}. \quad (24)$$

The remaining terms are defined as

$$\beta_3 = 1 + \frac{b_2}{3} \quad (25)$$

$$\beta_6 = 1 - \frac{b_2}{6} \quad (26)$$

$$\beta_{12} = 1 + \frac{b_2}{12} \quad (27)$$

$$y_1 = \frac{\beta_6}{\beta_{12}^2} \quad (28)$$

and

$$d_2 = \sqrt{\frac{\sum_{i=1}^n \rho_i \mu_i^2}{3 \varepsilon_o k T}} \quad (29)$$

$$d_o = \sqrt{\frac{q_e^2 \sigma^2}{\varepsilon_o k T} \sum_{i=1}^n \rho_i z_i^2} \quad (30)$$

where  $\rho_i$  is the number density of species  $i$ ,  $\mu_i$  is the dipole moment of species  $i$ ,  $k$  is the Boltzmann constant ( $k = 1.38066 \times 10^{-23} \text{ J} \cdot \text{K}^{-1}$ ),  $\varepsilon_o$  is the permittivity of a vacuum ( $\varepsilon_o = 8.85419 \times 10^{-12} \text{ C} \cdot \text{N}^{-1} \cdot \text{m}^{-2}$ ),  $\sigma$  is the diameter of the species in solution, and  $z_i$  is the charge of species  $i$ . The correct solution for the system of equations (16) - (18) may be verified by determining if  $b_o$ ,  $b_l$ , and  $b_2$  are within the correct ranges<sup>70</sup>. These ranges are shown in Table 1.

**Table 1: Range of acceptable values<sup>70</sup> for the solution of equations (16)-(18).**

Parameter	Range of Acceptable Values
$b_o$	-1.0 – 0.0
$b_1$	0.0 - $3\sqrt{2}$
$b_2$	0.0 – 6.0

Once the values of  $b_0, b_1, b_2$  are found using equations (16)-(18),  $A_{NPMSA}$  may be obtained by<sup>60</sup>

$$A_{NPMSA} = \frac{-kTV}{12\pi} \left( \frac{-2d_o^2 b_o}{\sigma^3} + \frac{2d_2 d_o b_1}{\sigma^3} + J' \right) \quad (31)$$

where

$$J' = \left( \frac{\beta_6}{D_f} - 2 - a_1 \right)^2 \frac{1}{\sigma^3} + 2\sigma b_1^2 \left[ \frac{[\beta_3 + a_1(3\Lambda - 2D_f)]^2}{\Delta^2 \sigma^4} \right] + 4 \left[ \left[ \beta_3^2 + \frac{\sigma b_1 a_2 (3\Lambda - 2D_f)}{2\sigma} \right] \frac{1}{\Delta} - 1 \right]^2 \frac{1}{\sigma^3} + \frac{2}{\sigma^3} \left( \frac{b_2 \beta_{24}}{\beta_{12}} \right)^2 \quad (32)$$

and

$$\beta_{24} = 1 - \frac{b_2}{24}. \quad (33)$$

The internal energy is obtained by

$$U_{NPMSA} = \frac{kTV}{4\pi\sigma^3} (d_o^2 b_o - 2d_2 d_o b_1 - 2b_2 d_2^2) \quad (34)$$

followed by obtaining pressure and  $Z$  with

$$P_{NPMSA} = \frac{U_{NPMSA} - A_{NPMSA}}{V} \quad (35)$$

$$Z_{NPMSA} = \frac{P_{NPMSA} V}{RT} \quad (36)$$

where  $R$  is the ideal gas constant ( $R = 8.314471 \text{ J}(\text{mol}\cdot\text{K})^{-1}$ ). All other thermodynamic quantities can be obtained through equations (34)-(36).

The van der Waals one-fluid mixing rules are used to calculate the diameter of the species in the NPMSA and are given by

$$\sigma^3 = \sum_{i=1}^n \sum_{j=1}^n \left( \frac{\sigma_i + \sigma_j}{2} \right)^3 x_i x_j \quad (37)$$

where  $\sigma_i$  and  $\sigma_j$  are the diameters of species  $i$  and  $j$ , respectively. The NPMSA diameters are allowed to be different from those in the hard-sphere term.

#### 4.4 The AP Perturbation Term

The perturbation term that Anderko and Pitzer<sup>1</sup> chose for the AP model comes from one used for a similar purpose by Dohrn and Prausnitz<sup>119</sup>. Dohrn and Prausnitz used the Carnahan and Starling hard-sphere equation of state<sup>118</sup> as the reference system for their equation of state for non-polar fluids. They added a perturbation term of a form empirically determined using experimental data from a variety of non-polar fluids. The final form for their perturbation term is

$$Z_{pert} = -\frac{4a}{RTb}\eta(1 + c\eta + d\eta^2) \quad (38)$$

where  $\eta$  is the reduced density given by

$$\eta = b\rho/4 \quad (39)$$

with  $\rho$  being the molar density.

Anderko and Pitzer adopted a slightly modified version of equation (38) given as

$$A_{pert} = -\frac{4a}{b}\eta(1 + c\eta + d\eta^2 + e\eta^3) \quad (40)$$

which contained an extra parameter,  $e$ , for the cubed reduced density. They then extended this equation to mixtures by relating the parameters to virial coefficients. They also changed the form of the equation to be a function of molar volume instead of  $\eta$  resulting in

$$A_{pert} = -\left(\frac{a}{v} + \frac{acb}{4v^2} + \frac{adb^2}{16v^3} + \frac{aeb^3}{64v^4}\right). \quad (41)$$

The corresponding  $Z$  contribution is

$$Z_{pert} = -\frac{1}{RT}\left(\frac{a}{v} + \frac{acb}{2v^2} + \frac{adb^2}{16v^3} + \frac{aeb^3}{16v^4}\right). \quad (42)$$

The mixing rules proposed for the parameters of equations (41) and (42) are

$$a = \sum_{i=1}^n \sum_{j=1}^n x_i x_j a_{ij} \quad (43)$$

$$acb = \sum_{i=1}^n \sum_{j=1}^n \sum_{k=1}^n x_i x_j x_k (ac)_{ijk} b_{ijk} \quad (44)$$

$$adb^2 = \sum_{i=1}^n \sum_{j=1}^n \sum_{k=1}^n \sum_{l=1}^n x_i x_j x_k x_l (ad)_{ijkl} b_{ijkl}^2 \quad (45)$$

$$aeb^3 = \sum_{i=1}^n \sum_{j=1}^n \sum_{k=1}^n \sum_{l=1}^n \sum_{m=1}^n x_i x_j x_k x_l x_m (ae)_{ijklm} b_{ijklm}^3 \quad (46)$$

where

$$b_{ijk} = \left[ \left( b_i^{1/3} + b_j^{1/3} + b_k^{1/3} \right) / 3 \right]^3 \quad (47)$$

$$b_{ijkl} = \left[ \left( b_i^{1/3} + b_j^{1/3} + b_k^{1/3} + b_l^{1/3} \right) / 4 \right]^3 \quad (48)$$

$$b_{ijklm} = \left[ (b_i^{1/3} + b_j^{1/3} + b_k^{1/3} + b_l^{1/3} + b_m^{1/3}) / 5 \right]^3. \quad (49)$$

The co-volume parameter is related to the diameters of the hard-sphere term by

$$\sigma_i = \left( \frac{3}{2\pi N_A} b_i \right)^{1/3}. \quad (50)$$

The remaining parameters in equations (43)-(46) are given by

$$a_{ij} = (a_i a_j)^{1/2} \alpha_{ij} \quad (51)$$

$$(ac)_{ijk} = [(ac)_i (ac)_j (ac)_k]^{1/3} \gamma_{ijk} \quad (52)$$

$$(ad)_{ijkl} = [(ad)_i (ad)_j (ad)_k (ad)_l]^{1/4} \delta_{ijkl} \quad (53)$$

$$(ae)_{ijklm} = [(ae)_i (ae)_j (ae)_k (ae)_l (ae)_m]^{1/5} \varepsilon_{ijklm} \quad (54)$$

where the undefined parameters in equations (51)-(54) are determined empirically for a specific system.

#### **4.5 Water Ligand Term**

In order to account for the changes in water ligand energies as a result of association with reacting species, it is necessary to incorporate a water ligand reaction term into the RIV model. There are many possible forms for this term including some theoretical models such

as SAFT.<sup>46</sup> In the RIV model, however, a simple term as a function of concentration is sufficient. The term is given as

$$A_{lig} = x_{ion} A_{lig}^* \quad (55)$$

where  $A_{lig}$  is the contribution to the residual Helmholtz energy,  $x_{ion}$  is the mole fraction of ions in solution, and  $A_{lig}^*$  is a solution specific parameter.

Water hydrates NaCl molecules in solution. When NaCl dissociates into ions, the  $\text{Na}^+$  and  $\text{Cl}^-$  species are also hydrated but more strongly. Because there is a net increase of individual species when NaCl dissociates and because ions have a much stronger interaction with water than NaCl, there is a large change in energy from this hydration, which can be thought of as ligand association. The form in equation (55) is designed to represent a linear change in the Helmholtz energy of solution as a result of the increase of concentration of ions.

#### **4.6 Determination of Ionic Speciation**

Thermodynamic theory specifies that at a constant temperature and density, the equilibrium state of the system coincides with the minimum of the total Helmholtz energy of the system. Thus, at a constant temperature and density, the speciation may be determined by minimizing the total Helmholtz energy of the system (in J) as a function of the extent of the dissociation reaction as in Figure 1. For example, for the NaCl dissociation reaction where the extent of reaction in moles is denoted by  $\varepsilon_{\text{NaCl}}$ , and the objective function that is

minimized is  $(1 \text{ mol} + \varepsilon_{\text{NaCl}})A$ . In this minimization, a starting amount of 1 mole of solution is assumed. The amount of solution after reaction, therefore, is  $(\varepsilon_{\text{NaCl}} + 1)$  moles.

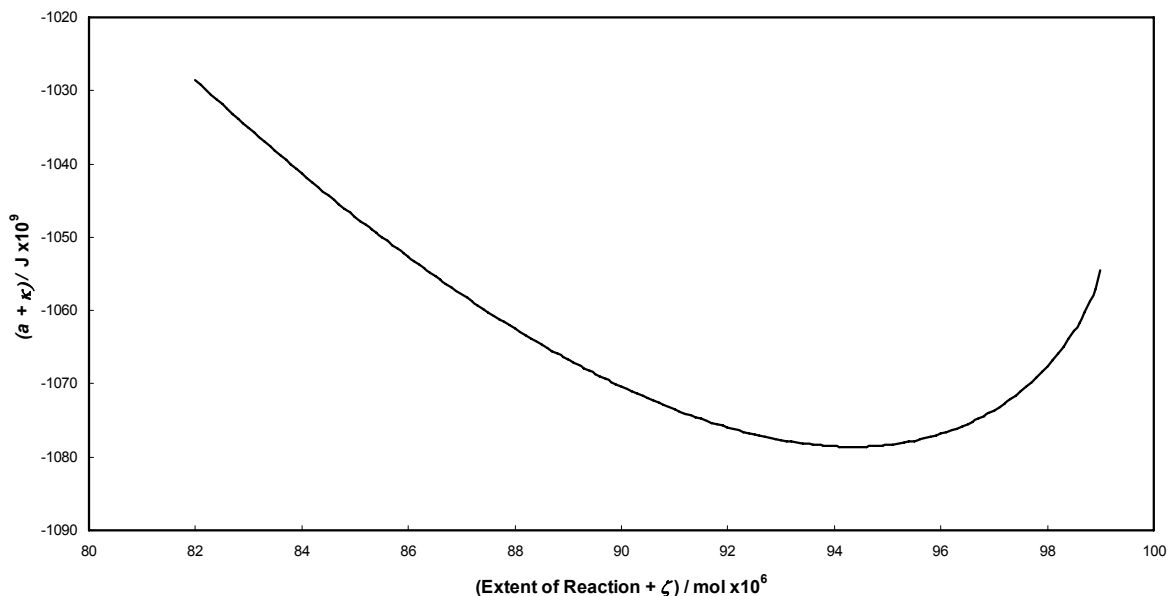


**Figure 1: The  $a$  of a system versus the extent of the dissociation reaction. The minimum in  $a$  coincides with the reaction equilibrium. The constants  $\kappa$  and  $\zeta$  are equal to 1273956.39196637 and -0.0853234, respectively, and are added to the plotted values to make the plot easier to read.**

## 4.7 Calculation of Volumes

The calculation of volumes as a function of temperature, pressure, and composition requires an algorithm that calculates equilibrium concentrations of the solute and ions at every value of molar volume. The algorithm is detailed in Figure 2. It is essentially a standard volume finding algorithm with an extra step added to determine speciation of the ionic species at every molar volume.

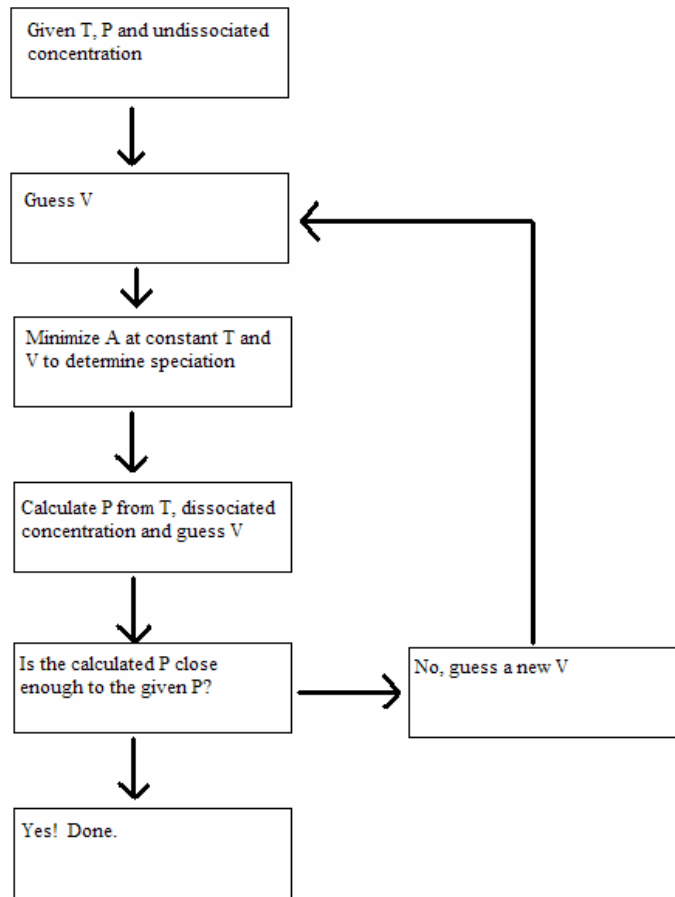


Figure 2: Algorithm used to determine molar volume from temperature, pressure, and composition.

#### 4.8 Calculation of $\Delta_{dil}H$ Values

The enthalpy of the solution is determined by

$$H = U + PV \quad (56)$$

where

$$U = -T^2 \left( \frac{\partial A/T}{\partial T} \right)_{V, x_i} . \quad (57)$$

The enthalpy at a given temperature, pressure, and solute concentration may be determined, therefore, by first determining the molar volume and the equilibrium concentration of aqueous species. Then internal energy is determined at the equilibrium concentration and the molar volume by equation (57). Finally, the quantity  $PV$  is added to  $U$ . The differentiation in equation (57) is accomplished numerically.

Values of  $\Delta_{dil}H$  are determined experimentally through calorimetric techniques. The data are normally reported in reference to the amount of associated salt that is involved in the aqueous phase reaction. For example, in NaCl solutions,  $\Delta_{dil}H$  values are normally reported in terms of energy/mole of NaCl.

The process of dilution for a NaCl solution is graphically described in Figure 3. In Figure 3,  $\varepsilon_1$  is the extent of the NaCl dissociation reaction for 1 mole of solution. Because there are two moles of ions generated for every mole of NaCl that reacts, the total number of moles in the solution at reaction equilibrium becomes  $(1+\varepsilon_1)$ .

When the stream of  $(1+\varepsilon_1)$  moles of NaCl solution mixes with the stream of  $n$  moles of pure water, it forms  $(1+n+\varepsilon_2)$  moles of solution where  $\varepsilon_2$  is the extent of the dissociation reaction for  $(1+n)$  moles of solution, i.e., the  $\varepsilon_2$  value is the extent of reaction for a solution of  $(1+n)$  moles of NaCl solution where the NaCl is initially all associated.

With this formalization of the process, the  $\Delta_{dil}H$  value may be calculated by

$$\Delta_{dil}H = \frac{(1+n+\varepsilon_2)H_f - nH_{H_2O} - (1+\varepsilon_1)H_i}{x_{NaCl_i}^o} \quad (58)$$

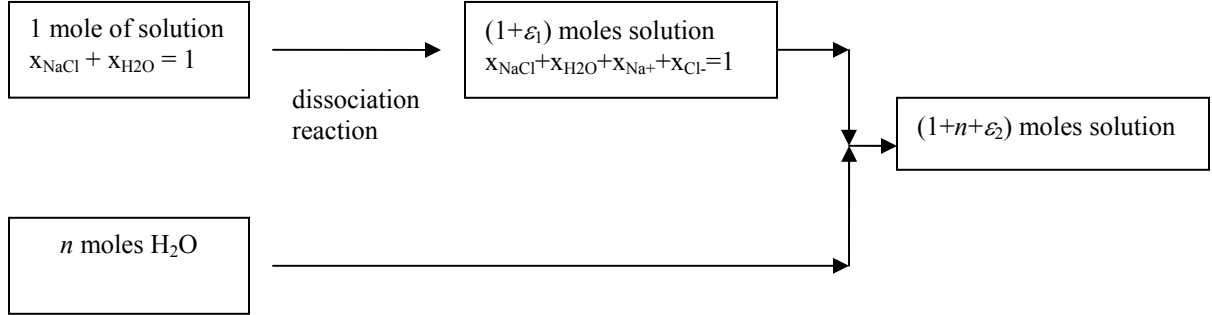


**Figure 3: The  $\Delta_{dil}H$  process.**

where  $H_f$  is the enthalpy of the final solution at the reaction equilibrium state;  $H_i$  is the enthalpy of the initial solution at the reaction equilibrium state;  $H_{H_2O}$  is the enthalpy of pure water; and  $x_{NaCl_i}^o$  is the mole fraction of NaCl in the initial solution assuming the NaCl is fully associated ( $x_{NaCl} + x_{H_2O} = 1$ ). The number of moles of pure water,  $n$ , is found by

$$n = \frac{x_{NaCl_i}^o}{x_{NaCl_f}^o} - 1 \quad (59)$$

where  $x_{NaCl_f}^o$  is the mole fraction of NaCl in the final solution assuming the NaCl is fully associated ( $x_{NaCl} + x_{H_2O} = 1$ ). The extents of reaction,  $\varepsilon_1$  and  $\varepsilon_2$ , may be determined by

$$\varepsilon_1 = \frac{x_{Na^+i}}{1 - x_{Na^+i}} \quad (60)$$

$$\varepsilon_2 = \frac{(n+1)x_{Na^+f}}{1 - x_{Na^+f}} \quad (61)$$

where  $x_{Na^+i}$  is the mole fraction of  $Na^+$  in the initial solution at the reaction equilibrium state, and  $x_{Na^+f}$  is the mole fraction of  $Na^+$  in the final solution at the reaction equilibrium state.

Thus,  $\Delta_{dil}H$  may be calculated for a given temperature, pressure, and the initial and final compositions of the solutions. The  $H_f$  and  $H_i$  values are determined by first calculating the system molar volume and equilibrium species concentrations and then calculating enthalpy at that molar volume and species composition.

## 4.9 Calculation of Heat Capacities

Heat capacities can be calculated as follows:

$$C_p = \left( \frac{\partial H}{\partial T} \right)_{P,x} \quad (62)$$

$$C_V = \left( \frac{\partial U}{\partial T} \right)_{V,x} \quad (63)$$

where  $C_p$  is the constant pressure heat capacity, and  $C_V$  is the constant volume heat capacity.

The enthalpy and internal energy are obtained from equations (56) and (57). Just as the

enthalpy and internal energy are evaluated numerically, so too derivatives in equations (62) and (63) are evaluated numerically.

#### 4.10 *log K<sub>o</sub> Calculation*

Literature values for  $K$  valid at infinite dilution are typically reported as molal equilibrium constants or  $K_{m_o}$ . The standard states used for this constant are asymmetric in that the solute and ionic species have a hypothetical infinite dilution standard state while the solvent (water) has a pure-component standard state. The  $K_{m_o}$  of the solute dissociation reaction at infinite dilution is defined as (using the NaCl dissociation reaction as an example)

$$K_{m_o} = \frac{m_{Na^+} m_{Cl^-}}{m_{NaCl}} \quad (64)$$

where  $m_i$  is the  $m$  of species  $i$ . At infinite dilution, activity coefficients are equal to unity. Since the infinite dilution standard state is hypothetical, it is not possible to calculate concentrations of the aqueous species for the standard state. As a result, the  $\log K_{m_o}$  must be calculated by extrapolation from finite concentrations.

Debye-Huckel theory shows that the  $\log K_m$  of an aqueous reaction should be a linear function of the square root of the ionic strength,  $I$ , in very dilute solutions. Because of numeric limitations stemming from the summation of very large values in evaluating residual Helmholtz energy, however, it is difficult to calculate precise concentrations in very dilute solutions. As a result, the method used for calculating infinite dilution  $\log K_m$  values, as shown in Figure 4, is to calculate  $\log Q$  values at several less dilute concentrations, fit a

quadratic function to these calculations versus the square root of ionic strength, and extrapolate to zero ionic strength.  $\log Q$  is defined as

$$\log Q = \frac{m_{Na^+} m_{Cl^-}}{m_{NaCl}} \quad (65)$$

and is equal to  $\log K_{mo}$  at infinite dilution.

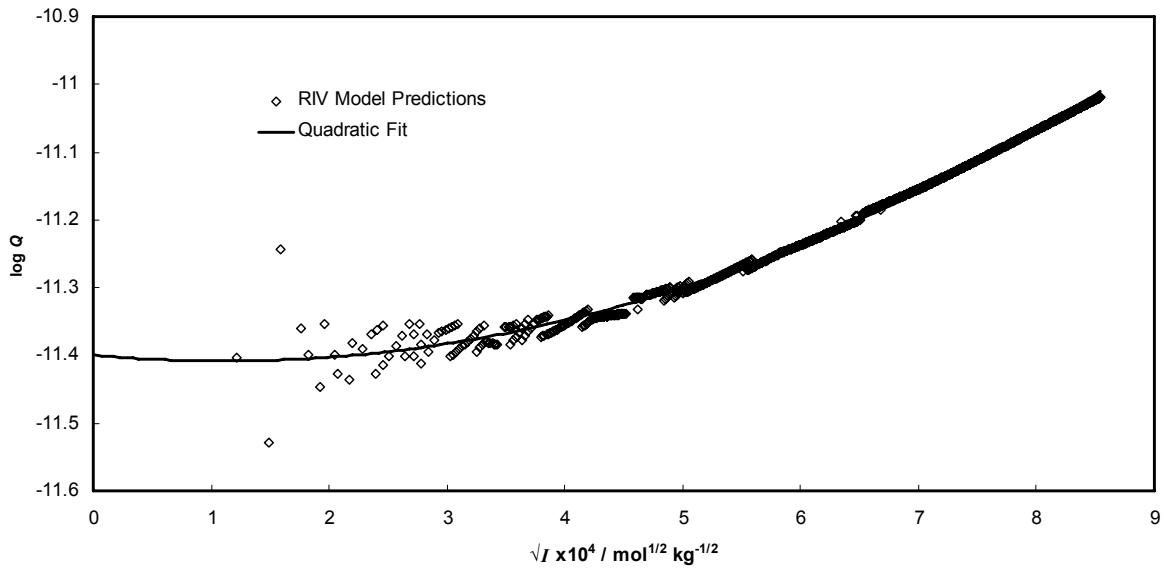


**Figure 4:** Plot of  $\log Q$  values predicted using the RIV model versus the square root of ionic strength. A quadratic function was fitted to the predictions and extrapolated to zero ionic strength to determine a  $\log K_{mo}$  value of about -11.4. As the solution becomes more dilute, numerical instability makes it difficult to calculate concentrations precisely.

## 5 Application of the RIV Model

In this chapter, the application of the RIV model to the aqueous NaCl and LiCl systems will be discussed. Visual Doc, a nonlinear optimization software package<sup>120</sup>, was used to regress the parameters in the RIV model. The parameters were regressed from experimental density and  $\Delta_{dil}H$  data in the case of the aqueous electrolyte solutions and from predictions from the IAPWS equation of state<sup>6</sup> in the case of pure water. The optimization objective function is given below as

$$Error = \frac{Error_V + Error_{\Delta_{dil}H}}{2} \quad (66)$$

$$Error_V = 100 \left( \sum_i \frac{|V_{dat_i} - V_{RIV_i}|}{V_{dat_i}} \right) / N_V \quad (67)$$

$$Error_{\Delta_{dil}H} = 100 \left( \sum_i \frac{|\Delta_{dil}H_{dat_i} - \Delta_{dil}H_{RIV_i}|}{\Delta_{dil}H_{dat_i}} \right) / N_{\Delta_{dil}H} \quad (68)$$

where  $Error_V$  and  $Error_{\Delta_{dil}H}$  are the differences between the molar volume predictions and the  $\Delta_{dil}H$  predictions and the literature molar volume values and literature  $\Delta_{dil}H$  values, respectively;  $V_{dat_i}$  and  $\Delta_{dil}H_{dat_i}$  are the literature values for molar volume and  $\Delta_{dil}H$ , respectively;  $V_{RIV_i}$  and  $\Delta_{dil}H_{RIV_i}$  are the RIV model predictions for molar volume and  $\Delta_{dil}H$ ,

respectively; and  $N_V$  and  $N_{\Delta_{dil}H}$  are the number of literature data points for molar volume and  $\Delta_{dil}H$ , respectively. *Error* is the total error with respect to literature data and the objective function for minimization. This function was chosen because it allowed the errors in the different kinds of data (i.e. molar volume versus  $\Delta_{dil}H$ ) to be measured on the same scale thus avoiding preferential treatment of one kind of data.

At the start of the regression, 10% of the data were randomly chosen and withheld. The random choice was made by assigning random numbers to each datum and then selecting the 10% of the random values with the lowest magnitude. This was done so that the model could be validated versus data that were not used in the regression. The sources of literature data for the electrolyte systems are listed in Table 2.

**Table 2: Sources for literature data used in the regression of parameters in the RIV model for the NaCl and LiCl solutions.**

<b>Literature Data Type</b>	<b>Source References</b>
NaCl Solution $V$	87, 121-123
NaCl Solution $\Delta_{dil}H$	2, 91-93, this study
LiCl Solution $V$	89, 90
LiCl Solution $\Delta_{dil}H$	94

First, the application of the model to water will be discussed followed by the application of the model to aqueous NaCl and LiCl solutions. The results from the application of the model to the NaCl and LiCl systems will be discussed in Chapter 6.

## **5.1 The Application of the RIV Model to Water**

The water model was regressed from densities and  $C_V$  values calculated using the IAPWS equation of state for water<sup>6</sup>. Values from the IAPWS equation of state were used

instead of experimental data because this equation can be used to reproduce data within experimental accuracy. The water model was fitted within the temperature range 100 °C – 1000°C. The dipole moment of water derived from experiment was used (1.85 D).

The AP water model<sup>1</sup> was regressed using density and vapor pressure data. Because the AP model was not intended to predict changes in enthalpy,  $C_v$  values, and other thermodynamic quantities derived by the differentiation of the Helmholtz energy with respect to temperature, these data were not used to regress the parameters in the AP model.

Consequently, the AP water model predicts  $C_v$  values poorly. In the present work, however, ionic speciation is a significant part of the model, and aqueous reaction is strongly tied to changes in enthalpy. For this reason, the water model parameters in the RIV approach was regressed from density values and  $C_v$  values which require the water model to fit quantities derived from the differentiation of the Helmholtz energy with respect to both density and temperature.

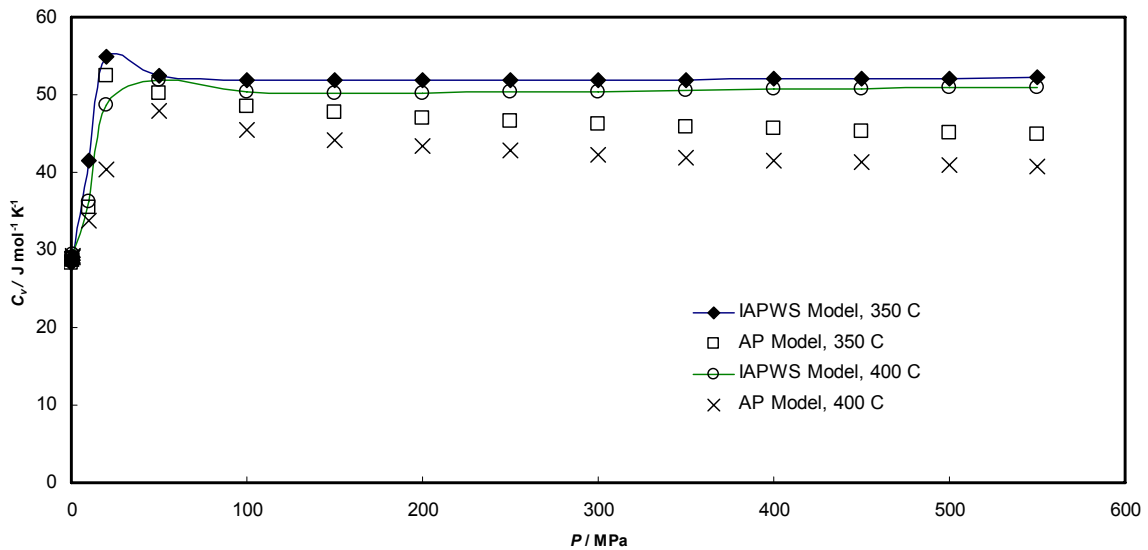


Figure 5: Pure water  $C_v$  predictions from both the AP model and the IAPWS model versus pressure.

The same functions used in the AP model for the perturbation term parameters were also chosen for this model. They are given as

$$\frac{a_{H_2O}}{Pa \cdot m^3 \cdot mol^{-1}} = a_{H_2O1} + \frac{a_{H_2O2}}{T_r} + \frac{a_{H_2O3}}{T_r^2} + \frac{a_{H_2O4}}{T_r^4} \quad (69)$$

$$c_{H_2O} = c_{H_2O1} + \frac{c_{H_2O2}}{T_r} + \frac{c_{H_2O3}}{T_r^2} + \frac{c_{H_2O4}}{T_r^4} \quad (70)$$

$$d_{H_2O} = d_{H_2O1} + \frac{d_{H_2O2}}{T_r} + \frac{d_{H_2O3}}{T_r^2} + \frac{d_{H_2O4}}{T_r^4} \quad (71)$$

where the reduced temperature value,  $T_r$ , is given by

$$T_r = T/T_c = T/647.067K. \quad (72)$$

The regressed values for the parameters in equations (69)-(71) are given in Table 3.

**Table 3: Regressed parameters for water in the perturbation term.**

<b>Parameters</b>	$a_{H_2O1}$ ,	$a_{H_2O2}$ ,	$a_{H_2O3}$ ,	$a_{H_2O4}$
<b>Values</b>	-0.137598,	0.7029259,	-0.2863362,	0.02026973
<b>Parameters</b>	$c_{H_2O1}$ ,	$c_{H_2O2}$ ,	$c_{H_2O3}$ ,	$c_{H_2O4}$
<b>Values</b>	-13.79992,	-0.9287413,	2.713971,	-0.361372
<b>Parameters</b>	$d_{H_2O1}$ ,	$d_{H_2O2}$ ,	$d_{H_2O3}$ ,	$d_{H_2O4}$
<b>Values</b>	9.182921,	11.89618,	-7.818237,	1.213452
<b>Parameters</b>	$e_{H_2O}$			
<b>Values</b>	-10.52253			

The van der Waals co-volume parameter,  $b$ , in the AP model is a constant. This, however, restricts the hard-sphere diameter to be constant. As has been noted by others<sup>124-128</sup>, the hard-sphere diameter should be allowed to change with temperature. Following the suggestion of Wilhelm<sup>127</sup>, the temperature dependence of the hard-sphere diameter as well as the NPMSA diameters is given by

$$\sigma_{NPMSA_i} = \sigma_{NPMSA1_i} + \sigma_{NPMSA2_i} (T - T_{ref}) \quad (73)$$

$$\sigma_{HS_i} = \sigma_{HS1_i} + \sigma_{HS2_i} (T - T_{ref}) \quad (74)$$

where  $\sigma_{NPMSA_i}$  is the hard-sphere diameter for species  $i$  (water in this case) for the NPMSA term,  $\sigma_{HS_i}$  is the hard-sphere diameter for the hard-sphere and perturbation terms, and  $T_{ref}$  is 573.15 K. The other values in equations (73) and (74) are given in Table 4.

**Table 4: Hard-sphere diameters in the water NPMSA and hard-sphere terms.**

<b>Parameters</b>	$\sigma_{NPMSA1}$ ,	$\sigma_{NPMSA2}$
<b>Values (angstroms)</b>	2.676105, 0.02009635 x10 <sup>-4</sup>	
<b>Parameters</b>	$\sigma_{HS1}$ ,	$\sigma_{HS2}$
<b>Values (angstroms)</b>	1.489643, 3.870141 x10 <sup>-4</sup>	

## **5.2 Application of the RIV Model to Aqueous NaCl and LiCl Solutions**

The parameters for the pure dipoles (NaCl, LiCl, KCl) and single ions (Na<sup>+</sup>, Li<sup>+</sup>, K<sup>+</sup>, and Cl<sup>-</sup>) in the model for aqueous solutions could not be determined separately since there

are no data available for single ions and because data for pure liquid NaCl are reported at much higher temperatures than those in this study. As a result, the pure parameters as well as the mixing parameters were regressed at the same time. These parameters were regressed from density and  $\Delta_{dil}H$  data.

Though the dipole moment of NaCl is known from gas-phase measurements, the value of the dipole moment in a solvating aqueous environment is likely to be different. Anderko and Pitzer allowed the dipole moment of NaCl to vary in the AP model<sup>1</sup> for this reason. The dipole moments of NaCl and LiCl were also allowed to vary during the model regression and are given in Table 5.

**Table 5: Dipole moments of NaCl and LiCl in the RIV model, AP Model, and from the literature.<sup>129</sup> The AP model has never been applied to LiCl solutions.**

Solute	RIV Value (D)	AP Value (D)	Literature Value (D)
NaCl	6.937	6.4	9.0443
LiCl	7.238	-	7.228

### 5.2.1 The Hard-Sphere Diameters

The hard-sphere diameters in the NPMSA term are independent from those used in the hard-sphere term and perturbation term. The functional form of the diameters is similar to that used for the water hard-sphere diameters but contains an extra term to increase accuracy. The term is given as

$$\sigma_{NPMSA_i} = \frac{\sigma_{NPMSA1_i} + \sigma_{NPMSA2_i} (T - T_{ref})}{1 + \sigma_{NPMSA3_i} (T - T_{ref})} \quad (75)$$

$$\sigma_{HS_i} = \frac{\sigma_{HS1_i} + \sigma_{HS2_i}(T - T_{ref})}{1 + \sigma_{HS3_i}(T - T_{ref})}. \quad (76)$$

The reference temperature,  $T_{ref}$ , is 623.15 K. The values for the parameters in equations (75) and (76) are given in Table 6 for NaCl solutions and in Table 7 for LiCl solutions.

**Table 6: Hard-sphere diameter function terms for the NaCl solution model.**

NaCl	Parameters	$\sigma_{NPMSA1}$ , $\sigma_{NPMSA2}$ , $\sigma_{NPMSA3}$
	Values (angstroms)	2.447379, -0.00635, -0.00963
NaCl	Parameters	$\sigma_{HS1}$ , $\sigma_{HS2}$ , $\sigma_{HS3}$
	Values (angstroms)	3.073261, 0.008138, -0.01346
Na <sup>+</sup>	Parameters	$\sigma_{NPMSA1}$ , $\sigma_{NPMSA2}$ , $\sigma_{NPMSA3}$
	Values (angstroms)	2.949513, -0.0108, 0.003968
Na <sup>+</sup>	Parameters	$\sigma_{HS1}$ , $\sigma_{HS2}$ , $\sigma_{HS3}$
	Values (angstroms)	4.061925, -0.00025, 0.003213
Cl <sup>-</sup>	Parameters	$\sigma_{NPMSA1}$ , $\sigma_{NPMSA2}$ , $\sigma_{NPMSA3}$
	Values (angstroms)	2.44611, -0.00978, -0.01478
Cl <sup>-</sup>	Parameters	$\sigma_{HS1}$ , $\sigma_{HS2}$ , $\sigma_{HS3}$
	Values (angstroms)	2.411284, -0.00086, -0.01526

**Table 7: Hard-sphere diameter function terms for the LiCl solution model.**

LiCl	Parameters	$\sigma_{NPMSA1}$ , $\sigma_{NPMSA2}$ , $\sigma_{NPMSA3}$
	Values (angstroms)	2.507244, -0.01216, -0.00745
LiCl	Parameters	$\sigma_{HS1}$ , $\sigma_{HS2}$ , $\sigma_{HS3}$
	Values (angstroms)	3.173677, 0.009411, -0.01527
Li <sup>+</sup>	Parameters	$\sigma_{NPMSA1}$ , $\sigma_{NPMSA2}$ , $\sigma_{NPMSA3}$
	Values (angstroms)	2.639198, -0.01618, -1.81 x 10 <sup>-05</sup>
Li <sup>+</sup>	Parameters	$\sigma_{HS1}$ , $\sigma_{HS2}$ , $\sigma_{HS3}$
	Values (angstroms)	4.71665, -0.00421, 0.005201
Cl <sup>-</sup>	Parameters	$\sigma_{NPMSA1}$ , $\sigma_{NPMSA2}$ , $\sigma_{NPMSA3}$
	Values (angstroms)	2.552215, -0.02271, -0.02409
Cl <sup>-</sup>	Parameters	$\sigma_{HS1}$ , $\sigma_{HS2}$ , $\sigma_{HS3}$
	Values (angstroms)	2.797408, 0.004144, -0.01157

## 5.2.2 The Perturbation Term Parameters

The functional forms for the empirical parameters in the perturbation term are identical to those in the perturbation term of the AP model. The pure dipole expressions are given below:

$$\frac{a}{Pa \cdot m^3 \cdot mol^{-1}} = a_1 + a_2 \exp[a_3(\theta - a_4)^2] - \exp[a_5(\theta - a_6)^{a_7}] \quad (77)$$

where  $\theta = T/100K$ . The parameters for NaCl are given in Table 8, and the parameters of LiCl are given in Table 9.

**Table 8: Pure NaCl parameter values.**

<b>Parameters</b>	$a_1,$	$a_2,$	$a_3,$	$a_4,$	$a_5,$	$a_6,$	$a_7$
<b>Values</b>	1.399069,	0.541709,	-0.47846,	-8.7667,	-0.70261,	-4.07533,	3.330227
<b>Parameters</b>			$c,$	$d,$	$e$		
<b>Values</b>			-1.95688,	7.291765,	-8.78801		

**Table 9: Pure LiCl parameter values.**

<b>Parameters</b>	$a_1,$	$a_2,$	$a_3,$	$a_4,$	$a_5,$	$a_6,$	$a_7$
<b>Values</b>	1.477184,	0.548648,	-0.46897,	-8.93819,	-0.78225,	-4.00911,	3.026675
<b>Parameters</b>			$c,$	$d,$	$e$		
<b>Values</b>			-1.96705,	9.807349,	-8.35237		

The mixing term equations are given below:

$$q = 0.1(\theta + q_{\text{var}}) \quad (78)$$

$$\tau = [\tau_1 + \tau_2 \exp[\tau_3(\theta + \tau_4)^{\tau_5}] \llbracket 1 + \tau_6 q + \tau_7 q^2 + \tau_8 q^3 + \tau_9 q^4 \rrbracket] \quad (79)$$

$$\alpha_{12} = \tau [\alpha_1 + \alpha_2 \theta + \alpha_3 \theta^2 + \alpha_4 \theta^3 + \alpha_5 \exp[\alpha_6(\theta + \alpha_7)^2]] \quad (80)$$

$$\gamma_{112} = \tau [\gamma_1 + \gamma_2(\theta + \gamma_3) + \gamma_4 \exp[\gamma_5(\theta + \gamma_6)^2]] \quad (81)$$

$$\gamma_{122} = \tau [\gamma_7 + \gamma_8 \theta + \gamma_9 \exp[\gamma_{10}(\theta + \gamma_{11})^8]] \quad (82)$$

$$\delta_{1112} = \tau [\delta_1 + \delta_2 \exp[\delta_3(\theta + \delta_4)^2]] \quad (83)$$

$$\delta_{1222} = \delta_5 \tau \quad (84)$$

$$\delta_{1122} = \delta_6 \tau \quad (85)$$

where the parameters for NaCl and LiCl are the same and are given in Table 10.

**Table 10: Mixing parameter values for NaCl and LiCl solutions.**

<b>Parameters</b>	$q_{\text{var}}$						
<b>Values</b>	-6.31649						
<b>Parameters</b>	$\tau_1,$	$\tau_2,$	$\tau_3,$	$\tau_4,$	$\tau_5,$	$\tau_6,$	$\tau_7$
<b>Values</b>	0.108246, 5.979269, -0.96106, -5.57296, 0.784699, 5.85684, -25.475						
<b>Parameters</b>	$\tau_8,$		$\tau_9$				
<b>Values</b>	127.5764, -132.591						
<b>Parameters</b>	$\alpha_1,$	$\alpha_2,$	$\alpha_3,$	$\alpha_4,$	$\alpha_5,$	$\alpha_6,$	$\alpha_7$
<b>Values</b>	-3.22274, 1.214036, -0.12127, 0.00996, 0.523238, -1.46802, -5.26022						
<b>Parameters</b>	$\gamma_1,$	$\gamma_2,$	$\gamma_3,$	$\gamma_4,$	$\gamma_5,$	$\gamma_6$	
<b>Values</b>	1.887113, 0.067941, -8.88195, 0.194301, -1.77404, -5.26081						
<b>Parameters</b>	$\gamma_7,$		$\gamma_8,$	$\gamma_9,$	$\gamma_{10},$	$\gamma_{11}$	
<b>Values</b>	0.832392, 0.143657, 0.227286, -0.00028, -0.53278						
<b>Parameters</b>	$\delta_1,$	$\delta_2,$	$\delta_3,$	$\delta_4,$	$\delta_5,$	$\delta_6$	
<b>Values</b>	1.257833, 0.086374, -1.84043, -5.33814, 1.37248, 1.607898						
<b>Parameters</b>	$\varepsilon$						
<b>Values</b>	1.09032						

### 5.2.3 Water Ligand Term Parameters

The values for the  $A_{lig^*}$  parameter for the aqueous NaCl and LiCl solutions are given in Table 11.

Table 11: The values for  $A_{lig^*}$  for the aqueous NaCl and LiCl solutions.

Solute	$A_{lig^*}$ (J/mol)
NaCl	$-5. \times 10^{-6}$
LiCl	$-1. \times 10^{-5}$

### 5.3 The Ideal Gas Term

The ideal gas contribution for  $Z$  is equal to 1 and is included in the  $Z_{HS}$  term implicitly.

The ideal gas term for the  $A_{IG}$  and the molar ideal gas internal energy,  $U_{IG}$ , may be calculated for a pure component by

$$A_{IG} = A_o + \int_{T_o}^T C_p^{IG} dT - T \int_{T_o}^T \frac{C_p^{IG}}{T} dT + RT \ln \left( \frac{TV_o}{T_oV} \right) - RT(T - T_o) + S_o(T_o - T) \quad (86)$$

$$U_{IG} = U_o + \int_{T_o}^T C_p^{IG} dT - R(T - T_o) \quad (87)$$

where the <sub>o</sub> subscript indicates that the property is evaluated at a standard state temperature and molar volume ( $T_o$ ,  $V_o$ ), and  $C_p^{IG}$  is the ideal gas constant pressure heat capacity. The reference state used for the ideal gas calculations involved in the development of the model is 273.15 K and 1.0 m<sup>3</sup>/mol. The mixture ideal gas term for molar Helmholtz energy and molar

internal energy,  $A_{IGmix}$  and  $U_{IGmix}$ , respectively, may be calculated from the pure components by

$$A_{IGmix} = \sum_i^N x_i A_{IGi} + RT \sum_{i=1}^n x_i \ln x_i \quad (88)$$

$$U_{IGmix} = \sum_i^N x_i U_{IGi} \quad (89)$$

The standard state Helmholtz energy, entropy, and internal energy for the pure species were determined by density functional (DFT) calculations using the b3lyp/6-311+g(3df,2p) model chemistry in Gaussian<sup>130</sup>. The values used are reported in Table 12. All standard state Helmholtz energies and internal energies are relative to the pure elements at their standard state.

**Table 12: Ideal Gas Standard State values (273.15 K, 1 m<sup>3</sup>/mol) from DFT calculations.**

<b>H<sub>2</sub>O</b>	<b>Parameters</b>	$A_o$ (J/mol),	$S_o$ (J/mol-K),	$U_o$ (J/mol)
	<b>Values</b>	$-1.17202 \times 10^6$ ,	217.2586,	$-1.11267 \times 10^6$
<b>NaCl</b>	<b>Parameters</b>	$A_o$ (J/mol),	$S_o$ (J/mol-K),	$U_o$ (J/mol)
	<b>Values</b>	$-4.51348 \times 10^5$ ,	258.0657,	$-3.80857 \times 10^5$
<b>Na<sup>+</sup></b>	<b>Parameters</b>	$A_o$ (J/mol),	$S_o$ (J/mol-K),	$U_o$ (J/mol)
	<b>Values</b>	$4.779248 \times 10^5$ ,	177.6041,	$5.26437 \times 10^5$
<b>Cl<sup>-</sup></b>	<b>Parameters</b>	$A_o$ (J/mol),	$S_o$ (J/mol-K),	$U_o$ (J/mol)
	<b>Values</b>	$-4.01868 \times 10^5$ ,	183.0092,	$-3.51879 \times 10^5$
<b>LiCl</b>	<b>Parameters</b>	$A_o$ (J/mol),	$S_o$ (J/mol-K),	$U_o$ (J/mol)
	<b>Values</b>	$-5.14728 \times 10^5$ ,	241.3579,	$-4.48801 \times 10^5$
<b>Li<sup>+</sup></b>	<b>Parameters</b>	$A_o$ (J/mol),	$S_o$ (J/mol-K),	$U_o$ (J/mol)
	<b>Values</b>	$5.00918 \times 10^5$ ,	162.6690,	$5.45352 \times 10^5$

The  $C_p^{IG}$  values for the  $\text{Na}^+$ ,  $\text{K}^+$ ,  $\text{Li}^+$ , and  $\text{Cl}^-$  are invariant with respect to temperature and are shown by theory to be  $5/2 R$  or approximately 20.786 J/mol-K. The  $C_p^{IG}$  values for the non-ionic pure components are calculated from a correlation used by DIPPR<sup>131</sup>. The correlation is given by

$$C_p^{IG} = a_{CP} + b_{CP} \left( \frac{c_{CP}/T}{\sinh(c_{CP}/T)} \right)^2 + d_{CP} \left( \frac{e_{CP}/T}{\cosh(e_{CP}/T)} \right)^2 \quad (90)$$

where  $a_{CP}$ ,  $b_{CP}$ ,  $c_{CP}$ ,  $d_{CP}$ , and  $e_{CP}$  are substance-specific parameters. The values of those parameters for  $\text{H}_2\text{O}$  and  $\text{NaCl}$  are reported by DIPPR<sup>131</sup>. For  $\text{LiCl}$ , the parameters were fitted to  $C_p^{IG}$  values from DFT calculations, again with the b3lyp/6-311+g(3df,2p) model chemistry, at a variety of temperatures as shown in Figure 6. The differences between model predictions and the DFT values for  $C_p^{IG}$  in this regression were found to range between  $5.85 \times 10^{-4} \%$  and  $6.96 \times 10^{-2} \%$  which is sufficient for the present application. The fit parameters are found in Table 13 and yield  $C_p^{IG}$  in J/(kmol-K).

**Table 13: Parameters for ideal gas  $C_p$  model for LiCl**

Parameters	$a_{CP}$ ,	$b_{CP}$ ,	$c_{CP}$ ,	$d_{CP}$ ,	$e_{CP}$
Values	29079.9017,	8320.3823,	872.9265,	7782.1883,	446.7259

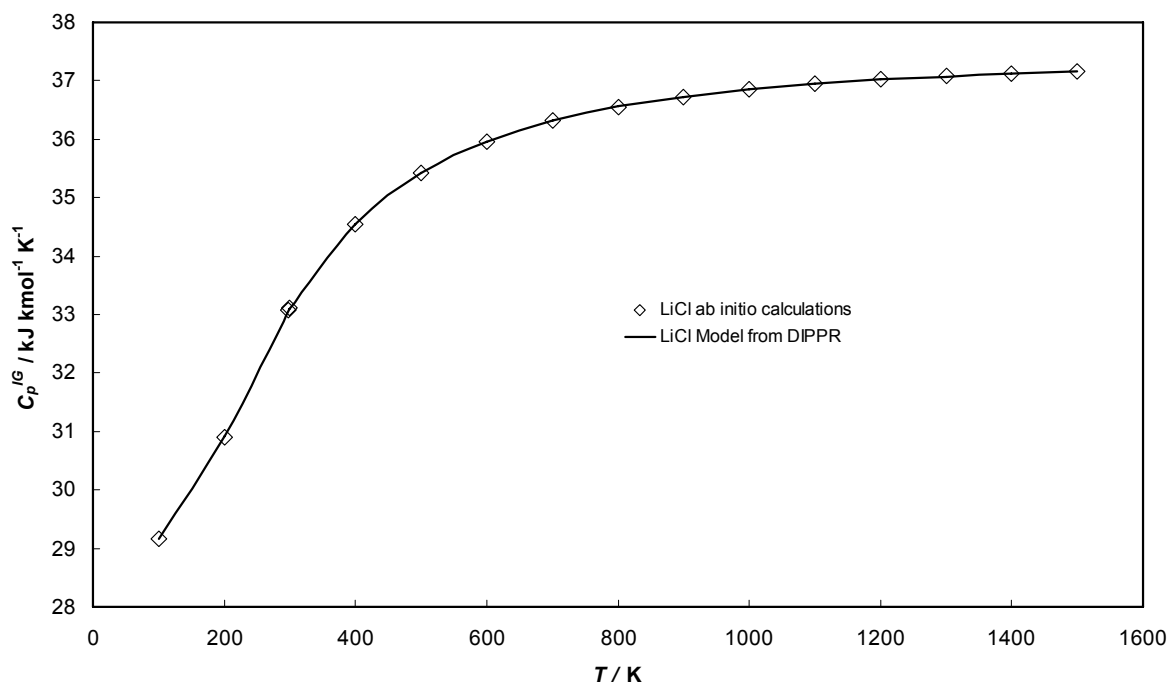


**Figure 6: Plot of LiCl  $C_p^{IG}$  versus temperature as predicted from DFT calculations and the DIPPR correlation (Equation 90).**



## 6 Model Results and Discussion

The results obtained from the RIV model will be discussed in this chapter. First, results from the application of the model to pure water will be discussed. The results for the application to NaCl and LiCl solutions will then be discussed.

### 6.1 *The Water Model*

The AP water model parameters were regressed from  $\rho$  values and vapor pressures. In developing the water portion of the RIV model, it was desirable to regress the parameters from property data related to changes in enthalpy because aqueous reactions in solution are closely tied to these changes. The water model, therefore, was regressed from  $C_v$  data as well as densities. Because the water model regression included  $C_v$  values with no additional parameters, the accuracy in density predictions is poorer than that of the AP model. The  $C_v$  predictions, however, are improved. The average difference between calculated values of density from the model and experimental values for the AP model is 0.72%, and the average difference for the RIV model is 4.72%. The average difference in  $C_v$  predictions versus experiment for the AP model is 21.82%, and the average difference in  $C_v$  predictions for the RIV model is 5.34%. The ranges in which the AP and present models are compared are 100 to 1000 °C and pressures up to 5 kbar which are close to the ranges used in regressing the AP model (99.85 °C to 926.85).

The increased accuracy in  $C_v$  predictions from the RIV model is gained at the expense of decreased accuracy in density predictions. This trade-off was deemed worthwhile, however, because accurate  $C_v$  predictions help to ensure the RIV model behaves properly with respect to changes in temperature. This behavior with respect to changes in temperature is important for modeling aqueous reactions since these reactions involve large enthalpy changes.

Interestingly, the vapor pressure predictions in the RIV model are not much less accurate than predictions from the AP model even though vapor pressure values were not used in regressing the parameters. As shown in Figure 7, while the AP model follows the IAPWS model trend better, the RIV model is not unreasonable in its predictions as indicated by the respective  $R^2$  values for the predictions. The  $R^2$  value for the RIV model fit is 0.995 whereas the  $R^2$  value for the AP model fit is 1.000.

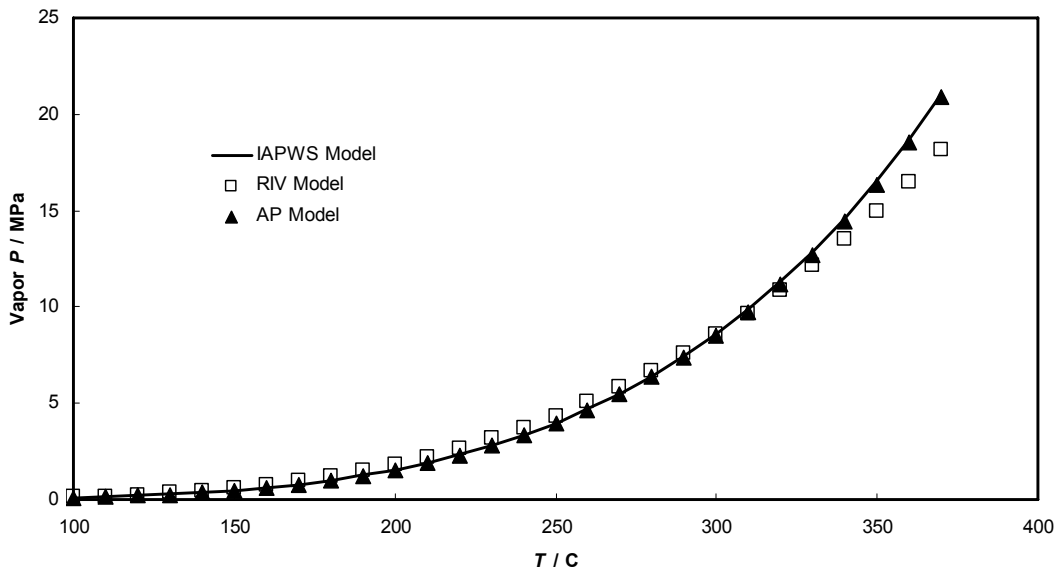


**Figure 7: Plot of vapor pressure versus temperature. Vapor pressure predictions from the AP and RIV models are compared with IAPWS model<sup>6</sup> predictions. The AP model predictions are closer to IAPWS model values, but RIV model predictions are reasonable.**

## 6.2 The NaCl Solution and LiCl Solution Models

The solution model parameters were regressed from molar volume and  $\Delta_{dil}H$  data. First, the molar volume results for both solutions will be discussed. Next, the  $\Delta_{dil}H$  results for both solutions will be discussed. The RIV model fit will be compared to the AP model fit for NaCl for both molar volume and  $\Delta_{dil}H$  data. Next, the trends in the RIV model for the fraction dissociated of the solute as a function of solute concentration will be discussed. Finally, predictions for the log  $K$  of the aqueous reaction will be discussed.

In the AP model, the solute is assumed to be fully associated in solution. In the RIV model, this assumption is relaxed allowing a more realistic model. In relaxing this assumption, however, there are no more regressible parameters included in the RIV model than in the AP model. Thus, one cannot explain a difference in the quality of the fit simply on the basis of a larger or smaller number of regressible parameters.

### 6.2.1 Results for Molar Volume

In Figure 8 and in Figure 9, the RIV model predictions of molar volume for the NaCl solutions and the LiCl solutions, respectively, are compared to the literature molar volumes. The AP model molar volume predictions for NaCl solutions are also shown. Overall, the average difference in calculated and experimental molar volumes for the AP model is 3.51% for the NaCl solution within a temperature range of 350 ° to 400 °C. The average difference for the RIV model calculated values of molar volume is 6.66% for the NaCl solution in the same range. The average difference for the RIII model calculated values of molar volume is 1.34% for the NaCl solution in the same range. The average difference for the RIV model

for molar volume is 10.90% for the LiCl solution. The AP model and the RIV model have never been applied to LiCl solutions.

A random selection of 10% of the experimental data was not used in the regression for the NaCl and the LiCl models. The difference between predicted molar volume and literature values of molar volume, on average, for the withheld NaCl data is 7.84%, and the average difference for the withheld LiCl data is 11.07%. These differences are displayed graphically in Figure 10 and in Figure 11. The average difference between the model predictions and the withheld sections of data corresponds well with the difference between the model predictions compared to data used in the regression.

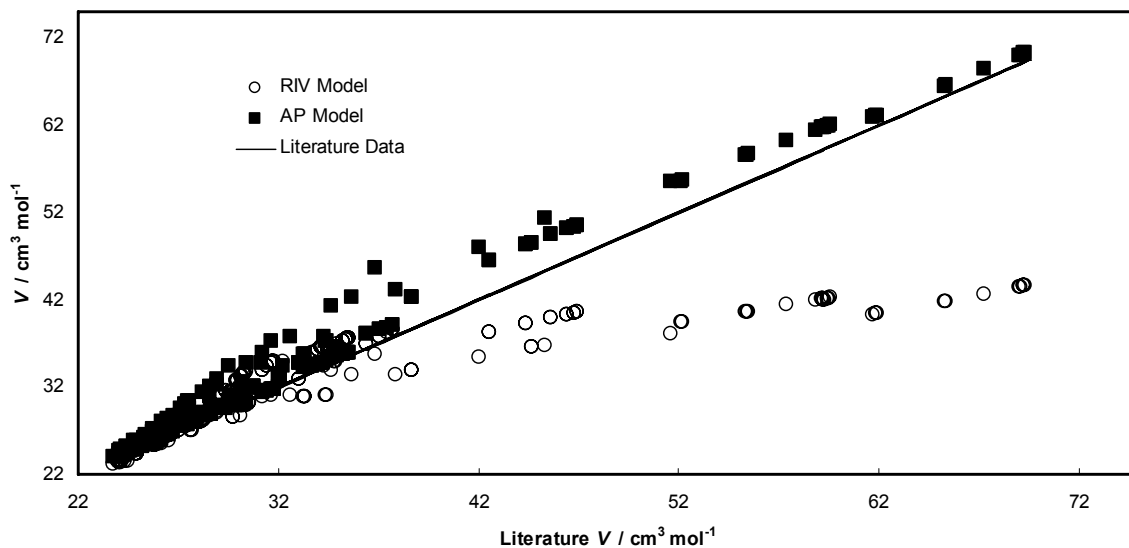


**Figure 8:** Plot of calculated molar volumes versus literature values of molar volume. Calculated values of molar volume of NaCl solutions from the RIV model and the AP model are compared to literature values.

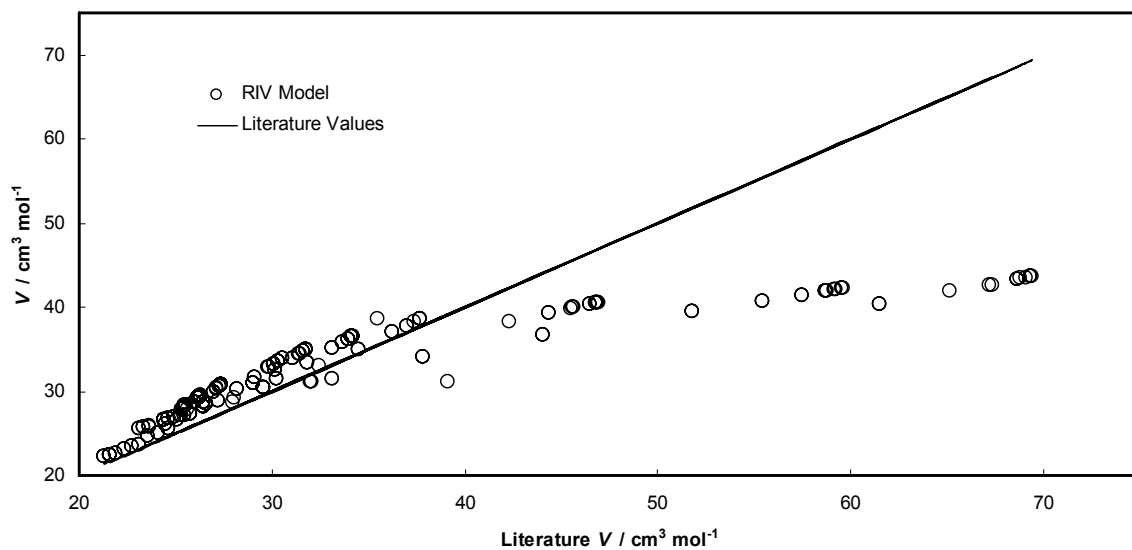


**Figure 9:** Plot of calculated molar volumes from the RIV model versus literature values of molar volume. Calculated values of the molar volume of LiCl solutions from the RIV model are compared to literature values.

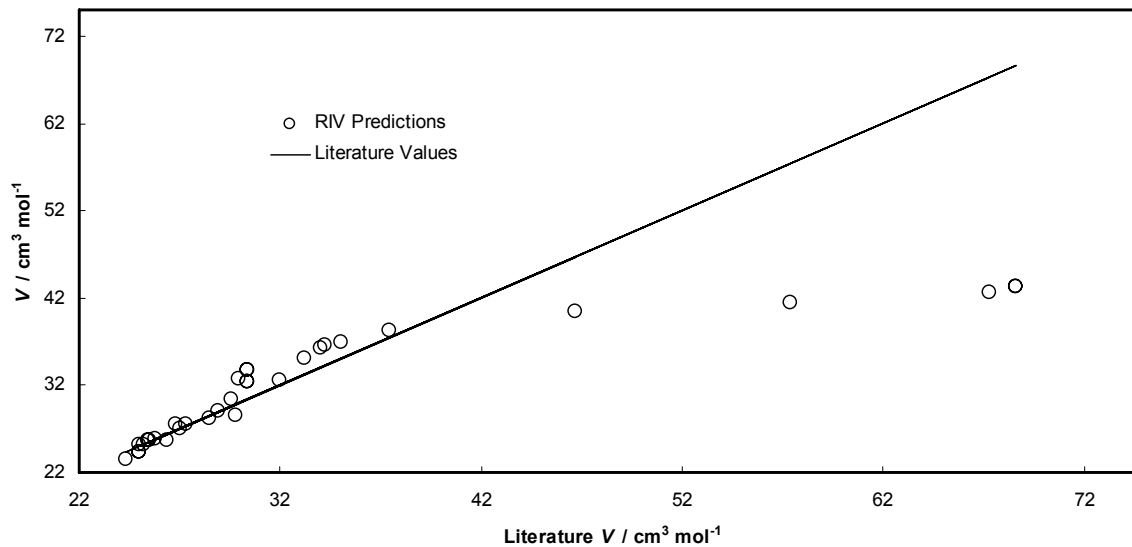


**Figure 10:** Plot of molar volume versus literature values of molar volume. Predictions from the RIV model for NaCl solution molar volume are compared to literature values that were not used to regress model parameters. Agreement between model predictions and literature values are similar to those in Figure 8.

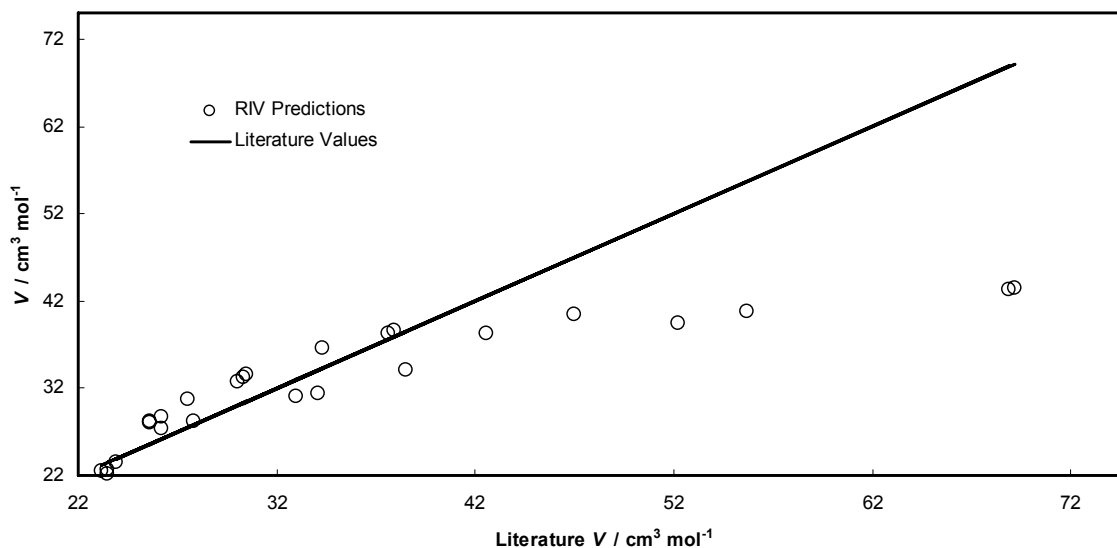


**Figure 11: Plot of molar volumes versus literature values of molar volume. Predictions from the RIV model for LiCl solution molar volume are compared to literature values that were not used to regress model parameters. Agreement between model predictions and literature values are similar to those in Figure 9.**

From Figure 8 and Figure 9, it is apparent that the RIV model can be used to more accurately reproduce experimental data at lower molar volumes than at higher molar volumes for both the NaCl solution and the LiCl solution. In fact, the accuracy of the RIV model appears to be greater than the accuracy of the AP model at lower molar volumes for the NaCl solution. Conversely, the accuracy of the RIV model is much poorer than the accuracy of the AP model at higher molar volumes.

One possible reason that the RIV model is more accurate at lower molar volumes is that there are many more data at lower molar volumes. As a result, the average difference between model predictions and experiment can be lowered more by improving the fit at lower molar volumes than at high molar volumes. Thus, this disparity in accuracy between the two molar volume regions may simply be a result of the method by which the model parameters were regressed.

Additionally, one reason posed<sup>1</sup> for not using an MSA term for the dipolar contribution in the AP model is that the MSA term is less accurate at lower molar volumes. There are two notable observations from this point. First, the NPMSA term can apparently function well enough at lower molar volumes indicating that the MSA dipole term is perhaps not a significant problem.

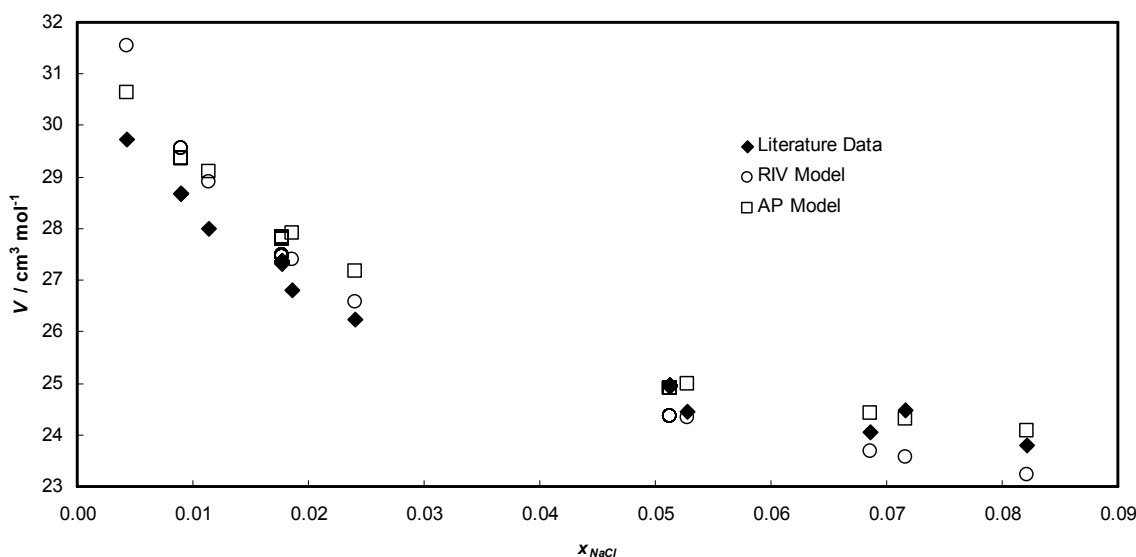


**Figure 12:** Plot of molar volumes versus mole fraction of NaCl as predicted using the AP model and the RIV model compared with literature molar volumes at 350 °C and pressure between 13.5 and 16.8 MPa.

Second, it is possible that the NPMSA is significantly less accurate at lower molar volumes. If this were true, the larger concentration of data at lower molar volumes would perhaps have forced a good fit at low molar volumes at the expense of a poor fit at high molar volumes. If the NPMSA were accurate at lower molar volumes, then perhaps fitting the data at lower molar volumes would have led to a good fit at high molar volumes as well.

Predicted molar volumes as a function of the concentration of NaCl or LiCl are compared with experimental molar volumes in Figure 12 and Figure 13, respectively. In

these cases, the molar volumes for the NaCl solution are within the range where the average difference between model predictions and experiment is low, while some of the molar volumes for the LiCl solution come from the region where the average difference for molar volumes is quite high. For both solutions, the trend with respect to the  $x$  of the solute appears to follow the data well except at lower concentrations where the molar volume is also larger.

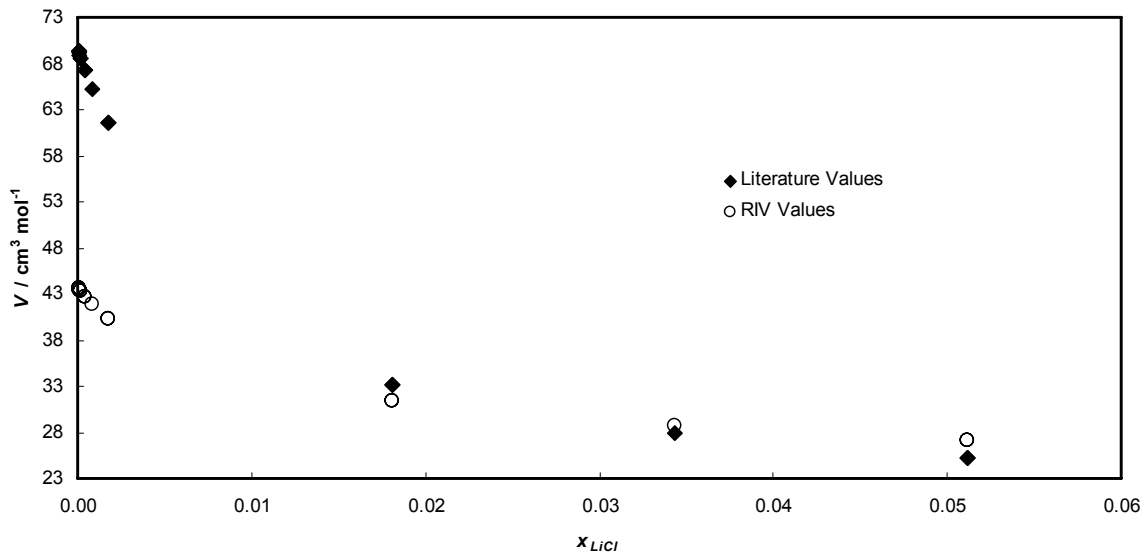


**Figure 13: Plot of molar volumes versus mole fraction of LiCl. Results from the RIV model are compared to literature values for the LiCl solution at 400 °C and 28 MPa.**

Indeed, as shown in Figure 14, the difference between calculated values and experimental values is more significant for both the AP model and the RIV model at lower concentrations. The difference at very low concentrations is more significant for the RIV model whereas the AP model has a more gradual increase in the difference between model and experiment as the concentration of NaCl decreases.

The increase in the discrepancy between model predictions and experiment at lower concentrations may be attributed to the change in the critical point for a solution as the solute

concentration changes. The addition of a solute, such as NaCl or LiCl, will dramatically increase the critical temperature and the critical pressure of a solution. As the solute concentration goes to zero, therefore, the solution will behave more like a near-critical fluid. Neither the AP model nor the RIV model may be used to give a qualitatively correct prediction near the critical point because they are of classical form in regard to critical point behavior. Thus, it is reasonable to suppose that the difference between model predictions and experiment would increase for smaller concentrations of solute where the critical point of the solution is close to that of pure water.

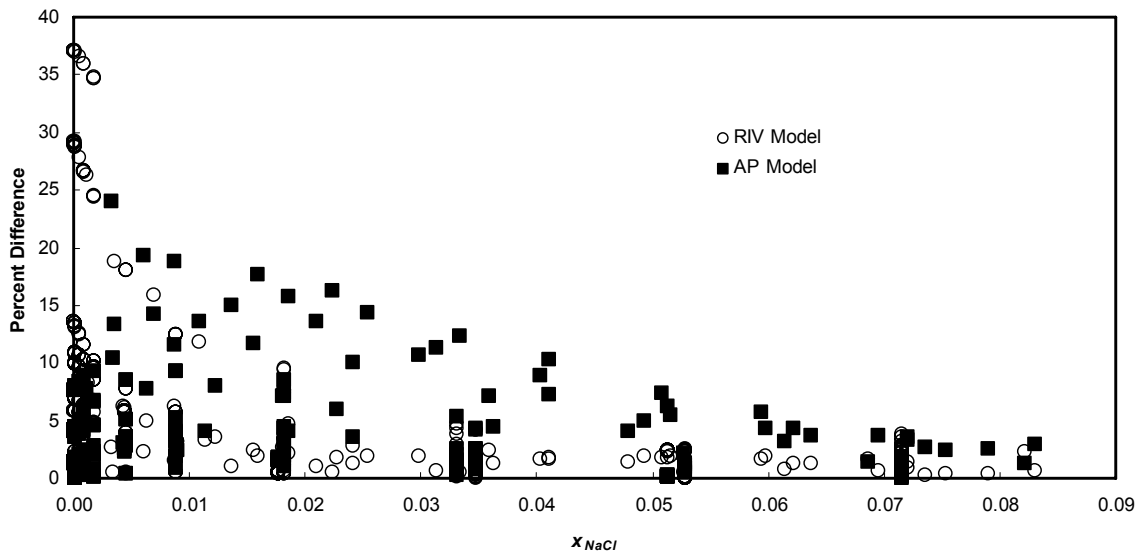


**Figure 14: Plot of the percent difference between experimental values and model values of molar volume versus mole fraction of NaCl. The percent differences for both the AP model and the RIV model are shown.**

It is also possible that the model for pure water is not sufficiently accurate, and solutions that have a low concentration of solute would not be well modeled using the AP or RIV models as a result.

A final possible explanation for the increase in difference between model predictions and experiment with a decrease in solute concentration lies with the aqueous reaction. As solute concentration decreases, a larger fraction of the associated solute will dissociate to form ions. Thus, aqueous reaction plays a larger role in dilute solutions. Since the AP model does not include dissociation, it is reasonable to suppose that the AP model would be less accurate when the solute concentration is low. The fraction dissociated of the solute predicted using the RIV model is likely lower than the true value leading to some discrepancy for the RIV model predictions as well. Solute dissociation, however, has a much more pronounced effect on  $\Delta_{dil}H$  predictions than on molar volume predictions.

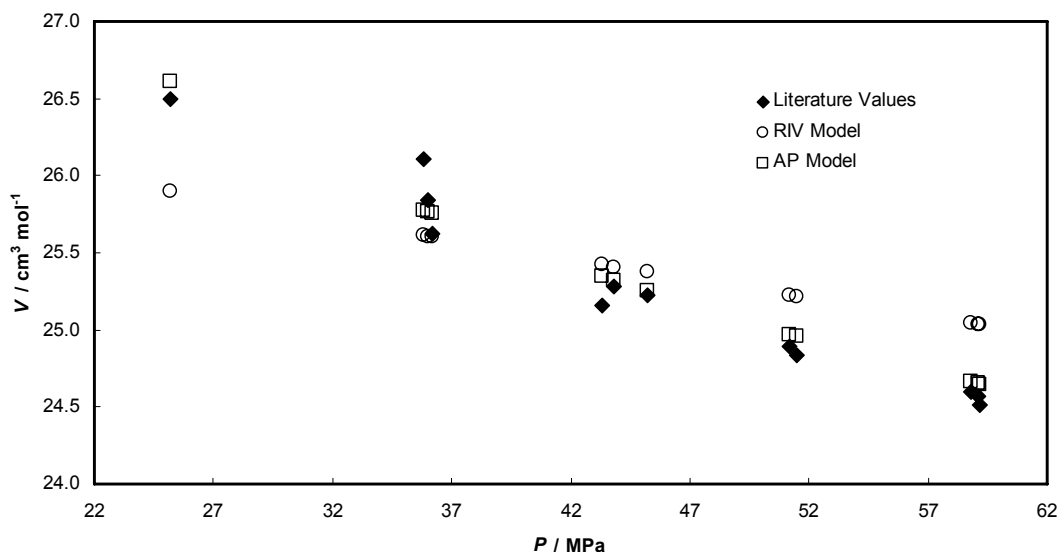


**Figure 15: Plot of molar volumes for the NaCl solution at 400 °C and  $7.16 \times 10^{-2}$  mole fraction of NaCl versus pressure. Predictions from the RIV model and AP model are compared to literature values.**

The trend for molar volumes as a function of pressure is shown for NaCl solutions and LiCl solutions in Figure 15 and in Figure 16, respectively. For the LiCl solution, the difference between predicted values and experimental values seems to be constant with

respect to pressure. For the NaCl solution, however, the discrepancy between predicted values and experimental values is not constant with respect to pressure.

The percent difference between predicted values and literature values for molar volume as a function of pressure is examined in Figure 17. Both the AP model and the RIV model evidence trends in the percent difference with respect to pressure. The difference distribution for both models is somewhat bell-shaped. In the AP model, the peak comes at 23.2 MPa which is close to the critical pressure (22.0640 MPa). In the RIV model, the peak comes at 28 MPa.

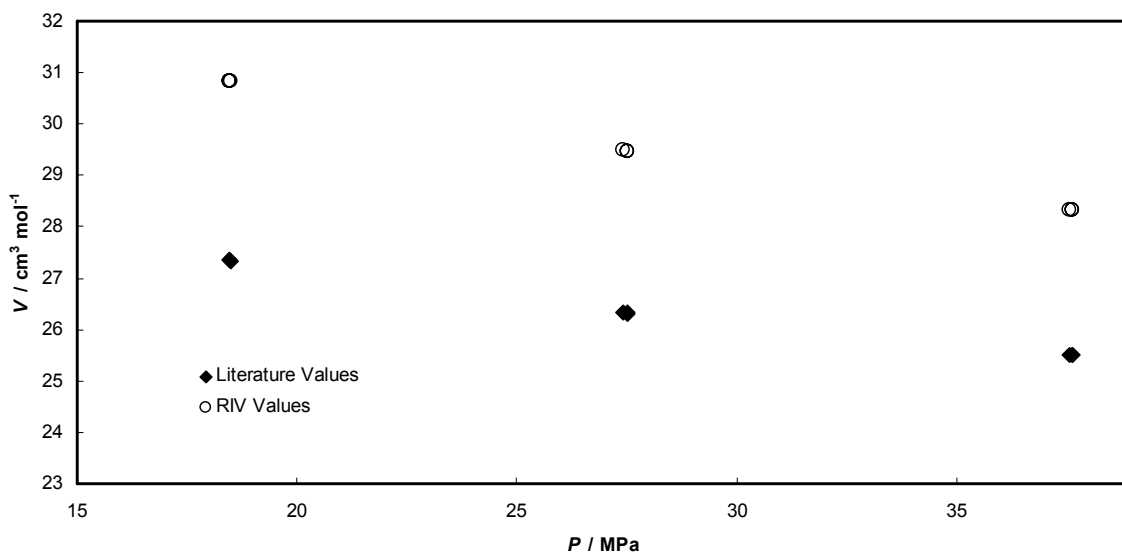


**Figure 16: Plot of molar volumes versus pressure for the LiCl solutions at 604 K and  $8.66 \times 10^{-5}$  mole fraction LiCl. Literature values are compared with RIV predictions.**

It seems likely that both trends in the percent difference are related to critical point phenomena. Neither the AP model nor the RIV model is capable of modeling the critical point exactly and are likely to diverge from experiment near the critical point of the solution.

The critical point of a NaCl solution is different from the critical point of pure water. In the AP model, all the NaCl is assumed to be associated which makes the solution more similar to pure water than the partially associated solution described in the RIV model. As a result, the critical point may not rise as quickly with the addition of NaCl to pure water in the AP model as in the RIV model. This would account for the shift in the peak discrepancy from 23 MPa in the AP model to 28 MPa in the RIV model.

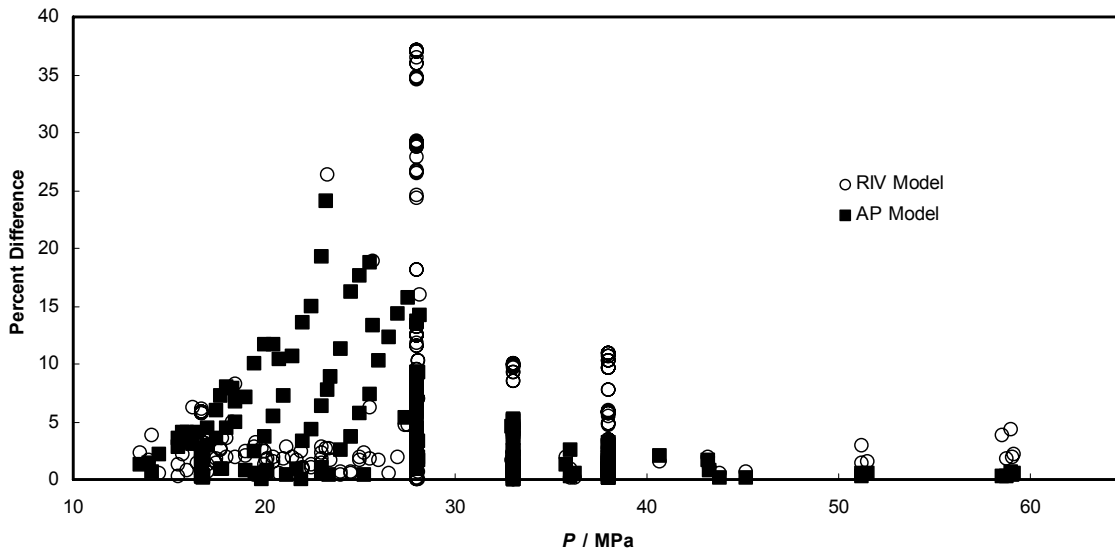


**Figure 17:** Plot of the percent difference between model predictions and literature values of molar volume for NaCl solutions as a function of pressure. The percent differences for both the RIV and the AP models are shown.

As seen in Figure 18 and in Figure 19, volume predictions from use of the RIV model generally diverge more strongly from experiment at higher temperatures. As shown in Figure 20, this is different from the AP model which has a peak in the percent difference around 380 °C and then has decreasing error as temperature increases. The peak at 380 °C is close to the critical temperature at 374 °C and can possibly be attributed to the difficulty of

modeling solutions near the critical point. It is possible that the increase in the error for the RIV model can be attributed to critical phenomena as well since it would likely predict a critical point at a higher temperature.

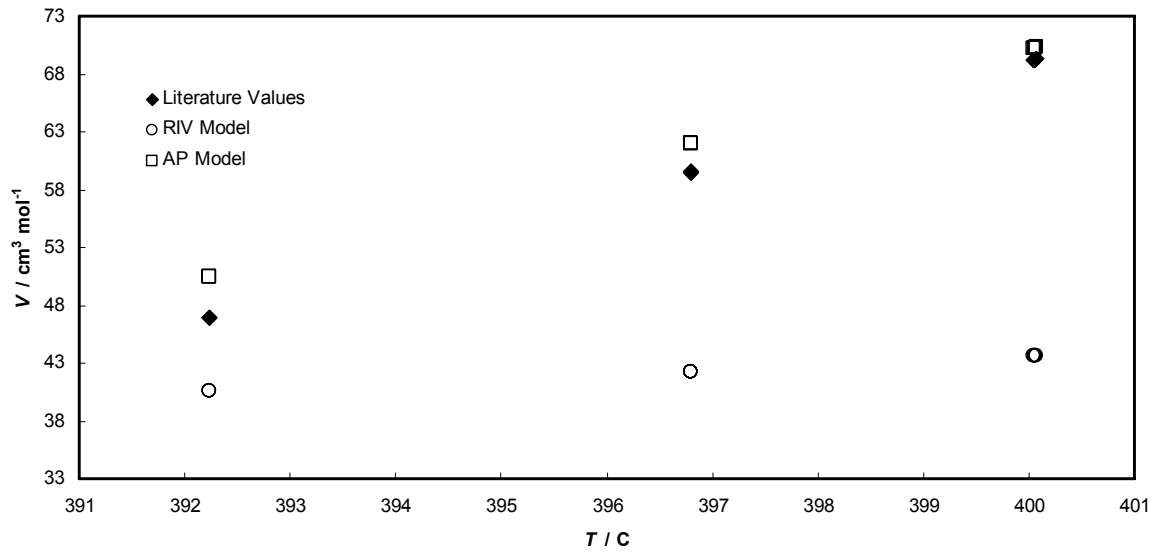


**Figure 18:** Plot of molar volumes versus temperature at 28 MPa and  $4.51 \times 10^{-5}$  mole fraction NaCl. The RIV model predictions and the AP model predictions are compared to literature values.

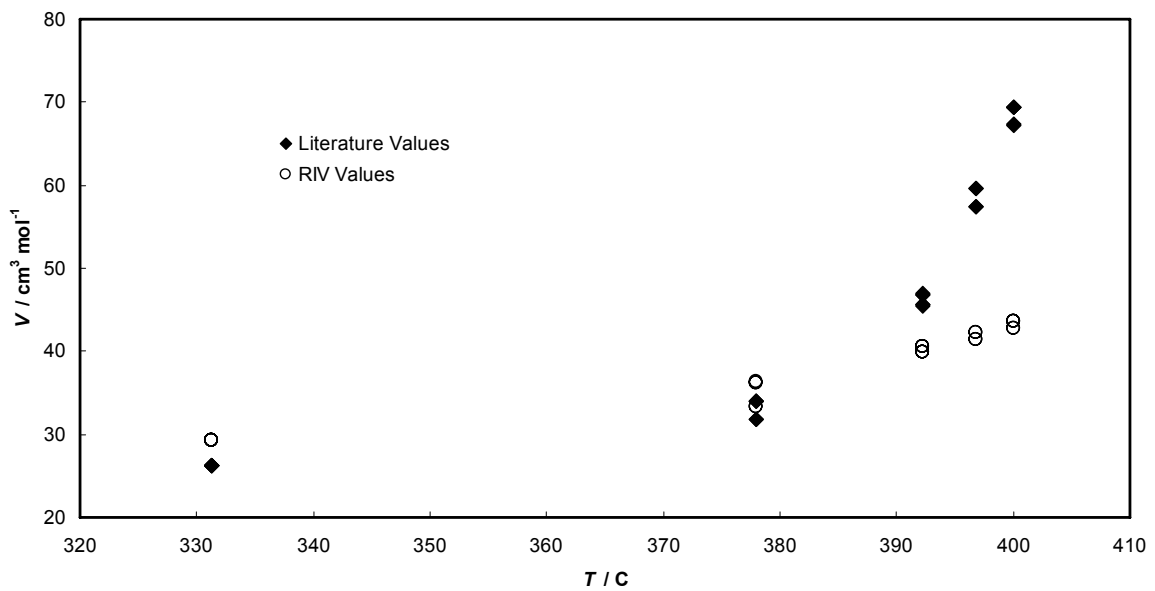


**Figure 19:** Plot of molar volumes of LiCl solutions at 28 MPa and  $4.44 \times 10^{-4}$  mole fraction LiCl as a function of temperature. The RIV model predictions are compared to literature values.

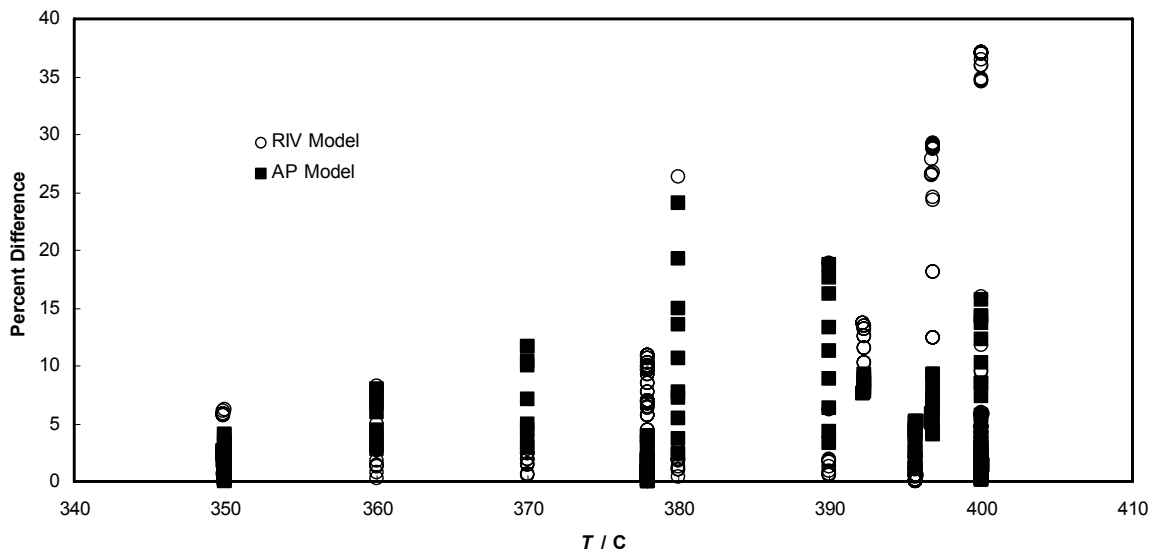


**Figure 20: Plot of the percent difference between model predictions and literature values of molar volume versus temperature. The percent differences for both the RIV and the AP models are shown.**

To summarize the molar volume results, the RIV model is overall less accurate than the AP model for molar volume predictions. The inaccuracy is greatest at larger molar volumes. In fact, the RIV model predictions are closer to the literature values than the AP model predictions at lower molar volumes. While many possible reasons for this have been discussed and all may play a part in the decrease in accuracy compared to the AP model, there are two points that seem most significant:

- 1) There are no more regressible parameters in the RIV model than in the AP model (which was not fit to  $\Delta_{dil}H$  data), yet the RIV model has been fit to both molar volume and  $\Delta_{dil}H$  data. An increase in the accuracy of the  $\Delta_{dil}H$  predictions is likely to correspond to a decrease in the accuracy of the molar volume predictions.

2) The water model is probably not accurate enough and leads to greater error. Many of the other possible causes of error may be connect to the water model.

### 6.2.2 Results for $\Delta_{dil}H$

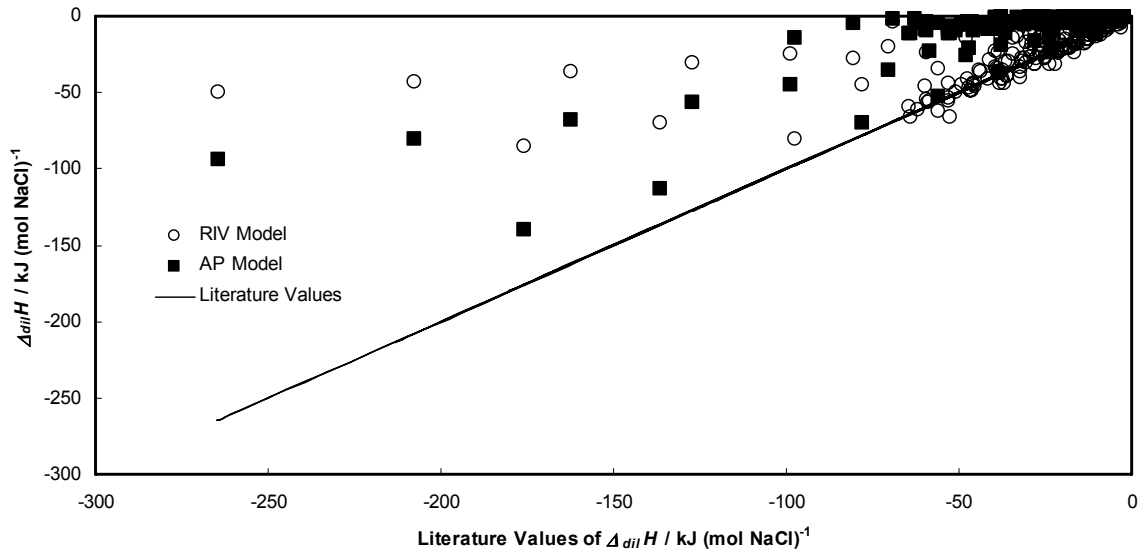


**Figure 21:** Plot of  $\Delta_{dil}H$  values versus literature values of  $\Delta_{dil}H$ . Predictions from the AP model and the RIV model for the NaCl solution are compared to literature values.

In Figure 21, the fit of the RIV model is compared to the fit of the AP model versus experimental data for the NaCl solutions. The experimental  $\Delta_{dil}H$  values collected as part of this study are included in this plot. The RIV model can be used to predict  $\Delta_{dil}H$  values with greater accuracy than those predictions generated using the AP model. The average difference between  $\Delta_{dil}H$  predictions from the RIV model and literature values is 25.16% for NaCl solutions. The average difference between predictions from the AP model and literature values is 78.78%. The average difference between predictions from the RIII model

and literature values is 22.03%. The average difference between predictions from the RIV model and literature values is 5.49% for LiCl solutions. These average differences were determined with each individual difference weighted equally. Again, the AP model and the RIV model have not been applied to LiCl solutions. The values predicted by the RIV model in Figure 21 that are less accurate than those predicted by the AP model are in extremely dilute solutions where measurements are far less accurate as well as where inaccuracies in the calculation of the NaCl dissociation have the greatest effect.

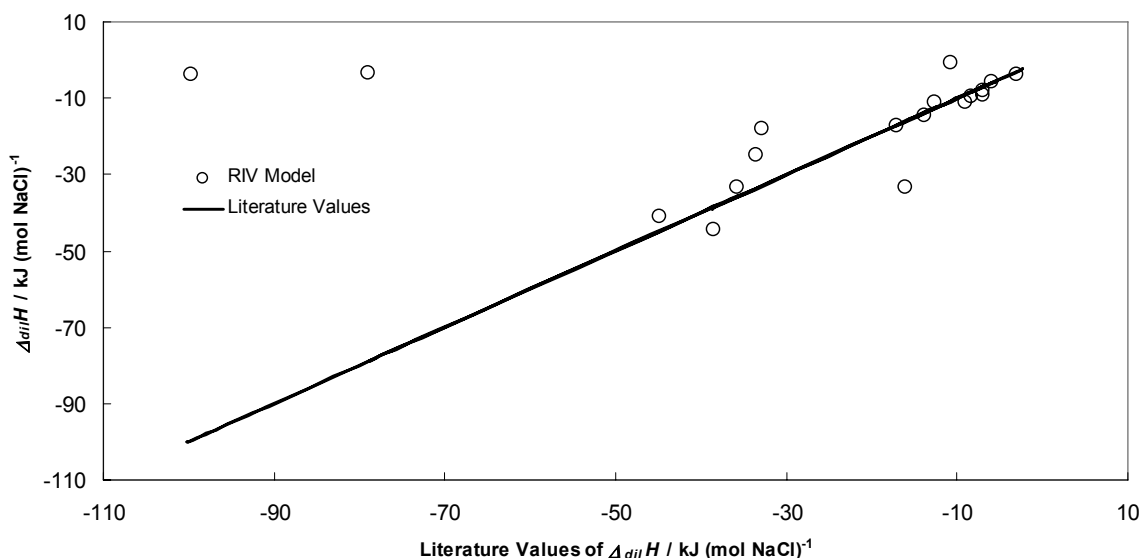


**Figure 22: Plot of  $\Delta_{dil}H$  values versus literature values of  $\Delta_{dil}H$  for NaCl solutions. RIV model predictions are compared to literature values that were not used to regress model parameters. Generally, the agreement between literature values and model predictions are similar to those in Figure 21.**

A random selection of 10% of the experimental data was withheld in the regression of the RIV model parameters for the NaCl solution (Figure 22). A random selection was not withheld for the LiCl solution since there are so few data available. The average difference for NaCl solution predictions from the RIV model when compared with the withheld

experimental data was 34.38%. The reason for the large difference, primarily, is that a few poor predictions influence the average a great deal because there are so few data points that were withheld.

By nature of the experimental method for determining  $\Delta_{dil}H$  values, the values are best plotted as a function of the final solution concentration rather than as a function of temperature or pressure. The results from the LiCl fit are shown in Figure 23 and in Figure 24. There does not appear to be a bias with respect to temperature, pressure, or initial concentration in the discrepancy between predictions from the RIV model and literature values for the NaCl solution, as seen in Figure 25-Figure 27.

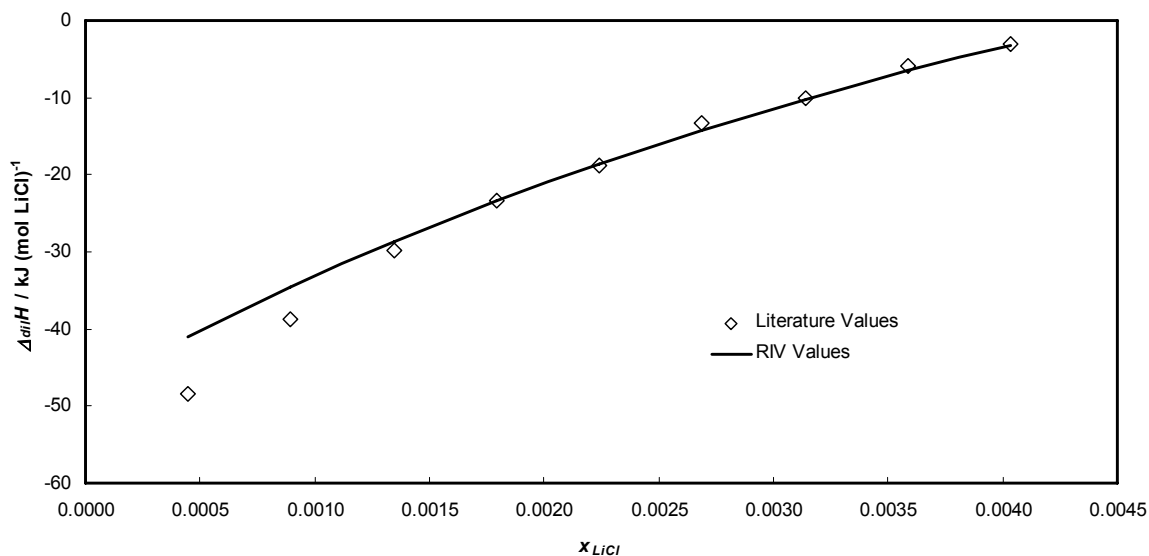


**Figure 23: Plot of  $\Delta_{dil}H$  values for LiCl solutions at 350 °C and 17.6 MPa as a function of final solute concentration. The initial mole fraction of LiCl is  $4.48 \times 10^{-3}$ . RIV predictions are compared with literature values.**

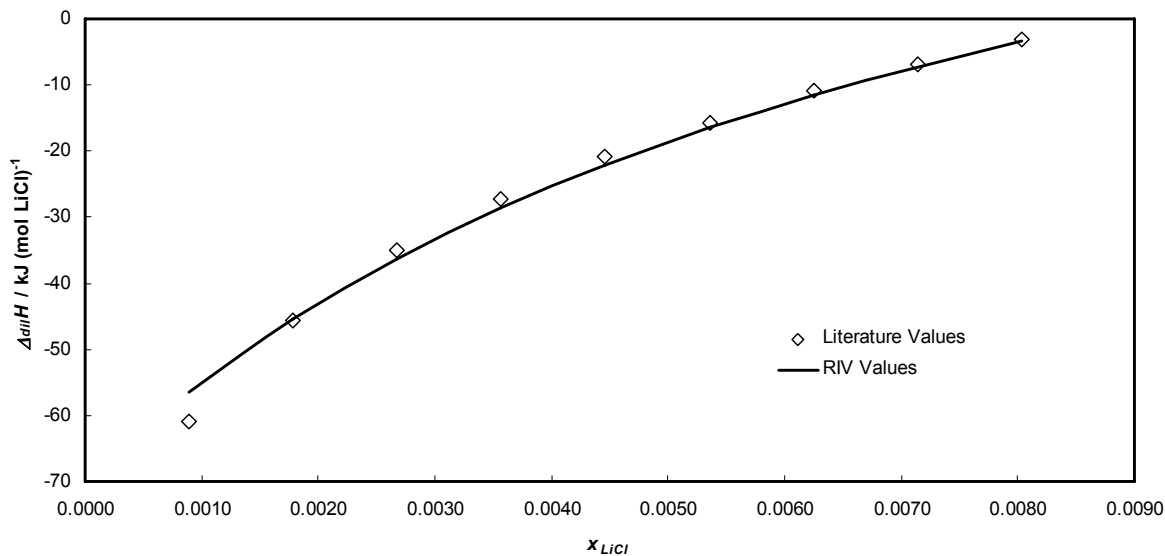


Figure 24: Plot of  $\Delta_{diff}H$  values for LiCl solutions at 350 °C and 17.6 MPa as a function of final solute concentration. The initial mole fraction of LiCl is  $8.93 \times 10^{-3}$ . RIV predictions are compared with literature values.

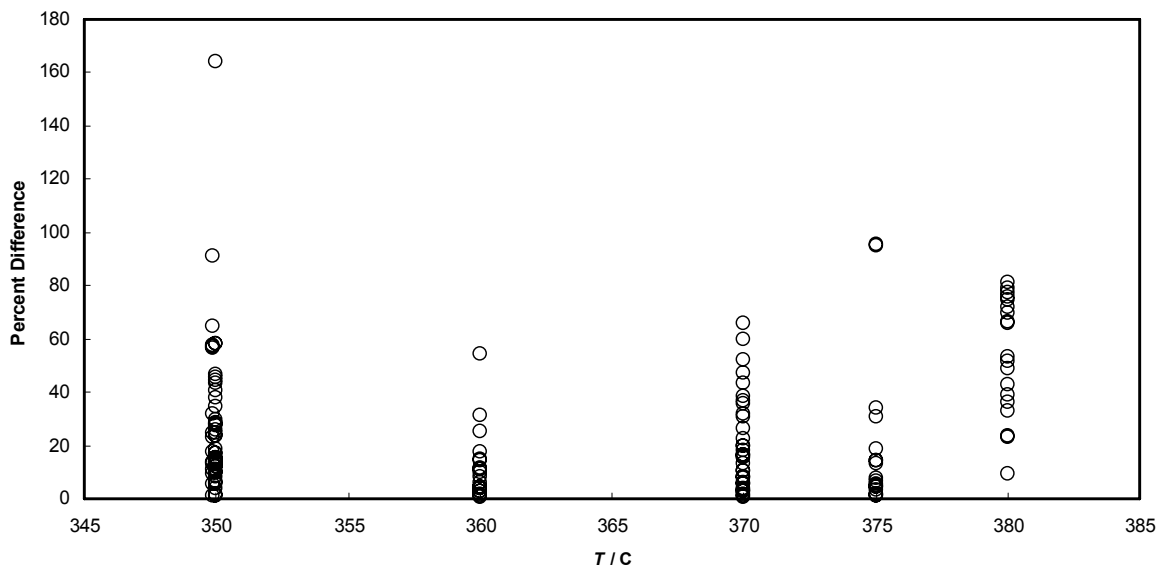


Figure 25: Plot of the percent difference between predictions from the RIV model and literature values of  $\Delta_{diff}H$  as a function of temperature for NaCl solutions.

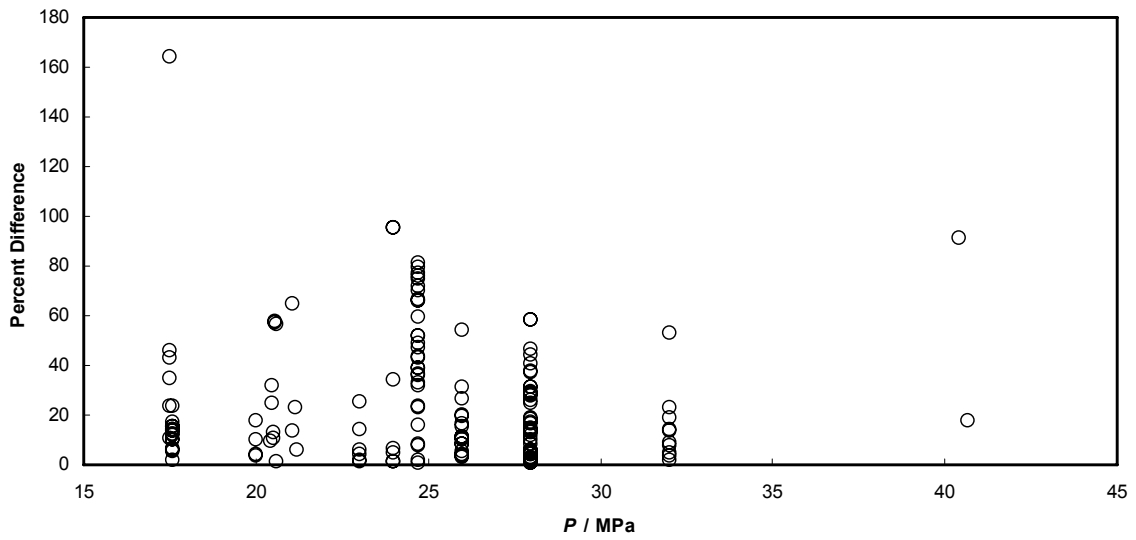


Figure 26: Plot of the percent difference between predictions from the RIV model and literature values of  $\Delta_{lit}H$  as a function of pressure for NaCl solutions.

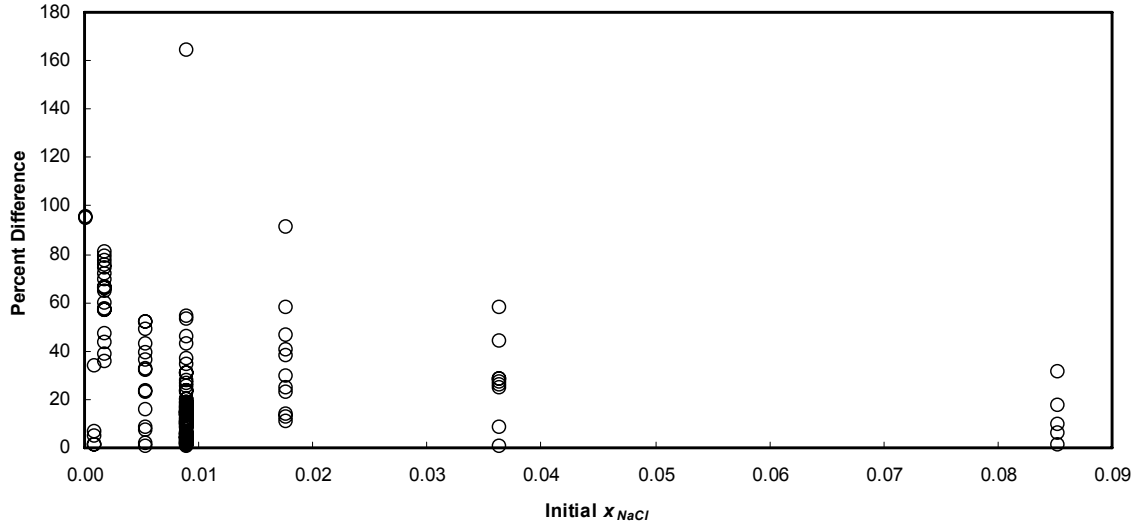


Figure 27: Plot of the percent difference between predictions from the RIV model and literature values of  $\Delta_{lit}H$  as a function of the mole fraction of NaCl.

### 6.2.3 Fraction of the Solute Dissociated

It is interesting to examine the trend of the fraction dissociated as a function of solute concentration, temperature, and pressure. The degree to which this trend agrees with generally observed trends indicates the success of the model in incorporating aqueous phase reactions.

As seen in Figure 28, the fraction dissociated of the solute, NaCl, decreases as  $x_{NaCl}$  increases. This matches the trend observed in all known aqueous electrolyte solutions. That is, the dissociation into ions is driven by the lower energy the ions may achieve by coordinating with waters in solution. As more NaCl is added to solution, there are fewer waters available for coordination per ion. Additionally, as the solution becomes increasingly concentrated in NaCl, the theoretical line between an associated and a dissociated NaCl molecule becomes ambiguous because there are many other NaCl molecules in close proximity.

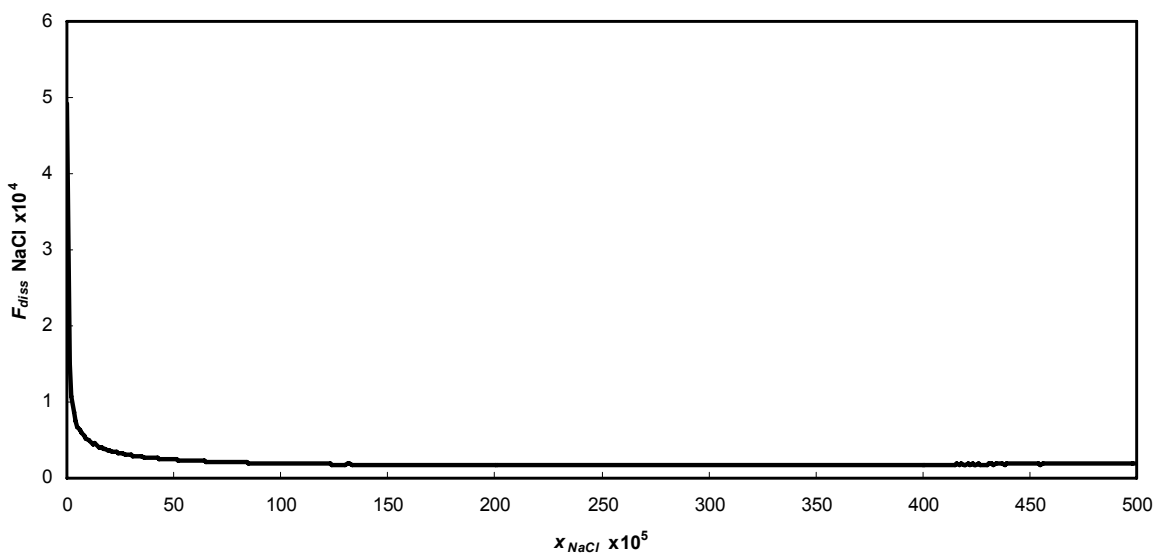
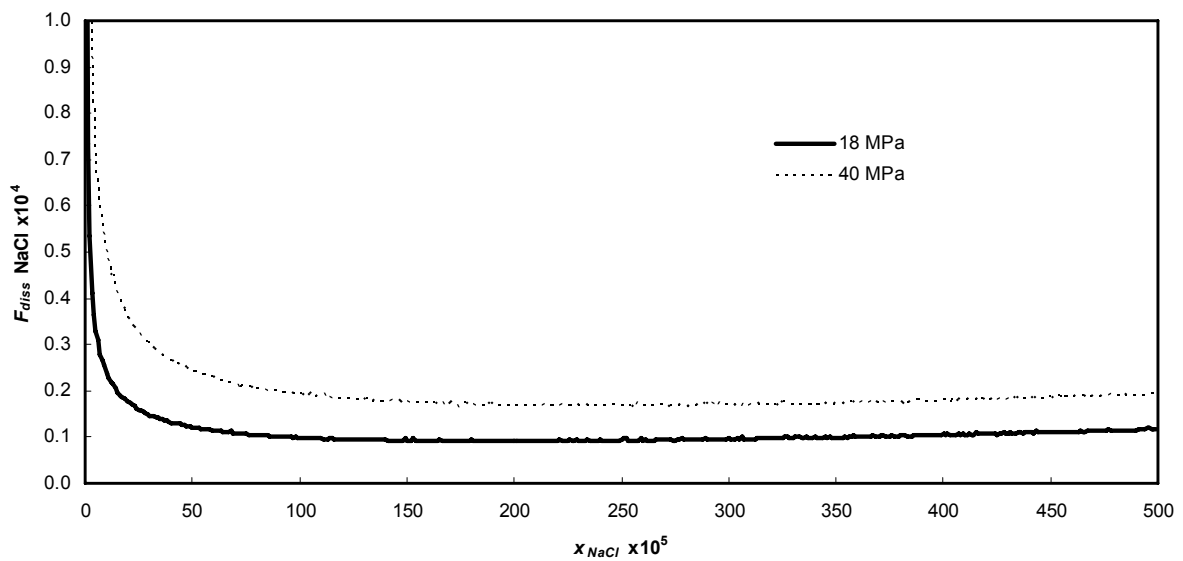


Figure 28: Plot of the fraction dissociated of NaCl versus  $x_{NaCl}$  as predicted using the RIV model at 350 °C and 40 MPa.

In Figure 29, fraction dissociated of NaCl is shown at different pressures but at the same temperature. At the higher pressure, the fraction dissociated is higher. The higher pressure at the same temperature leads to a higher solution density and therefore brings the NaCl into closer proximity to water. As a result, the water interactions that lead to the NaCl reacting to form ions are stronger. This leads to more dissociation.

At higher temperatures, the fraction dissociated also increases as would be expected. At higher temperatures, the energetics for the dissociation reaction are more favorable leading to more dissociation. This is shown graphically in Figure 30.

Because the RIV model can be used to qualitatively predict trends in the fraction of the solute that is dissociated into ions in solution, some confidence may be had in the soundness of the theoretical portion of the model.



**Figure 29:** Plot of the fraction dissociated of NaCl versus the  $x_{NaCl}$  as predicted using the RIV model at 350 °C and different pressures.

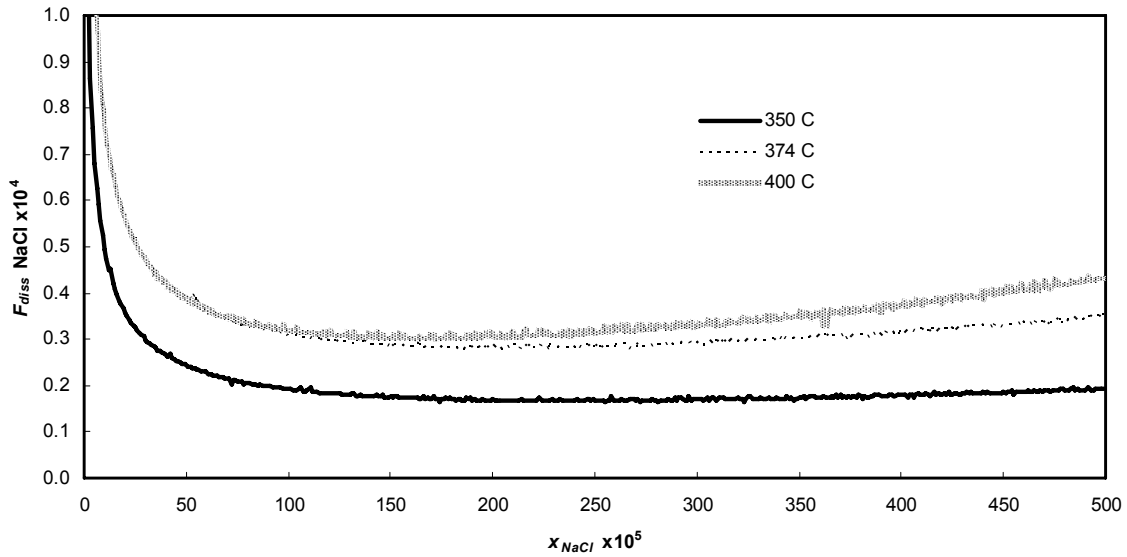


Figure 30: Plot of the fraction dissociated of NaCl versus the mole fraction of NaCl as predicted using the RIV model at 40 MPa and varying temperatures.

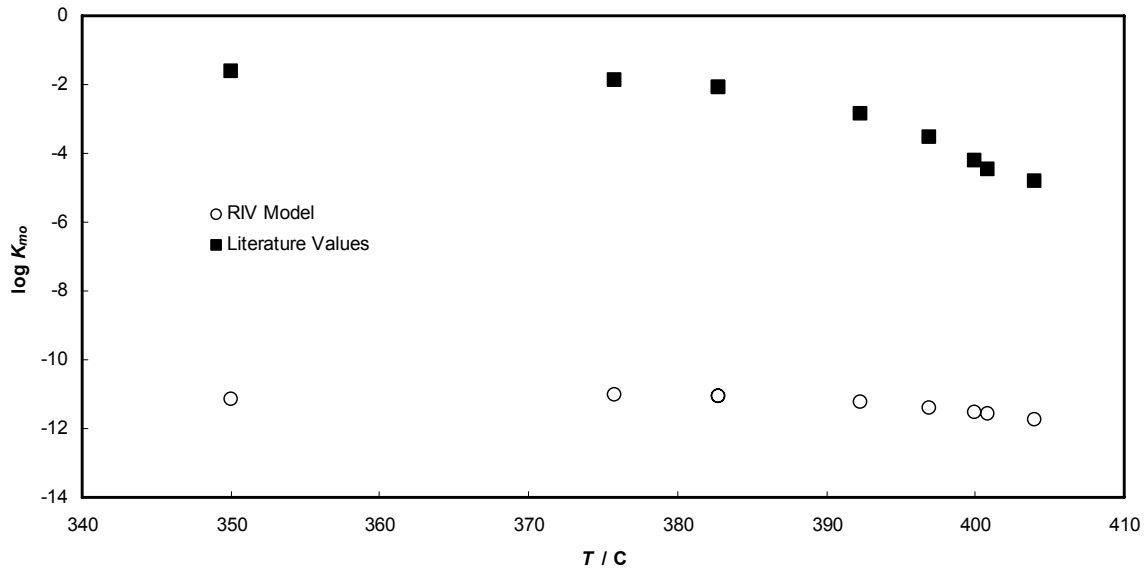


Figure 31: Plot of  $\log K_{mo}$  values versus temperature at 28 MPa.  $\log K_{mo}$  values are taken from the literature and compared to those calculated using the RIV model.

## 6.2.4 log $K$ Predictions Valid at Infinite Dilution

While the RIV model was not regressed using log  $K_o$  data for either the NaCl or the LiCl system, it is interesting to use the RIV model to predict log  $K_o$  values. As may be seen in Figure 31, the predicted log  $K_o$  values are significantly more negative than the literature values they are compared against.

These results indicate that there is more dissociation of the solute into ions than is predicted using the RIV model. Therefore, while the trends in dissociation with respect to the concentration of solute are qualitatively correct, it is doubtful that the trends are quantitatively correct.

Ideally, the parameters in the RIV model would be regressed from log  $K_o$  data as well as  $\Delta_{dil}H$  data and molar volume data. Because the evaluation of a log  $K_o$  prediction is so expensive in terms of time, regressing from log  $K_o$  data was not feasible. If sufficient computing power were available, a regression from log  $K_o$  data may significantly improve the accuracy of the RIV model.



## 7 Experimental Work

In order to provide additional  $\Delta_{dil}H$  values from which to regress parameters in the RIV model and to evaluate the RIV model for aqueous NaCl solutions, several  $\Delta_{dil}H$  values were collected experimentally. It was vital to have a broad range of temperature, pressure, and concentration conditions represented in the  $\Delta_{dil}H$  data so that the model could model temperature, pressure, and concentration dependencies accurately. Very few  $\Delta_{dil}H$  data are available at conditions near the critical point of water.

Additionally,  $\Delta_{dil}H$  values were collected for aqueous sodium acetate solutions. The objective of this research originally included the application of the RIV model to a system, such as the aqueous sodium acetate solution, in which there are multiple significant aqueous reactions. This scope of research was discovered to be too great for a single project, however. It would be desirable in future work to apply the RIV model to the sodium acetate solution though and, therefore, the data for this system are reported here as well.

### 7.1 *Recent Improvements Made to the Calorimeter*

Improvements have been made to the previously reported calorimeter<sup>93</sup> that increase the accuracy of the measurements made with the calorimeter as well as the versatility of the calorimeter. By replacing thermistors in the calorimeter with platinum RTDs, measurements

at temperatures as high as 600 °C may be possible. The RTDs are more robust than the thermistors and last longer during use so that less maintenance time is necessary.

In addition, a new pump, the Digital Positive Displacement Pump Model 2219-DO726 from Chandler Engineering, was obtained. This new pump can deliver high precision flow rates that are much lower than those the previous pumps were capable of delivering. As a result, higher concentrations of solutions can be mixed because the resulting high heats will not exceed the calorimeter's capabilities.

## **7.2 Methodology**

The following is a description of how the calorimeter is used to collect the  $\Delta_{dil}H$  values reported in the appendices. Further details may be obtained from the cited literature. A reaction vessel is submerged in a temperature controlled bath. The temperature in the reaction vessel is controlled at the temperature of the bath using a PID controller with a resistance heater output.

A “baseline” is established by activating a thermoelectric refrigeration device inside the reaction vessel necessitating an input of heat from the PID controller in order to maintain the bath temperature. After the baseline is established, two solutions at the bath temperature are mixed. The resulting solution made up of the mixture of the two original solutions exits the calorimeter.

As a result of the enthalpy change from the solutions being mixed, the PID controller changes the voltage through the resistance heater to maintain a constant temperature in the reaction vessel. The difference between the baseline voltage and the reaction voltage, when multiplied by a calibration constant, yields the enthalpy change due to the reaction (Figure 32).

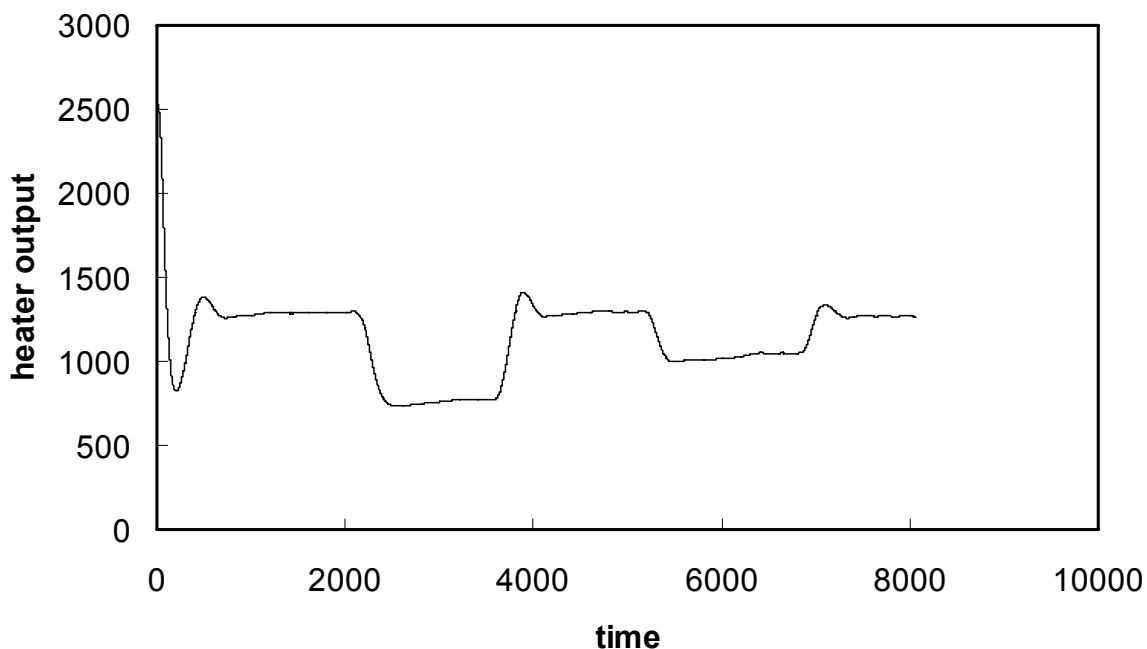


**Figure 32: Plot of heater output from the calorimeter versus time. This shows a series of baselines and reaction lines obtained from the calorimeter in our laboratory for two reaction conditions. The lines near 1350 on the y-axis are base lines and are obtained when there is no reaction occurring. The lines near 750 and near 1000 are reaction lines and are obtained when a reaction is occurring. The differences between the reaction lines and baselines, combined with a calibration constant, yield enthalpy changes for the reaction.**

Corrosion is a significant issue with electrolyte solutions at temperature values of 350 °C and above. Problems with corrosion are avoided by only allowing the solutions to contact corrosion resistant surfaces made either of Teflon or a platinum/rhodium alloy. The solutions are stored in Teflon bags before flowing into the calorimeter. The bags are kept in containers with water surrounding them. When pumps inject more water into the containers, the increase in pressure causes the Teflon bags to compact and force the solutions into tubes. The tubes are made from a 90%/10% platinum/rhodium alloy. The tubes lead to the temperature controlled bath where the two solutions are combined in a pure platinum mixing

cell. This generates the enthalpy change measured in the experiment. When the mixed solution exits the calorimeter, it is received into another Teflon bag.

Because a single baseline or reaction line takes one to two hours to measure, small fluctuations in temperature or pressure do not effect the measurement. Measurements are accurate to within 5% to 10%.

### **7.3 Experimental Conditions**

The experimental conditions for NaCl solutions and for sodium acetate solutions at which  $\Delta_{dil}H$  values were collected are summarized in Table 14 and in Table 15, respectively. The results are found in Appendix C for NaCl solutions and in Appendix E for sodium acetate solutions.

NaCl solution  $\Delta_{dil}H$  values had been experimentally determined previously at 350 °C and 17.6 MPa with an undiluted concentration of 0.5 *m* NaCl. In order to confirm the accuracy of the new  $\Delta_{dil}H$  values by comparison to these previous studies,  $\Delta_{dil}H$  values were collected at 350 °C, 17.5 MPa, and 0.5 *m* NaCl. All other experimental conditions in this study were different from those previously reported in the literature for NaCl solution  $\Delta_{dil}H$  data. This was done order to provide the needed diversity of experimental conditions in the data from which the RIV model parameters were regressed. Before these values were determined, there were 82  $\Delta_{dil}H$  values at temperature values of 350 °C or higher reported. This study determined 117 new  $\Delta_{dil}H$  values and thereby more than doubled the amount of  $\Delta_{dil}H$  data for NaCl solutions available at high temperatures. It was not possible to experimentally determine  $\Delta_{dil}H$  values for LiCl solutions as part of this study.

Previous to this study, there were no experimental  $\Delta_{dil}H$  values for sodium acetate solutions at conditions near the critical point of water reported in the literature. These data will be crucial in applying the RIV model to the sodium acetate solution in the future.

**Table 14: Summary of  $\Delta_{dil}H$  experiments conducted for NaCl solutions.**

$m$ (mol NaCl/kg H <sub>2</sub> O)	$T$ (°C)	$P$ (MPa)	Number of dilution ratios from $\Delta_{dil}H$ measurements
0.05	375	24 Mpa	6
0.01	375	24 MPa	5
0.5	380	32 MPa	3
	375	32 MPa	7
		28 Mpa	8
	370	28 MPa	10
		26 MPa	12
	360	28 MPa	10
		26 Mpa	10
		23 Mpa	8
		20 Mpa	8
		350	17.5 Mpa
		28 MPa	8
1	350	28 Mpa	6
2	350	28 MPa	10

Table 15: Summary of  $\Delta_{dil}H$  experiments conducted for sodium acetate solutions.

$m$ (mol NaAce/kg H <sub>2</sub> O)	$T$ (°C)	$P$ (MPa)	Number of dilution ratios from $\Delta_{dil}H$ measurements
0.5	350	28	10
		26	11
		24	16
		28	7
		26	8
		24	11
1	360	28	2

#### 7.4 Comparison to Literature Data

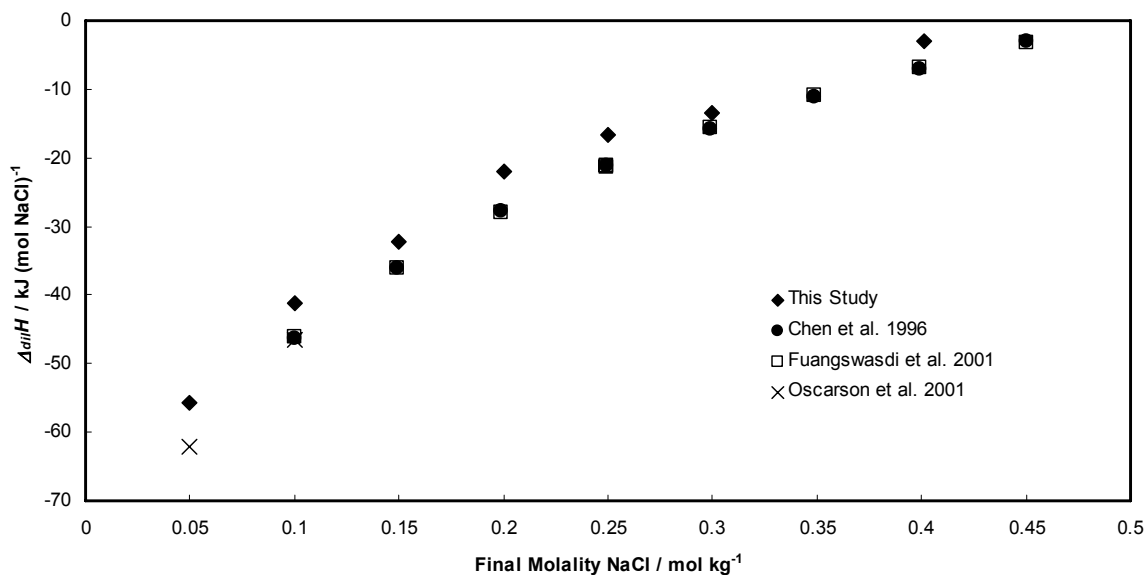


Figure 33: Plot of  $\Delta_{dil}H$  values versus final NaCl molality. This compares results from three previous studies reported in the literature to those from this study. The conditions are at 350 °C and 17.5 MPa for this study and 17.6 MPa for the three literature studies.

Initially,  $\Delta_{dil}H$  values were collected at 350 °C, 17.5 MPa, and an initial NaCl concentration of 0.5 *m* in order to compare to results from previous experiments. Three previous studies<sup>2,92,93</sup> have been conducted at 350 °C, 17.6 MPa, and an initial NaCl concentration of 0.5 *m*. There is close agreement among the data sets despite a 0.1 MPa pressure difference.



## 8 Conclusions and Recommendations

This dissertation has presented the development of the RIV model as well as the results from the application of this model to aqueous NaCl and LiCl solutions in a temperature range from 350 °C to 400 °C and in a pressure range from 17 MPa to 40 MPa. A model that can be used to predict thermodynamic quantities as well as the species concentrations as a result of aqueous phase reactions is useful in a variety of fields. A specific application is the supercritical water oxidation technology where issues concerning corrosion and species solubilities are of vital concern.

### 8.1 Development of the RIV Model

Conventional models such as the Pitzer Ion Interaction Model, rely upon excess Gibbs energy functions and are ineffective above temperatures of 300 °C<sup>25-27</sup>. Models that rely upon residual Helmholtz energy functions are more effective above temperatures of 300 °C.

A difficulty in modeling electrolyte solutions is the manner in which the incomplete reactions in the aqueous phase are handled. One approach is to assume that all the electrolyte solute is associated. The AP model<sup>1</sup> is a notable and successful example of this.

Another approach is to include aqueous phase reactions in the model and allow species concentrations to vary as a function of temperature, pressure, and solute

concentration. While this is clearly a more realistic approach, it is much more difficult to employ. Very few models using this approach have been developed.

The RIII model was developed to allow for partial aqueous reactions of the solute. It uses a separate model for infinite dilution  $\log K$  values to include aqueous reactions. It is more accurate than the AP model for density and  $\Delta_{dil}H$  predictions. The RIII model has substantial thermodynamic inconsistencies, however, and is not well suited for application to systems with multiple reactions in solution or to mixtures of solutes.

The RIV model has been developed to address the concerns in the RIII model while still allowing aqueous phase reactions to be modeled. The RIV model is a residual Helmholtz energy model and relies upon fundamental interactions to model the aqueous phase reactions rather than a separate empirical model. The model contains a hard-sphere term to account for repulsion between species. It also contains a NPMSA term that accounts for interactions between hard-sphere dipoles and hard-sphere ions. Additionally, the RIV model contains a term to account for water-ligand interactions during aqueous reactions. Finally the perturbation term used in the AP model is included to account for all other interactions in solution.

Dissociation of the solute into ions is determined by the minimization of the total Helmholtz energy of solution as a function of the extent of the dissociation reaction. As a result, the speciation is a result of the interactions of the species in solution rather than an outside empirical  $K$  equation. This approach to accounting for speciation in solution is novel.

The RIV model was regressed against molar volume and  $\Delta_{dil}H$  values. In order to have a  $\Delta_{dil}H$  data set that extended over a broader range of conditions, values of  $\Delta_{dil}H$  for NaCl solutions were determined using flow calorimetry methods.

## 8.2 Results Using the RIV Model

The RIV model is less accurate than the AP model in predicting experimental molar volumes. The main region of inaccuracy in the RIV model is at higher molar volumes. This could be an artifact of the regression since there are fewer data at higher molar volumes, and this would place less emphasis on minimizing error at higher molar volumes. Additionally, the discrepancy is higher in regions that are more dilute. As the solution becomes more dilute, however, the critical point of the solution becomes closer and closer to pure water. The RIV model will be less accurate closer to the critical point of the solution because it treats critical point phenomena classically. It seems the water model may be the source of much of this inaccuracy.

The RIV model is significantly more accurate than the AP model in predicting experimental  $\Delta_{dil}H$  values except at very dilute conditions. There does not appear to be any trend in the differences between model predictions and experimental values with respect to temperature, pressure, or concentration.

Although the objective of the research was not to improve upon the RIII model in terms of accuracy, it is worthwhile to compare the accuracy of the RIV model with that of the RIII model. Calculated values of both molar volume and  $\Delta_{dil}H$  from the RIII model are closer to experimental values on average than calculated values from the RIV model. A comparison of the accuracy of the three models is given in Table 16.

While the predictions of the fraction dissociated of the solute as a function of solute concentration are qualitatively good, the predictions are likely quantitatively inaccurate. The  $\log K_o$  values predicted using the model, when compared with experimental values, indicate

too little solute dissociation. This indicates that the predictions for species concentrations at finite concentrations are not accurate.

**Table 16: The average percent difference between calculated values and literature values of molar volume and  $\Delta_{dil}H$  from the AP model, the RIII model, and the RIV model.**

<b>Type of Data</b>	<b>AP % Difference</b>	<b>RIII % Difference</b>	<b>RIV % Difference</b>
$V$	3.51	1.34	6.66
$\Delta_{dil}H$	78.78	22.03	25.16

### **8.3 Contributions this Work Makes to the Body of Knowledge**

There are three primary advances this work makes:

- 1) The RIV model improves upon the AP model without the inconsistencies and limitations of the RI and RIII models. The accuracy of the RIII model is greater, but it is not as theoretically sound.
- 2) The approach for modeling aqueous electrolyte reactions in the RIV model is novel and significant.
- 3) A significant number of experimental values for  $\Delta_{dil}H$  for NaCl solutions and sodium acetate solutions have been determined.

The contribution of this work to the body of knowledge may be reduced most simply to the three items above. To expand upon the first advance listed above, the RIV model is an advance from the AP model in two ways:

- 1) The RIV model allows for ions to be included in solution and is therefore a more conceptually realistic model. The AP model cannot be used to explore aqueous ion behavior.

2) While  $\rho$  predictions from the RIV model are slightly less accurate with regard to experiment as compared to the AP model, the  $\Delta_{dil}H$  predictions are much more accurate.

**Table 17: A comparison of the characteristics between the RI, RIII, AP, and RIV Models**

Characteristic	RI Model	RIII Model	AP Model	RIV Model
An $A^{res}$ model	✓	✓	✓	✓
Includes aqueous ion dissociation reactions	✓	✓		✓
Includes dipole-dipole term	✓	✓	✓	✓
Includes ion-dipole term				✓
Includes ion-ion term		✓		✓
Does not need solution dielectric constant	✓		✓	✓
Predicts $\Delta_{dil}H$ values near experimental values	✓	✓		✓
Does not mix discrete and continuum models			✓	✓
Does not have standard state inconsistencies			✓	✓

The RIV model avoids the difficulties of the RI and RIII models because the RIV model is thermodynamically sound. While the RI and RIII models do allow for ions in solution, the RI and RIII approaches are not thermodynamically consistent. Thus, the RIV model is an advance over the RI and RIII models in terms of building upon the AP model in a thermodynamically sound manner. The RIV model is not an advance in accuracy over the

RIII model and is not as accurate for molar volume predictions as the AP model. It is much more accurate than the AP model for  $\Delta_{dil}H$  calculations, however. A summary of the characteristics of the several models is found in Table 17.

## 8.4 Recommendations

The following recommendations are made for future work:

- 1) The water model portion of the RIV model may be improved. It seems a likely cause of inaccuracy in the RIV model is insufficient accuracy of the water model. A more complicated function for the hard sphere diameter or modifications of the perturbation term may be effective in increasing the accuracy of the water model. Improving the behavior at the critical point may especially improve the RIV model.
- 2) The RIV model is a successful approach for describing aqueous electrolyte solutions. While it has only been applied to simple 1:1 electrolyte solutions thus far, the RIV model requires no change in form to apply it to multiply charged ions. Application of the model to  $\text{CaCl}_2$  or  $\text{MgCl}_2$  solutions would demonstrate the degree of effectiveness with which the RIV model may be used.
- 3) Additionally, with multiply charged solutes (e.g. +2 or -2 charge) as well as many other solutes, there will be more than one significant reaction in solution. The RIV model needs no change in form to account for more than one reaction. The minimization routine for determining reaction equilibrium will require the minimization of more extent of reaction variables. Sodium acetate would be an interesting system to apply the RIV model to because it has multiple significant reactions in solution. Data for  $\Delta_{dil}H$  are reported for this system in Appendix E.

- 4) Gases dissolved in solution would also provide an interesting system to model for the RIV model. For example, CO<sub>2</sub> dissolved in water requires the modeling of a neutral dissolved gas with multiple reactions in solution.
- 5) Also, regressing the parameters for the RIV model from log  $K_m$  data as well as density and  $\Delta_{dil}H$  data may provide a better fit and more realistic predictions for the concentrations of ions in solution. The calculation of values for log  $K_m$  is very expensive computationally, however.
- 6) Finally, the RIV model has not been applied to solution vapor pressure predictions but may be applied without changing the form of the model. This may be a realistic next step in developing the models for NaCl and LiCl solutions. In order to do this, the water model will likely need to be modified and regressed against vapor pressures since the vapor pressure predictions were less accurate than the AP model.



## 9 References

1. Anderko, A.; Pitzer, K. S., Equation-of-State Representation of Phase-Equilibria and Volumetric Properties of the System NaCl-H<sub>2</sub>O above 573 K. *Geochimica Et Cosmochimica Acta* **1993**, 57, (8), 1657-1680.
2. Oscarson, J. L.; Palmer, B. A.; Fuangswasdi, S.; Izatt, R. M., A New Model Incorporating Ion Dissociation for Sodium Chloride Solutions near the Critical Point of Water. *Industrial & Engineering Chemistry Research* **2001**, 40, (9), 2176-2182.
3. Palmer, B. A. Properties model for dilute sodium chloride solutions near the critical point of water. Thesis (M.S.), Brigham Young University. Dept. of Chemical Engineering, 2000.
4. Liu, B.; Oscarson, J. L.; Peterson, C. J.; Izatt, R. M., Improved Thermodynamic Model for Aqueous NaCl Solutions from 350 to 400 DegC. *Industrial & Engineering Chemistry Research* **2006**, 45, (9), 2929-2939.
5. Liu, B. Properties model for aqueous sodium chloride solutions near the critical point of water. Thesis (Ph. D.), Brigham Young University. Dept. of Chemical Engineering, 2005.
6. Wagner, W.; Pruss, A., The IAPWS formulation 1995 for the thermodynamic properties of ordinary water substance for general and scientific use. *Journal of Physical and Chemical Reference Data* **2002**, 31, (2), 387-535.
7. Huang, S. H.; Radosz, M., Equation of State for Small, Large, Polydisperse, and Associating Molecules. *Industrial & Engineering Chemistry Research* **1990**, 29, (11), 2284-2294.
8. Gidner, A. V.; Stenmark, L. B.; Carlsson, K. M. In *Treatment of different wastes by supercritical water oxidation*, International Conference on Incineration and Thermal Treatment Technologies, Philadelphia, PA, United States, May 14-18, 2001, 2001; Philadelphia, PA, United States, 2001; pp 23-27.
9. Crain, N.; Shanableh, A.; Gloyna, E., Supercritical water oxidation of sludges contaminated with toxic organic chemicals. *Water Science and Technology* **2000**, 42, (7-8), 363-368.
10. Minett, S.; Fenwick, K., Supercritical water oxidation - the environmental answer to organic waste disposal? *European Water Management* **2001**, 4, (3), 54-56.

11. Weber, R.; Yoshida, S.; Miwa, K., PCB destruction in subcritical and supercritical water - Evaluation of PCDF formation and initial steps of degradation mechanisms. *Environmental Science & Technology* **2002**, 36, (8), 1839-1844.
12. Shaw, R. W.; Brill, T. B.; Clifford, A. A.; Eckert, C. A.; Franck, E. U., Supercritical water. A medium for chemistry. *Chemical & Engineering News* **1991**, 69, (51), 26-39.
13. Tester, J. W.; Holgate, H. R.; Armellini, F. J.; Webley, P. A.; Killilea, W. R.; Hong, G. T.; Barner, H. E., Supercritical Water Oxidation Technology. Process Development and Fundamental Research. In *Emerging Technologies in Hazardous Waste Management*, Tedder, D. W.; Pohland, F. G., Eds. American Chemical Society: Washington, D. C., 1993.
14. Gloyna, E. F.; Li, L., Supercritical water oxidation research and development update. *Environmental Progress* **1995**, 14, (3), 182-92.
15. Modell, M., Supercritical-Water Oxidation. In *Standard Handbook of Hazardous Waste Treatment and Disposal*, Freeman, H. M., Ed. McGraw-Hill Book Co.: New York, 1989; pp 8.153-8.168.
16. Griffith, J. W., Design and operation of the first supercritical wet oxidation industrial waste destruction facility, 1995. *Chemical Oxidation* **1997**, 5, 22-38.
17. Spritzer, M. H.; Hazlebeck, D. A.; Downey, K. W., Supercritical water oxidation of chemical agents, and solid propellants. *Journal of Energetic Materials* **1995**, 13, (3&4), 185-212.
18. Bleyl, H. J.; Abeln, J.; Boukis, N.; Goldacker, H.; Kluth, M.; Kruse, A.; Petrich, G.; Schmieder, H.; Wiegand, G., Hazardous waste disposal by supercritical fluids. *Separation Science and Technology* **1997**, 32, (1-4), 459-485.
19. Alonso, M. J. C.; Sanchez, E. A.; Fernandez-Polanco, F., Supercritical water oxidation of wastewater and sludges - design considerations. *Engineering in Life Sciences* **2002**, 2, (7), 195-200.
20. Shaw, R. W.; Dahmen, N., Destruction of Toxic Organic Materials Using Supercritical Water Oxidation: Current State of Technology. In *Supercritical Fluids: Fundamentals and Applications*, Kiran, E.; Debenedetti, P. G.; Peters, C. J., Eds. Kluwer Academic: Dordrecht, The Netherlands, 2000; pp 427-437.
21. Eliaz, N.; Mitton, D. B.; Latanision, R. M., Review of materials issues in supercritical water oxidation systems and the need for corrosion control. *Transactions of the Indian Institute of Metals* **2003**, 56, (3), 305-314.
22. Macdonald, D. D.; Kriksunov, L. B., Probing the chemical and electrochemical properties of SCWO systems. *Electrochimica Acta* **2001**, 47, (5), 775-790.

23. Armellini, F. J.; Tester, J. W., Solubility of Sodium-Chloride and Sulfate in Subcritical and Supercritical Water-Vapor from 450-550 °C and 100-250 Bar. *Fluid Phase Equilibria* **1993**, 84, 123-142.
24. Pitzer, K. S., *Activity coefficients in electrolyte solutions* 2ed.; CRC Press: 1991; p 542.
25. Pitzer, K. S., Aqueous electrolytes at near-critical and supercritical temperatures. *International Journal of Thermophysics* **1998**, 19, (2), 355-366.
26. Pitzer, K. S., Thermodynamics of Natural and Industrial Waters. *Journal of Chemical Thermodynamics* **1993**, 25, (1), 7-26.
27. Sengers, J. M. H.; Harvey, A. H.; Weigand, S., Ionic Fluids Near the Critical Points and at High  $T$ 's. In *Equations of State for Fluids and Fluid Mixtures*, 1st ed.; Sengers, J. V.; Kayser, R. F.; Peters, C. J.; White, H. J. J., Eds. Elsevier: Amsterdam ; New York, 2000; Vol. 2, pp 805-847.
28. Anderko, A.; Pitzer, K. S., Phase equilibria and volumetric properties of the systems potassium chloride-water and sodium chloride-potassium chloride-water above 573 K: equation of state representation. *Geochimica et Cosmochimica Acta* **1993**, 57, (20), 4885-97.
29. Gruskiewicz, M. S.; Wood, R. H., Conductance of dilute LiCl, NaCl, NaBr, and CsBr solutions in supercritical water using a flow conductance cell. *Journal of Physical Chemistry B* **1997**, 101, (33), 6549-6559.
30. Sengers, A. L.; Hocken, R.; Sengers, J. V., Critical-point universality and fluids. *Physics Today* **1977**, 30, (12), 42-8, 50-1.
31. Anisimov, M. A.; Sengers, J. V., Critical Region. In *Equations of State for Fluids and Fluid Mixtures*, 1st ed.; Sengers, J. V.; Kayser, R. F.; Peters, C. J.; White, H. J. J., Eds. Elsevier: Amsterdam ; New York, 2000; Vol. 1, pp 381-434.
32. Anisimov, M. A.; Kiselev, S. B.; Sengers, J. V.; Tang, S., Crossover Approach to Global Critical Phenomena in Fluids. *Physica A* **1992**, 188, (4), 487-525.
33. Ho, P. C.; Bianchi, H.; Palmer, D. A.; Wood, R. H., Conductivity of dilute aqueous electrolyte solutions at high temperatures and pressures using a flow cell. *Journal of Solution Chemistry* **2000**, 29, (3), 217-235.
34. Zimmerman, G. H.; Gruskiewicz, M. S.; Wood, R. H., New Apparatus for Conductance Measurements at High-Temperatures - Conductance of Aqueous-Solutions of LiCl, NaCl, NaBr, and CsBr at 28 MPa and Water Densities from 700 to 264 kg·m<sup>-3</sup>. *Journal of Physical Chemistry* **1995**, 99, (29), 11612-11625.
35. Chialvo, A. A.; Cummings, P. T.; Simonson, J. M.; Mesmer, R. E., Molecular simulation study of speciation in supercritical aqueous NaCl solutions. *Journal of Molecular Liquids* **1997**, 73-4, 361-372.

36. Chialvo, A. A.; Cummings, P. T.; Cochran, H. D.; Simonson, J. M.; Mesmer, R. E., Na<sup>+</sup>-Cl<sup>-</sup> Ion-Pair Association in Supercritical Water. *Journal of Chemical Physics* **1995**, 103, (21), 9379-9387.
37. Chialvo, A. A.; Simonson, J. M., Aqueous Na<sup>+</sup>Cl<sup>-</sup> pair association from liquidlike to steamlike densities along near-critical isotherms. *Journal of Chemical Physics* **2003**, 118, (17), 7921-7929.
38. Boublik, T., Perturbation Theory. In *Equations of State for Fluids and Fluid Mixtures*, 1st ed.; Sengers, J. V.; Kayser, R. F.; Peters, C. J.; White, H. J. J., Eds. Elsevier: Amsterdam ; New York, 2000; Vol. 1, pp 127 - 168.
39. Li, Y., Recent advances in the use of statistical mechanics to establish molecular thermodynamic models for electrolyte solutions. *Tsinghua Science and Technology* **2004**, 9, (4), 444-454.
40. Stell, G.; Rasaiah, J. C.; Narang, H., Thermodynamic perturbation theory for simple polar fluids. II. *Molecular Physics* **1974**, 27, (5), 1393-414.
41. Stell, G.; Rasaiah, J. C.; Narang, H., Thermodynamic perturbation theory for simple polar fluids. I. *Molecular Physics* **1972**, 23, (2), 393-406.
42. Rushbrooke, G. S.; Stell, G.; Hoyer, J. S., Theory of polar liquids. I. Dipolar hard spheres. *Molecular Physics* **1973**, 26, (5), 1199-215.
43. Barker, J. A.; Henderson, D., Perturbation theory and equation of state for fluids. II. Successful theory of liquids. *Journal of Chemical Physics* **1967**, 47, (11), 4714-21.
44. Donohue, M. D.; Vimalchand, P., Thermodynamics of Multi-Polar Molecules - the Perturbed-Anisotropic-Chain-Theory. *Abstracts of Papers of the American Chemical Society* **1985**, 189, (Apr-), 68-Inde.
45. Vimalchand, P.; Donohue, M. D., Thermodynamics of Quadrupolar Molecules - the Perturbed-Anisotropic-Chain Theory. *Industrial & Engineering Chemistry Fundamentals* **1985**, 24, (2), 246-257.
46. GilVillegas, A.; Galindo, A.; Whitehead, P. J.; Mills, S. J.; Jackson, G.; Burgess, A. N., Statistical associating fluid theory for chain molecules with attractive potentials of variable range. *Journal of Chemical Physics* **1997**, 106, (10), 4168-4186.
47. Henderson, D., Perturbation theory, ionic fluids, and the electric double layer. *Advances in Chemistry Series* **1983**, 204, (Mol.-Based. Study Fluids), 47-71.
48. Jin, G.; Donohue, M. D., An Equation of State for Electrolyte-Solutions .2. Single Volatile Weak Electrolytes in Water. *Industrial & Engineering Chemistry Research* **1988**, 27, (9), 1737-1743.

49. Jin, G.; Donohue, M. D., An Equation of State for Electrolyte-Solutions .1. Aqueous Systems Containing Strong Electrolytes. *Industrial & Engineering Chemistry Research* **1988**, 27, (6), 1073-1084.
50. Jin, G.; Donohue, M. D., An Equation of State for Electrolyte-Solutions .3. Aqueous-Solutions Containing Multiple Salts. *Industrial & Engineering Chemistry Research* **1991**, 30, (1), 240-248.
51. Larsen, B.; Rasaiah, J. C.; Stell, G., Thermodynamic perturbation theory for multipolar and ionic liquids. *Molecular Physics* **1977**, 33, (4), 987-1027.
52. Henderson, D.; Blum, L.; Tani, A., Equations of state : theories and applications. In *ACS symposium series 300*, Chao, K.-c.; Robinson, R. L., Eds. American Chemical Society: Washington, D.C., 1986; pp ix, 597.
53. Wu, J. Z.; Lu, J. F.; Li, Y. G., A New Perturbation Method for Electrolyte-Solutions Based on Msa. *Fluid Phase Equilibria* **1994**, 101, 121-136.
54. Chan, K. Y., Comparison of a Primitive Model Perturbation-Theory with Experimental-Data of Simple Electrolytes. *Journal of Physical Chemistry* **1990**, 94, (22), 8472-8477.
55. Ornstein, L. S. Z., F., *Proc. Acad. Sci., Amsterdam* **1914**, 17, 793.
56. Wertheim, M. S., Exact solution of the mean spherical model for fluids of hard spheres with permanent electric dipole moments. *Journal of Chemical Physics* **1971**, 55, (9), 4291-8.
57. Waisman, E. M.; Lebowitz, J. L., Mean spherical model integral equation for charged hard spheres. II. Results. *Journal of Chemical Physics* **1972**, 56, (6), 3093-9.
58. Waisman, E. M.; Lebowitz, J. L., Mean spherical model integral equation for charged hard spheres. I. Method of solution. *Journal of Chemical Physics* **1972**, 56, (6), 3086-93.
59. Blum, L., Mean spherical model for asymmetric electrolytes. I. Method of solution. *Molecular Physics* **1975**, 30, (5), 1529-35.
60. Blum, L., Mean spherical model for a mixture of charged spheres and hard dipoles. *Chemical Physics Letters* **1974**, 26, (2), 200-2.
61. Adelman, S. A.; Deutch, J. M., Exact solution of the mean spherical model for strong electrolytes in polar solvents. *Journal of Chemical Physics* **1974**, 60, (10), 3935-49.
62. Vericat, F.; Blum, L., Mean Spherical Model for Hard Ions and Dipoles - Thermodynamics and Correlation-Functions. *Journal of Statistical Physics* **1980**, 22, (5), 593-604.

63. Perezhernandez, W.; Blum, L., Explicit Solution of the Mean Spherical Model for Ions and Dipoles. *Journal of Statistical Physics* **1981**, 24, (3), 451-454.
64. Blum, L., Solution of the Mean Spherical Approximation for Hard Ions and Dipoles of Arbitrary Size. *Journal of Statistical Physics* **1978**, 18, (5), 451 - 474.
65. Blum, L.; Wei, D. Q., Analytical Solution of the Mean Spherical Approximation for an Arbitrary Mixture of Ions in a Dipolar Solvent. *Journal of Chemical Physics* **1987**, 87, (1), 555-565.
66. Wei, D. Q.; Blum, L., The Mean Spherical Approximation for an Arbitrary Mixture of Ions in a Dipolar Solvent - Approximate Solution, Pair Correlation-Functions, and Thermodynamics. *Journal of Chemical Physics* **1987**, 87, (5), 2999-3007.
67. Blum, L.; Vericat, F.; Fawcett, W. R., On the Mean Spherical Approximation for Hard Ions and Dipoles. *Journal of Chemical Physics* **1992**, 96, (4), 3039-3044.
68. Wei, D. Q.; Blum, L., Solvation Thermodynamic Functions in the Mean Spherical Approximation - Behavior near the Solvent Critical Region. *Journal of Chemical Physics* **1995**, 102, (10), 4217-4226.
69. Protsykevich, I. A., Analytic solution of the mean spherical approximation for arbitrary mixture of hard ions and hard dipoles. *Journal of Molecular Liquids* **1996**, 68, (1), 13-21.
70. Lvov, S. N.; Wood, R. H., Equation of State of Aqueous NaCl Solutions over a Wide-Range of Temperatures, Pressures and Concentrations. *Fluid Phase Equilibria* **1990**, 60, (3), 273-287.
71. Liu, W. B.; Li, Y. G.; Lu, J. F., A new equation of state for real aqueous ionic fluids based on electrolyte perturbation theory, mean spherical approximation and statistical associating fluid theory. *Fluid Phase Equilibria* **1999**, 160, 595-606.
72. Liu, W. B.; Li, Y. G.; Lu, J. F., Nonprimitive model of mean spherical approximation applied to aqueous electrolyte solutions. *Industrial & Engineering Chemistry Research* **1998**, 37, (10), 4183-4189.
73. Gao, G. H.; Tan, Z. Q.; Yu, Y. X., Calculation of high-pressure solubility of gas in aqueous electrolyte solution based on non-primitive mean spherical approximation and perturbation theory. *Fluid Phase Equilibria* **1999**, 165, (2), 169-182.
74. Lotfikian, M.; Modarress, H., Modification and application of a non-primitive mean spherical approximation model for simple aqueous electrolyte solutions. *Fluid Phase Equilibria* **2003**, 209, (1), 13-27.
75. Li, C. X.; Li, Y. G.; Lu, J. F.; Yang, L. Y., Study of the ionic activity coefficients in aqueous electrolytes by the non-primitive mean spherical approximation equation. *Fluid Phase Equilibria* **1996**, 124, (1-2), 99-110.

76. Liu, W. B.; Liu, Z. P.; Li, Y. G.; Lu, J. F., Comparison of perturbation theory and mean spherical approximation for polar fluids and ion-dipole mixtures based on molecular simulation data. *Fluid Phase Equilibria* **2001**, 178, (1-2), 45-71.
77. Knight, C. L.; Bodnar, R. J., Synthetic fluid inclusions: IX. Critical PVTX properties of sodium chloride-water solutions. *Geochimica et Cosmochimica Acta* **1989**, 53, (1), 3-8.
78. Anderko, A.; Pitzer, K. S., Equation of State for Pure Fluids and Mixtures Based on a Truncated Virial Expansion. *Aiche Journal* **1991**, 37, (9), 1379-1391.
79. Myers, J. A.; Sandler, S. I.; Wood, R. H., An equation of state for electrolyte solutions covering wide ranges of temperature, pressure, and composition. *Industrial & Engineering Chemistry Research* **2002**, 41, (13), 3282-3297.
80. Archer, D. G.; Wang, P. M., The Dielectric-Constant of Water and Debye-Huckel Limiting Law Slopes. *Journal of Physical and Chemical Reference Data* **1990**, 19, (2), 371-411.
81. Oelkers, E. H.; Helgeson, H. C., Calculation of Dissociation-Constants and the Relative Stabilities of Polynuclear Clusters of 1-1 Electrolytes in Hydrothermal Solutions at Supercritical Pressures and Temperatures. *Geochimica Et Cosmochimica Acta* **1993**, 57, (12), 2673-2697.
82. Khaibullin, I. K.; Borisov, N. M., Experimental investigation of the thermal properties of aqueous and vapor phases of sodium and potassium chlorides in phase equilibrium. *Teplofizika Vysokikh Temperatur* **1966**, 4, (4), 518-23.
83. Khaibullin, I. K.; Borisov, N. M., Phase equilibrium diagrams in the sodium chloride-water and potassium chloride-water systems. *Doklady Akademii Nauk SSSR* **1965**, 165, (3), 590-2.
84. Khaibullin, K.; Borisov, N. M., Phase equilibrium in the system NaCl-H<sub>2</sub>O at high temperatures. I. *Zhurnal Fizicheskoi Khimii* **1965**, 39, (3), 688-92.
85. Borisov, N. M.; Khaibullin, I. K., Volatility of components and the coefficient of distribution in the two-phase system of NaCl-H<sub>2</sub>O at high temperatures. *Zhurnal Fizicheskoi Khimii* **1965**, 39, (6), 1380-7.
86. Bodnar, R. J., Experimental-Determination of the PVTX Properties of Aqueous-Solutions at Elevated-Temperatures and Pressures Using Synthetic Fluid Inclusions - H<sub>2</sub>O-NaCl as an Example. *Pure and Applied Chemistry* **1995**, 67, (6), 873-880.
87. Urusova, M. A., Volumetric properties of sodium chloride aqueous solutions at elevated temperatures and pressures. *Zhurnal Neorganicheskoi Khimii* **1975**, 20, (11), 3103-10.
88. Bodnar, R. J.; Sterner, S. M., Synthetic Fluid Inclusions in Natural Quartz .2. Application to PVT Studies. *Geochimica Et Cosmochimica Acta* **1985**, 49, (9), 1855-1859.

89. Majer, V.; Hui, L.; Crovetto, R.; Wood, R. H., Volumetric properties of aqueous 1-1 electrolyte solutions near and above the critical temperature of water. II. Densities and apparent molar volumes of lithium chloride(aq) and sodium bromide(aq) at molalities from 0.0025 mol/kg to 3.0 mol/kg, temperatures from 604.4 K to 725.5 K, and pressures from 18.5 MPa to 38.0 MPa. *Journal of Chemical Thermodynamics* **1991**, 23, (4), 365-78.
90. Pepinov, R. I.; Lobkova, N. V.; Panakhov, I. A., Density and viscosity of aqueous lithium chloride solutions over a wide range of state parameters. *Teplofizika Vysokikh Temperatur* **1989**, 27, (6), 1086-9.
91. Busey, R. H.; Holmes, H. F.; Mesmer, R. E., The Enthalpy of Dilution of Aqueous Sodium-Chloride to 673 K Using a New Heat-Flow and Liquid-Flow Microcalorimeter - Excess Thermodynamic Properties and Their Pressure Coefficients. *Journal of Chemical Thermodynamics* **1984**, 16, (4), 343-372.
92. Chen, X. M.; Oscarson, J. L.; Cao, H. J.; Gillespie, S. E.; Izatt, R. M., A new flow calorimeter designed for operation to 450 °C and 50 MPa. *Thermochimica Acta* **1996**, 285, (1), 11-23.
93. Fuangswasdi, S.; Oscarson, J. L.; Zhou, L.; Izatt, R. M., A new flow calorimeter using a eutectic molten salt as the temperature control medium. *Thermochimica Acta* **2001**, 373, (1), 13-22.
94. Gillespie, S. E.; Chen, X.; Oscarson, J. L.; Izatt, R. M., Enthalpies of dilution of aqueous solutions of LiCl, KCl, and CsCl at 300, 325, and 350 DegC. *Journal of Solution Chemistry* **1997**, 26, (1), 47-61.
95. Franck, E. U., Super-critical water as electrolytic solvent. *Angewandte Chemie* **1961**, 73, 309-22.
96. Ho, P. C.; Palmer, D. A.; Mesmer, R. E., Electrical conductivity measurements of aqueous sodium chloride solutions to 600 DegC and 300 MPa. *Journal of Solution Chemistry* **1994**, 23, (9), 997-1018.
97. Oelkers, E. H.; Helgeson, H. C., Calculation of the thermodynamic and transport properties of aqueous species at high pressures and temperatures: dissociation constants for supercritical alkali metal halides at temperatures from 400 to 800 DegC and pressures from 500 to 4000 bar. *Journal of Physical Chemistry* **1988**, 92, (6), 1631-9.
98. Ho, P. C.; Palmer, D. A., Determination of Ion Association in Dilute Aqueous Lithium Chloride and Lithium Hydroxide Solutions to 600 DegC and 300 MPa by Electrical Conductance Measurements. *Journal of Chemical and Engineering Data* **1998**, 43, (2), 162-170.
99. Christensen, J. J.; Johnston, H. D.; Izatt, R. M., Isothermal titration calorimeter. *Review of Scientific Instruments* **1968**, 39, (9), 1356-9.

100. Christensen, J. J.; Hansen, L. D.; Eatough, D. J.; Izatt, R. M.; Hart, R. M., Isothermal high pressure flow calorimeter. *Review of Scientific Instruments* **1976**, 47, (6), 730-4.
101. Christensen, J. J.; Hansen, L. D.; Izatt, R. M.; Eatough, D. J.; Hart, R. M., Isothermal, Isobaric, Elevated-Temperature, High-Pressure, Flow Calorimeter. *Review of Scientific Instruments* **1981**, 52, (8), 1226-1231.
102. Christensen, J. J.; Izatt, R. M., An Isothermal Flow Calorimeter Designed for High-Temperature, High-Pressure Operation. *Thermochimica Acta* **1984**, 73, (1-2), 117-129.
103. Christensen, J. J.; Brown, P. R.; Izatt, R. M., An Isothermal Flow Calorimeter for High-Temperature Aqueous-Solutions. *Thermochimica Acta* **1986**, 99, 159-168.
104. Oscarson, J. L.; Chen, X. M.; Gillespie, S. E.; Izatt, R. M., An Isothermal Flow Calorimeter for High-Temperature Basic Solutions. *Thermochimica Acta* **1991**, 185, (1), 51-61.
105. Chen, X. M.; Gillespie, S. E.; Oscarson, J. L.; Izatt, R. M., Enthalpy of Dissociation of Water at 325 °C and LogK,  $\Delta H$ ,  $\Delta S$ , and  $\Delta C_p$  Values for the Formation of NaOH(Aq) from 250 °C to 325 °C. *Journal of Solution Chemistry* **1992**, 21, (8), 803-824.
106. Chen, X. M.; Izatt, R. M.; Oscarson, J. L., Thermodynamic Data for Ligand Interaction with Protons and Metal-Ions in Aqueous-Solutions at High-Temperatures. *Chemical Reviews* **1994**, 94, (2), 467-517.
107. Chen, X. M.; Gillespie, S. E.; Oscarson, J. L.; Izatt, R. M., Calorimetric Determination of Thermodynamic Quantities for Chemical-Reactions in the System CO<sub>2</sub>-NaOH-H<sub>2</sub>O from 225 Degrees to 325 DegreesC. *Journal of Solution Chemistry* **1992**, 21, (8), 825-848.
108. Gillespie, S. E.; Oscarson, J. L.; Chen, X.; Izatt, R. M.; Pando, C., Thermodynamic Quantities for the Interaction of Cl<sup>-</sup> with Mg<sup>2+</sup>, Ca<sup>2+</sup> and H<sup>+</sup> in Aqueous-Solution from 250 to 325 °C. *Journal of Solution Chemistry* **1992**, 21, (8), 761-788.
109. Oscarson, J. L.; Gillespie, S. E.; Christensen, J. J.; Izatt, R. M.; Brown, P. R., Thermodynamic Quantities for the Interaction of H<sup>+</sup> and Na<sup>+</sup> with C<sub>2</sub>H<sub>3</sub>O<sub>2</sub> and Cl<sup>-</sup> in Aqueous-Solution from 275 °C to 320 °C. *Journal of Solution Chemistry* **1988**, 17, (9), 865-885.
110. Oscarson, J. L.; Gillespie, S. E.; Izatt, R. M.; Chen, X.; Pando, C., Thermodynamic Quantities for the Ionization of Nitric-Acid in Aqueous-Solution from 250 °C to 319 °C. *Journal of Solution Chemistry* **1992**, 21, (8), 789-801.
111. Oscarson, J. L.; Izatt, R. M.; Brown, P. R.; Pawlak, Z.; Gillespie, S. E.; Christensen, J. J., Thermodynamic Quantities for the Interaction of (SO<sub>4</sub>)<sup>2-</sup> with H<sup>+</sup> and Na<sup>+</sup> in Aqueous-Solution from 150 °C to 320 °C. *Journal of Solution Chemistry* **1988**, 17, (9), 841-863.

112. Christensen, J. J.; Cordray, D. R.; Oscarson, J. L.; Izatt, R. M., The Excess-Enthalpies of 4 (Carbon-Dioxide + an Alkanol) Mixtures from 308.15 K to 573.15 K at 7.50 to 12.50 MPa. *Journal of Chemical Thermodynamics* **1988**, 20, (7), 867-875.
113. Pando, C.; Renuncio, J. A. R.; Hanks, R. W.; Christensen, J. J., The Prediction of Vapor Liquid Equilibrium from Heat of Mixing Data for Binary Hydrocarbon Ketone Mixtures. *Thermochimica Acta* **1983**, 63, (2), 173-190.
114. Pando, C.; Renuncio, J. A. R.; Hanks, R. W.; Christensen, J. J., The Prediction of Vapor Liquid Equilibrium from Heat of Mixing Data of Binary Hydrocarbon Ether and Hydrocarbon Aldehyde Mixtures. *Thermochimica Acta* **1983**, 62, (1), 113-124.
115. Cordray, D. R.; Christensen, J. J.; Izatt, R. M., A Calorimetric Method for the Determination of Binary Phase Compositions at High-Temperatures and Pressures. *Separation Science and Technology* **1987**, 22, (2-3), 1169-1181.
116. Boublik, T., Hard-sphere equation of state. *Journal of Chemical Physics* **1970**, 53, (1), 471-2.
117. Mansoori, G. A.; Carnahan, N. F.; Starling, K. E.; Leland, T. W., Jr., Equilibrium thermodynamic properties of mixture of hard spheres. *Journal of Chemical Physics* **1971**, 54, (4), 1523-5.
118. Carnahan, N. F.; Starling, K. E., Equation of state for nonattracting rigid spheres. *Journal of Chemical Physics* **1969**, 51, (2), 635-6.
119. Dohrn, R.; Prausnitz, J. M., A simple perturbation term for the Carnahan-Starling equation of state. *Fluid Phase Equilibria* **1990**, 61, (1-2), 53-69.
120. VR&D *VisualDOC Design Integration and Optimization Software*, Release 6.1; Vanderplaats Research & Development, Inc.: Colorado Springs, CO, 2008.
121. Crovetto, R.; Lvov, S. N.; Wood, R. H., Vapor pressures and densities of sodium chloride(aq) and potassium chloride(aq) at the temperature 623 K and calcium chloride(aq) at the temperatures 623 K and 643 K. *Journal of Chemical Thermodynamics* **1993**, 25, (1), 127-38.
122. Bischoff, J. L., Densities of Liquids and Vapors in Boiling NaCl-H<sub>2</sub>O Solutions - a PVT Summary from 300 Degrees C to 500 °C. *American Journal of Science* **1991**, 291, (4), 309-338.
123. Majer, V.; Hui, L.; Crovetto, R.; Wood, R. H., Volumetric properties of aqueous 1-1 electrolyte solutions near and above the critical temperature of water. I. Densities and apparent molar volumes of sodium chloride (aq) from 0.0025 mol.kg<sup>-1</sup> to 3.1 mol.kg<sup>-1</sup>, 604.4 K to 725.5 K, and 18.5 MPa to 38.0 MPa. *Journal of Chemical Thermodynamics* **1991**, 23, (3), 213-29.

124. Weeks, J. D.; Andersen, H. D.; Chandler, D. *Relation between the hard sphere fluid and fluids with realistic repulsive forces*; Dep. Chem., Univ. California, San Diego, CA, USA.: 1971; p 40 pp.
125. Elliott, J. R., Jr.; Daubert, T. E., The temperature dependence of the hard sphere diameter. *Fluid Phase Equilibria* **1986**, 31, (2), 153-60.
126. Cosgrove, B. A.; Walkley, J., Scaled particle theory of gas solubility-inclusion of the temperature dependent hard sphere term. *Canadian Journal of Chemistry* **1982**, 60, (14), 1896-900.
127. Wilhelm, E., Temperature dependence of the effective hard sphere diameter. *Journal of Chemical Physics* **1973**, 58, (9), 3558-60.
128. Wilhelm, E., Thermodynamic properties of a hard sphere fluid with temperature dependent effective hard sphere diameter. *Journal of Chemical Physics* **1974**, 60, (10), 3896-900.
129. McClellan, A. L., *Tables of Experimental Dipole Moments*. W. H. Freeman: San Francisco 1963; Vol. 2.
130. M. J. Frisch, G. W. T., H. B. Schlegel, G. E. Scuseria, ; M. A. Robb, J. R. C., J. A. Montgomery, Jr., T. Vreven, ; K. N. Kudin, J. C. B., J. M. Millam, S. S. Iyengar, J. Tomasi, ; V. Barone, B. M., M. Cossi, G. Scalmani, N. Rega, ; G. A. Petersson, H. N., M. Hada, M. Ehara, K. Toyota, ; R. Fukuda, J. H., M. Ishida, T. Nakajima, Y. Honda, O. Kitao, ; H. Nakai, M. K., X. Li, J. E. Knox, H. P. Hratchian, J. B. Cross, ; C. Adamo, J. J., R. Gomperts, R. E. Stratmann, O. Yazyev, ; A. J. Austin, R. C., C. Pomelli, J. W. Ochterski, P. Y. Ayala, ; K. Morokuma, G. A. V., P. Salvador, J. J. Dannenberg, ; V. G. Zakrzewski, S. D., A. D. Daniels, M. C. Strain, ; O. Farkas, D. K. M., A. D. Rabuck, K. Raghavachari, ; J. B. Foresman, J. V. O., Q. Cui, A. G. Baboul, S. Clifford, ; J. Cioslowski, B. B. S., G. Liu, A. Liashenko, P. Piskorz, ; I. Komaromi, R. L. M., D. J. Fox, T. Keith, M. A. Al-Laham, ; C. Y. Peng, A. N., M. Challacombe, P. M. W. Gill, ; B. Johnson, W. C., M. W. Wong, C. Gonzalez, and J. A. Pople *Gaussian 03*, Revision C.02; Gaussian, Inc.: Wallingford CT, 2004.
131. R. L. Rowley, W. V. W., J. L. Oscarson, N. F. Giles, Y. Yang *DIPPR® Data Compilation of Pure Chemical Properties*, Design Institute for Physical Properties, AIChE: New York, NY 2008.



## Appendix A Measured Molar Volumes and Those Predicted Using the RIV Model for NaCl Solutions

$T$ (°C)	$P$ (MPa)	$m$ (mol/kg H <sub>2</sub> O)	Measured (cm <sup>3</sup> /mol)	RIV (cm <sup>3</sup> /mol)	Reference
349.9	16.7	0.25	29.7	31.4	121
349.9	16.7	0.25	29.7	31.4	121
349.9	16.7	0.25	29.6	31.4	121
349.9	16.7	0.25	29.6	31.4	121
349.9	16.7	0.25	29.6	31.4	121
349.9	16.7	0.25	29.6	31.4	121
349.9	16.8	1	27.3	27.5	121
349.9	16.8	1	27.3	27.5	121
350	16.8	1	27.3	27.5	121
350	16.8	1	27.3	27.5	121
350	16.8	1	27.3	27.5	121
350	16.7	1	27.4	27.5	121
350	16.7	1	27.4	27.5	121
350	16.7	1	27.4	27.5	121
350	16.7	3	25.0	24.4	121
350	16.7	3	25.0	24.4	121
350	16.7	3	25.0	24.4	121
350	16.7	3	25.0	24.4	121
350	16.7	3	25.0	24.4	121
350	13.5	4.97	23.8	23.2	122
350	14	4.09	24.1	23.7	122
350	14.5	3.09	24.5	24.3	122
350	15	2.2	25.2	25.2	122
350	23	1.9	25.7	25.3	87
350	21.7	1.9	25.8	25.4	87
350	20.2	1.9	25.9	25.4	87
350	20.1	1.9	25.9	25.4	87
350	19	1.9	26.0	25.5	87
350	17.7	1.9	26.2	25.5	87
350	15.5	1.9	26.4	25.6	87
350	23.4	4.28	24.0	23.4	87
350	23	4.28	24.1	23.4	87
350	21.9	4.28	24.0	23.4	87
350	21.2	4.28	24.1	23.4	87
350	17.9	4.28	24.3	23.5	87

$T$ (°C)	$P$ (MPa)	$m$ (mol/kg H <sub>2</sub> O)	Measured (cm <sup>3</sup> /mol)	RIV (cm <sup>3</sup> /mol)	Reference
350	17.8	4.28	24.4	23.5	87
350	14.1	4.28	24.5	23.6	87
350	15.5	1.37	26.2	26.6	122
350	15.7	1.05	26.8	27.4	122
350	16	0.64	28.0	28.9	122
350	16.3	0.24	29.7	31.6	122
350	16.5	0	31.6	34.6	122
350	16.7	1	27.4	27.5	121
350	16.7	1	27.3	27.5	121
350	16.8	3	25.0	24.4	121
350	16.7	1	27.4	27.5	121
350	16.7	3	25.0	24.4	121
350	16.7	3	25.0	24.4	121
350	16.7	3	25.0	24.4	121
350	16.7	3	25.0	24.4	121
350	16.8	3	25.0	24.4	121
350	16.8	3	24.9	24.4	121
350	16.8	3	25.0	24.4	121
350	16.8	0.5	28.7	29.6	121
350	16.8	0.5	28.7	29.6	121
350	16.8	0.5	28.7	29.6	121
360	15.5	4.41	24.1	24.1	122
360	16	3.63	24.4	24.6	122
360	16.5	2.79	24.9	25.3	122
360	17	2.09	25.7	26.1	122
360	17.5	1.29	27.0	27.5	122
360	17.7	1.02	27.6	28.3	122
360	18	0.69	28.6	29.6	122
360	18.3	0.35	30.2	31.7	122
360	18.5	0.07	32.3	34.9	122
360	18.7	0	34.1	36.2	122
370	17	5.03	24.2	24.3	122
370	17.5	4.31	24.4	24.7	122
370	18	3.53	24.8	25.2	122
370	18.5	2.88	25.3	25.8	122
370	19	2.07	26.1	26.8	122
370	19.5	1.37	27.3	28.1	122
370	20	0.88	28.9	29.6	122
370	20.2	0.71	29.6	30.3	122
370	20.5	0.49	31.1	31.6	122
370	20.8	0.19	34.3	34.4	122
370	21	0	39.9	37.8	122
380	19.5	4.52	25.0	25.0	122
380	20	3.78	25.3	25.6	122
380	21	2.38	26.4	26.9	122

<i>T</i> (°C)	<i>P</i> (MPa)	<i>m</i> (mol/kg H <sub>2</sub> O)	Measured (cm <sup>3</sup> /mol)	RIV (cm <sup>3</sup> /mol)	Reference
380	21.5	1.71	27.5	28.0	122
380	22	1.19	29.0	29.3	122
380	22.5	0.77	31.2	30.9	122
380	23	0.34	34.7	33.9	122
380	23.2	0.18	36.8	35.8	122
380	23.3	0.06	51.6	38.0	122
390	21.5	4.83	25.0	25.2	122
390	22	4.31	25.3	25.6	122
390	22.5	3.68	25.8	26.1	122
390	23	3	26.3	26.7	122
390	23.5	2.33	27.1	27.5	122
390	24	1.8	28.2	28.4	122
390	24.5	1.27	29.6	29.7	122
390	25	0.9	31.6	31.0	122
390	25.5	0.49	35.7	33.5	122
390	25.7	0.2	45.3	36.8	122
400	24	4.76	25.6	25.5	122
400	24.5	4.15	25.9	26.0	122
400	25	3.51	26.2	26.7	122
400	25.5	2.97	26.8	27.2	122
400	26	2.38	27.5	28.0	122
400	26.5	1.92	28.6	28.7	122
400	27	1.45	30.4	29.8	122
400	27.5	1.05	32.6	31.1	122
400	28	0.61	37.9	33.4	122
400	28.1	0.39	42.1	35.4	122
400	59	1.9	26.1	27.2	87
400	58.6	1.9	26.2	27.2	87
400	51.2	1.9	26.8	27.5	87
400	50	1.9	26.8	27.6	87
400	43.2	1.9	27.4	27.9	87
400	40.7	1.9	27.6	28.0	87
400	36	1.9	28.3	28.3	87
400	35.8	1.9	28.5	28.3	87
400	27.4	1.9	30.1	28.7	87
400	59.2	4.28	24.5	25.0	87
400	59.1	4.28	24.6	25.0	87
400	58.8	4.28	24.6	25.0	87
400	51.5	4.28	24.8	25.2	87
400	51.2	4.28	24.9	25.2	87
400	45.2	4.28	25.2	25.4	87
400	43.8	4.28	25.3	25.4	87
400	43.3	4.28	25.2	25.4	87
400	36	4.28	25.8	25.6	87

<i>T</i> (°C)	<i>P</i> (MPa)	<i>m</i> (mol/kg H <sub>2</sub> O)	Measured (cm <sup>3</sup> /mol)	RIV (cm <sup>3</sup> /mol)	Reference
400	35.8	4.28	26.1	25.6	87
400	25.2	4.28	26.5	25.9	87
377.96	27.99	0.01	34.2	36.6	123
377.97	28	0.01	34.2	36.6	123
377.96	28.04	0.01	34.2	36.6	123
377.96	28.04	0.01	34.2	36.6	123
377.95	28	0.01	34.2	36.5	123
377.96	28	0.01	34.2	36.5	123
377.96	28	0.01	34.2	36.5	123
377.96	28	0.02	34.0	36.3	123
377.97	28	0.02	34.0	36.3	123
377.97	28	0.02	34.0	36.3	123
377.96	28	0.05	33.7	35.8	123
377.97	28	0.05	33.7	35.8	123
377.96	28	0.1	33.2	35.1	123
377.96	28	0.1	33.2	35.1	123
377.95	28	0.25	32.1	33.4	123
377.95	28	0.25	32.1	33.4	123
377.95	27.99	0.5	30.8	31.5	123
377.95	27.99	0.5	30.8	31.5	123
377.96	27.99	0.5	30.8	31.5	123
377.96	27.99	0.5	30.8	31.5	123
377.95	28.02	1.03	28.9	29.1	123
377.96	28.02	1.03	28.9	29.1	123
377.95	28	2	27.0	27.0	123
377.96	28.02	2	27.0	27.0	123
377.96	28.03	2	27.0	27.0	123
377.94	27.99	3.1	25.8	25.8	123
377.95	28	3.1	25.8	25.8	123
377.96	28	3.1	25.8	25.8	123
377.96	28	3.1	25.8	25.8	123
377.95	33	0.01	31.8	35.0	123
377.95	33	0.01	31.8	35.0	123
377.96	33.02	0.01	31.7	34.9	123
377.96	33.02	0.01	31.7	34.9	123
377.97	33.02	0.01	31.7	34.9	123
377.96	33	0.02	31.6	34.7	123
377.97	33	0.02	31.6	34.7	123
377.95	33	0.05	31.5	34.4	123
377.95	33	0.05	31.5	34.4	123
377.96	32.99	0.1	31.2	33.8	123
377.95	33	0.1	31.2	33.8	123
377.96	33	0.25	30.4	32.4	123
377.95	33.01	0.5	29.5	30.8	123

<i>T</i> (°C)	<i>P</i> (MPa)	<i>m</i> (mol/kg H <sub>2</sub> O)	Measured (cm <sup>3</sup> /mol)	RIV (cm <sup>3</sup> /mol)	Reference
377.95	33.01	0.5	29.5	30.8	123
377.95	33	1.03	28.1	28.7	123
377.95	33	1.03	28.1	28.7	123
377.95	33	2	26.5	26.8	123
377.95	33	2	26.5	26.8	123
377.97	32.99	3.1	25.5	25.7	123
377.95	33	3.1	25.4	25.7	123
377.96	33	3.1	25.4	25.7	123
377.96	33	3.1	25.5	25.7	123
377.96	33	3.1	25.5	25.7	123
377.95	37.98	0.01	30.4	33.7	123
377.97	37.98	0.01	30.4	33.7	123
377.97	37.99	0.01	30.4	33.7	123
377.95	37.98	0.01	30.4	33.7	123
377.94	38	0.01	30.4	33.6	123
377.96	38	0.01	30.3	33.6	123
377.96	38	0.02	30.3	33.5	123
377.96	38	0.02	30.3	33.5	123
377.95	37.98	0.05	30.2	33.3	123
377.96	38	0.05	30.1	33.2	123
377.96	38	0.05	30.2	33.2	123
377.95	37.98	0.1	29.9	32.8	123
377.96	37.98	0.1	29.9	32.8	123
377.95	37.99	0.1	29.9	32.8	123
377.96	38.01	0.1	29.9	32.8	123
377.96	38.02	0.1	29.9	32.8	123
377.95	38.01	0.25	29.4	31.6	123
377.95	38.02	0.25	29.4	31.6	123
377.95	38	0.5	28.6	30.2	123
377.95	38	0.5	28.6	30.2	123
377.93	38	1.03	27.5	28.4	123
377.93	38	1.03	27.5	28.4	123
377.95	37.97	2	26.1	26.6	123
377.96	37.97	2	26.1	26.6	123
377.96	38.02	2	26.1	26.6	123
377.95	37.96	3.1	25.2	25.5	123
377.96	37.96	3.1	25.2	25.5	123
377.96	37.97	3.1	25.2	25.5	123
377.95	38	3.1	25.2	25.5	123
377.95	38	3.1	25.2	25.5	123
392.23	28	0	46.9	40.5	123
392.23	28	0	46.9	40.5	123
392.24	28.01	0.01	46.7	40.5	123
392.24	28	0.01	46.8	40.5	123

<i>T</i> (°C)	<i>P</i> (MPa)	<i>m</i> (mol/kg H <sub>2</sub> O)	Measured (cm <sup>3</sup> /mol)	RIV (cm <sup>3</sup> /mol)	Reference
392.24	28	0.01	46.4	40.3	123
392.24	28	0.01	46.4	40.3	123
392.24	28	0.02	45.6	39.9	123
392.25	28	0.02	45.6	39.9	123
392.24	28.01	0.05	44.4	39.3	123
392.24	28.01	0.05	44.4	39.3	123
392.24	28.02	0.1	42.5	38.2	123
392.24	28.02	0.1	42.5	38.2	123
395.71	33	0.01	37.7	38.6	123
395.71	33	0.01	37.7	38.6	123
395.71	33	0.02	37.4	38.3	123
395.71	33	0.02	37.4	38.3	123
395.71	33.01	0.05	37.0	37.8	123
395.71	33.01	0.05	37.0	37.8	123
395.71	32.97	0.1	36.4	37.0	123
395.71	32.99	0.1	36.4	37.0	123
395.71	33	0.25	34.8	35.0	123
395.71	32.99	0.25	34.8	35.0	123
395.71	32.99	0.5	33.0	32.8	123
395.72	32.99	0.5	33.0	32.8	123
395.7	33	1.03	30.6	30.3	123
395.7	33	1.03	30.6	30.3	123
395.71	33	1.03	30.6	30.3	123
395.7	33	2	28.1	28.0	123
395.7	33	2	28.1	28.0	123
395.71	33	2	28.1	28.0	123
395.71	33	2	28.1	28.0	123
395.7	33.02	3.1	26.6	26.6	123
395.7	33.02	3.1	26.6	26.6	123
395.7	33.02	3.1	26.6	26.6	123
395.7	33	3.1	26.6	26.6	123
395.7	33	3.1	26.6	26.6	123
395.71	33	3.1	26.6	26.6	123
396.8	28	0	59.6	42.2	123
396.8	28.01	0	59.5	42.2	123
396.8	28.01	0	59.5	42.2	123
396.8	28.01	0.01	59.2	42.1	123
396.8	28.01	0.01	59.2	42.1	123
396.8	28.01	0.01	59.1	42.1	123
396.79	28	0.01	58.8	41.9	123
396.8	27.97	0.01	59.2	42.0	123
396.82	27.97	0.01	59.3	42.0	123
396.78	28	0.02	57.4	41.4	123
396.78	28	0.05	55.3	40.7	123

<i>T</i> (°C)	<i>P</i> (MPa)	<i>m</i> (mol/kg H <sub>2</sub> O)	Measured (cm <sup>3</sup> /mol)	RIV (cm <sup>3</sup> /mol)	Reference
396.78	27.99	0.05	55.4	40.7	123
396.79	27.99	0.05	55.5	40.7	123
396.81	27.98	0.1	52.2	39.4	123
396.81	27.99	0.1	52.1	39.4	123
396.79	28.01	0.25	44.6	36.6	123
396.79	28.01	0.25	44.6	36.6	123
396.82	28.01	0.5	38.7	33.9	123
396.82	28.01	0.5	38.7	33.9	123
396.82	28.01	0.5	38.7	33.9	123
396.82	28.01	1.03	33.4	30.8	123
396.82	28.01	1.03	33.3	30.8	123
396.82	28.01	1.03	33.4	30.8	123
400.04	28	0	69.2	43.6	123
400.05	28	0	69.3	43.6	123
400.07	28	0	69.3	43.6	123
400.02	28	0.01	69.0	43.5	123
400.05	28.01	0.01	69.0	43.5	123
400.04	28	0.01	68.6	43.3	123
400.05	28	0.01	68.6	43.3	123
400.03	28	0.02	67.3	42.7	123
400.05	28.01	0.02	67.2	42.7	123
400.02	28	0.05	65.3	41.8	123
400.04	28	0.05	65.3	41.8	123
400.04	27.99	0.1	61.8	40.4	123
400.05	27.99	0.1	61.9	40.4	123
400.03	28	0.1	61.7	40.4	123
400.06	28	1.03	34.4	31.1	123
400.07	28	1.03	34.4	31.1	123
400.03	28	2	29.8	28.5	123
400.03	28.01	2	29.8	28.5	123
400.04	28.01	2	29.8	28.5	123
400.02	28	3.1	27.6	27.0	123
400.03	28	3.1	27.7	27.0	123
400.03	28.01	3.1	27.6	27.0	123
400.04	37.99	0	35.5	37.6	123
400.03	38	0	35.5	37.6	123
400.03	37.97	0.01	35.5	37.6	123
400.08	37.98	0.01	35.5	37.6	123
400.04	37.99	0.01	35.4	37.5	123
400.04	38	0.01	35.4	37.5	123
400.04	38	0.01	35.4	37.5	123
400.03	37.99	0.02	35.2	37.2	123
400.04	38	0.02	35.2	37.2	123
400.03	38	0.05	35.0	36.9	123

<b><i>T</i> (°C)</b>	<b><i>P</i> (MPa)</b>	<b><i>m</i> (mol/kg H<sub>2</sub>O)</b>	<b>Measured (cm<sup>3</sup>/mol)</b>	<b>RIV (cm<sup>3</sup>/mol)</b>	<b>Reference</b>
400.03	38.01	0.05	35.0	36.8	123
400.05	38	0.1	34.5	36.2	123
400.05	38	0.1	34.5	36.2	123
400.02	38.01	0.1	34.5	36.2	123
400.03	38	0.25	33.4	34.5	123
400.04	38	0.25	33.4	34.5	123
400.03	37.97	0.5	32.1	32.6	123
400.03	37.99	0.5	32.0	32.6	123
400.03	38.01	0.5	32.0	32.6	123
400.04	37.99	1.03	30.1	30.2	123
400.04	38	1.03	30.1	30.2	123
400.03	37.99	2	27.9	28.0	123
400.02	38	2	27.9	28.0	123
400.02	38	2	27.9	28.0	123
400.04	38.01	3.1	26.5	26.7	123
400.04	38.01	3.0955	26.5	26.7	123

## Appendix B Measured Molar Volumes and Those Predicted Using the RIV Model for LiCl Solutions

<i>T</i> (°C)	<i>P</i> (MPa)	<i>m</i> (mol/kg H <sub>2</sub> O)	Measured (cm <sup>3</sup> /mol)	RIV (cm <sup>3</sup> /mol)	Reference
331.25	27.4	2.9940	23.2	22.4	89
331.25	27.4	2.9940	23.2	22.4	89
331.25	27.4	2.9940	23.2	22.4	89
331.25	37.3	0.2555	25.2	27.0	89
331.25	37.3	0.2555	25.2	27.0	89
331.26	18.4	0.0103	27.5	30.8	89
331.26	18.42	0.0103	27.5	30.8	89
331.26	18.42	0.0103	27.5	30.8	89
331.26	18.45	0.0048	27.5	30.8	89
331.26	18.47	0.0247	27.4	30.6	89
331.26	18.48	0.0247	27.4	30.6	89
331.26	18.48	0.2555	26.7	28.7	89
331.26	18.49	0.5008	26.2	27.3	89
331.26	18.5	0.0247	27.4	30.6	89
331.26	18.5	0.2555	26.7	28.7	89
331.26	18.5	0.2555	26.7	28.7	89
331.26	18.5	0.5008	26.2	27.3	89
331.26	18.51	0.5008	26.2	27.3	89
331.26	18.52	2.9940	23.5	22.6	89
331.26	18.54	1.9760	24.3	23.7	89
331.26	18.55	1.9760	24.3	23.7	89
331.26	18.58	0.0490	27.3	30.4	89
331.26	18.58	2.9940	23.5	22.6	89
331.26	18.6	0.0490	27.3	30.4	89
331.26	27.35	1.0232	24.8	25.1	89
331.26	27.35	1.0250	24.8	25.1	89
331.26	27.38	2.9940	23.2	22.4	89
331.26	27.38	2.9940	23.2	22.4	89
331.26	27.38	2.9940	23.2	22.4	89
331.26	27.39	1.9760	23.9	23.5	89
331.26	27.39	1.9760	23.9	23.5	89
331.26	27.4	0.0048	26.5	29.5	89
331.26	27.4	0.0490	26.3	29.1	89
331.26	27.4	0.0490	26.3	29.1	89

<i>T</i> (°C)	<i>P</i> (MPa)	<i>m</i> (mol/kg H <sub>2</sub> O)	Measured (cm <sup>3</sup> /mol)	RIV (cm <sup>3</sup> /mol)	Reference
331.26	27.4	0.1005	26.2	28.8	89
331.26	27.42	0.0490	26.3	29.1	89
331.26	27.42	0.0490	26.3	29.1	89
331.26	27.43	0.0247	26.4	29.3	89
331.26	27.43	0.0247	26.4	29.3	89
331.26	27.43	0.0247	26.4	29.3	89
331.26	27.44	0.5008	25.5	26.7	89
331.26	27.45	0.5008	25.5	26.7	89
331.26	27.51	0.0048	26.5	29.5	89
331.26	27.52	0.0048	26.5	29.5	89
331.26	27.57	0.0247	26.4	29.3	89
331.26	27.65	0.0103	26.4	29.4	89
331.26	37.23	0.0490	25.6	28.1	89
331.26	37.23	0.0490	25.6	28.1	89
331.26	37.3	0.5008	24.9	26.1	89
331.26	37.4	1.0250	24.3	24.7	89
331.27	18.45	0.0048	27.5	30.8	89
331.27	18.49	0.0048	27.5	30.8	89
331.27	18.49	0.0048	27.5	30.8	89
331.27	18.5	0.5008	26.2	27.3	89
331.27	18.52	1.0250	25.3	25.5	89
331.27	18.56	0.1005	27.2	29.9	89
331.27	18.56	0.1005	27.1	29.9	89
331.27	27.4	0.0247	26.4	29.3	89
331.27	27.5	0.1005	26.2	28.8	89
331.27	27.55	0.1005	26.2	28.8	89
331.27	27.65	0.0103	26.4	29.4	89
331.27	37.22	0.0247	25.6	28.2	89
331.27	37.41	0.1005	25.5	27.8	89
331.27	37.49	0.1005	25.5	27.8	89
331.27	37.6	0.0103	25.6	28.3	89
331.27	37.6	0.0103	25.6	28.3	89
331.27	37.62	0.0048	25.6	28.3	89
331.27	37.62	0.0048	25.6	28.3	89
331.28	18.47	1.0250	25.3	25.5	89
331.28	27.52	0.2555	25.9	27.8	89
331.28	27.58	0.2555	25.9	27.8	89
331.28	37.27	0.0247	25.6	28.2	89
331.28	37.35	1.0250	24.3	24.7	89
331.28	37.37	0.5008	24.9	26.1	89
331.28	37.58	0.0048	25.6	28.3	89
331.28	37.63	1.9760	23.5	23.2	89
331.29	37.32	0.0247	25.6	28.2	89
331.29	37.67	1.9760	23.5	23.2	89

<i>T</i> (°C)	<i>P</i> (MPa)	<i>m</i> (mol/kg H <sub>2</sub> O)	Measured (cm <sup>3</sup> /mol)	RIV (cm <sup>3</sup> /mol)	Reference
331.29	37.7	2.9940	22.9	22.3	89
377.92	27.99	0.0048	34.4	36.6	89
377.93	27.98	0.0048	34.4	36.6	89
377.93	38	1.0250	27.4	28.5	89
377.95	27.99	0.0103	34.3	36.5	89
377.95	27.99	0.5008	30.8	31.5	89
377.95	28	0.0247	34.1	36.3	89
377.95	28	0.0247	34.1	36.3	89
377.95	28	0.0247	34.1	36.3	89
377.95	28.02	1.0250	28.8	29.3	89
377.95	28.02	1.0250	28.8	29.3	89
377.95	32.99	0.0247	31.8	34.7	89
377.95	33	0.1005	31.3	33.8	89
377.95	33	1.0250	28.0	28.9	89
377.95	33	1.0250	28.0	28.9	89
377.95	33	2.9940	25.1	25.7	89
377.95	33.01	0.0048	31.9	35.0	89
377.95	33.01	0.5008	29.5	30.9	89
377.95	33.01	0.5008	29.5	30.9	89
377.95	33.01	0.5008	29.5	30.9	89
377.95	33.01	1.9760	26.2	26.9	89
377.95	33.01	1.9760	26.2	26.9	89
377.95	33.02	2.9940	25.1	25.7	89
377.95	37.92	1.9760	25.9	26.7	89
377.95	37.93	1.9760	25.9	26.7	89
377.95	37.97	2.9940	24.8	25.5	89
377.95	37.98	0.0103	30.5	33.7	89
377.95	37.98	0.0103	30.5	33.7	89
377.95	37.98	0.0490	30.3	33.3	89
377.95	37.98	0.0490	30.3	33.3	89
377.95	37.99	2.9940	24.8	25.5	89
377.95	38	0.1005	30.0	32.8	89
377.95	38	0.5008	28.6	30.3	89
377.95	38	0.5008	28.6	30.3	89
377.95	38	2.9940	24.8	25.5	89
377.95	38.02	0.2555	29.4	31.7	89
377.95	38.13	1.9760	25.9	26.7	89
377.96	27.99	0.0048	34.4	36.6	89
377.96	27.99	0.2555	32.2	33.4	89
377.96	27.99	0.5008	30.8	31.5	89
377.96	28	0.0048	34.4	36.6	89
377.96	28	0.0103	34.3	36.5	89
377.96	28	0.0103	34.3	36.5	89
377.96	28	0.0490	33.8	35.9	89

<i>T</i> (°C)	<i>P</i> (MPa)	<i>m</i> (mol/kg H <sub>2</sub> O)	Measured (cm <sup>3</sup> /mol)	RIV (cm <sup>3</sup> /mol)	Reference
377.96	28	0.0490	33.8	35.9	89
377.96	28	0.1005	33.3	35.1	89
377.96	28	0.2555	32.2	33.4	89
377.96	28	0.2555	32.2	33.4	89
377.96	28.02	2.9940	25.4	25.8	89
377.96	28.03	1.9760	26.7	27.1	89
377.96	28.03	1.9760	26.7	27.1	89
377.96	28.03	2.9940	25.4	25.8	89
377.96	32.99	0.0048	32.0	35.0	89
377.96	32.99	0.0048	31.9	35.0	89
377.96	32.99	0.0048	32.0	35.0	89
377.96	32.99	0.0247	31.8	34.7	89
377.96	32.99	2.9940	25.1	25.7	89
377.96	33	0.0103	31.9	34.9	89
377.96	33	0.0490	31.6	34.4	89
377.96	33	0.1005	31.3	33.8	89
377.96	33.01	0.0048	31.9	35.0	89
377.96	33.01	0.0490	31.6	34.4	89
377.96	33.01	0.2555	30.5	32.4	89
377.96	33.02	0.2555	30.5	32.4	89
377.96	33.02	0.5008	29.5	30.9	89
377.96	38	0.0103	30.5	33.6	89
377.96	38	0.0103	30.5	33.6	89
377.96	38	1.0250	27.4	28.5	89
377.96	38.02	0.1005	30.0	32.8	89
377.96	38.02	0.1005	30.0	32.8	89
377.96	38.02	0.2555	29.4	31.7	89
377.97	28	0.0247	34.1	36.3	89
377.97	33.03	0.0103	31.9	34.9	89
377.97	37.99	0.0490	30.3	33.3	89
377.97	37.99	1.0250	27.4	28.5	89
377.97	38.02	0.0490	30.3	33.3	89
378.97	37.98	0.0048	30.7	33.9	89
378.97	37.99	0.0048	30.7	33.9	89
392.23	28.01	0.0025	47.1	40.5	89
392.23	28.01	0.0025	47.1	40.5	89
392.24	27.99	0.0103	46.7	40.3	89
392.24	27.99	0.0103	46.7	40.3	89
392.24	27.99	0.0247	45.9	39.9	89
392.24	27.99	0.0247	45.9	39.9	89
392.24	28	0.0025	47.2	40.6	89
392.24	28	0.0048	47.0	40.5	89
392.24	28	0.0048	47.0	40.5	89
392.24	28	0.0490	44.6	39.3	89

<i>T</i> (°C)	<i>P</i> (MPa)	<i>m</i> (mol/kg H <sub>2</sub> O)	Measured (cm <sup>3</sup> /mol)	RIV (cm <sup>3</sup> /mol)	Reference
392.24	28.01	0.0247	45.8	39.9	89
392.24	28.01	0.1005	42.6	38.2	89
392.25	28.01	0.0490	44.6	39.3	89
392.25	28.02	0.1005	42.6	38.2	89
395.7	33	0.0247	37.6	38.3	89
395.7	33	0.0247	37.6	38.3	89
395.7	33	1.0250	30.5	30.5	89
395.7	33	1.0250	30.5	30.5	89
395.7	33	1.9760	27.8	28.2	89
395.7	33	2.9940	26.2	26.7	89
395.7	33.01	1.0250	30.5	30.5	89
395.7	33.01	2.9940	26.2	26.7	89
395.7	33.02	2.9940	26.2	26.7	89
395.7	33.02	2.9940	26.2	26.7	89
395.71	32.99	0.0103	35.6	38.6	89
395.71	32.99	0.0103	37.9	38.6	89
395.71	32.99	0.2555	34.9	35.0	89
395.71	32.99	1.9760	27.8	28.2	89
395.71	32.99	1.9760	27.8	28.2	89
395.71	32.99	1.9760	27.8	28.2	89
395.71	32.99	1.9760	27.8	28.2	89
395.71	32.99	2.9940	26.2	26.7	89
395.71	33	0.0103	37.9	38.6	89
395.71	33	0.0490	37.2	37.8	89
395.71	33	0.0490	37.2	37.8	89
395.71	33	0.5008	33.0	33.0	89
395.71	33	0.5008	33.0	33.0	89
395.71	33	2.9940	26.2	26.7	89
395.71	33	2.9940	26.2	26.7	89
395.71	33.01	0.1005	36.5	37.0	89
395.71	33.01	1.0250	30.5	30.5	89
395.72	32.99	0.0103	37.9	38.6	89
395.72	33.01	0.1005	36.5	37.0	89
395.72	33.01	2.9940	26.2	26.7	89
395.73	32.99	0.2555	34.9	35.1	89
396.77	27.99	0.0247	57.8	41.5	89
396.78	27.99	0.0247	57.8	41.5	89
396.78	27.99	0.0490	55.7	40.7	89
396.78	27.99	0.2555	44.5	36.6	89
396.78	27.99	0.2555	44.5	36.6	89
396.78	28	0.0025	59.8	42.2	89
396.78	28	0.0103	59.0	41.9	89
396.78	28	0.5008	38.5	34.0	89
396.78	28	0.5008	38.5	34.0	89

<i>T</i> (°C)	<i>P</i> (MPa)	<i>m</i> (mol/kg H <sub>2</sub> O)	Measured (cm <sup>3</sup> /mol)	RIV (cm <sup>3</sup> /mol)	Reference
396.78	28.01	1.0250	33.0	31.1	89
396.79	27.98	0.1005	52.2	39.4	89
396.79	27.98	0.1005	52.2	39.4	89
396.79	27.99	0.0490	55.8	40.7	89
396.79	28	0.0103	59.1	41.9	89
396.79	28.01	0.0048	59.5	42.1	89
396.79	28.01	1.0250	40.3	31.1	89
396.8	28	0.0025	59.9	42.2	89
396.8	28.01	0.0103	59.0	41.9	89
396.81	28.01	0.0048	59.5	42.1	89
400.01	28	2.9940	27.1	27.1	89
400.01	28	2.9940	27.2	27.1	89
400.03	27.99	0.1005	62.0	40.4	89
400.03	27.99	1.0250	34.1	31.4	89
400.03	28	1.9760	29.4	28.7	89
400.03	28.01	0.0490	65.6	41.9	89
400.03	28.01	0.0490	65.6	41.9	89
400.03	28.01	1.9760	29.4	28.7	89
400.04	27.99	0.1005	62.0	40.4	89
400.04	28	0.0103	68.9	43.3	89
400.04	28.02	0.0048	69.2	43.5	89
400.04	28.02	0.0048	69.2	43.5	89
400.05	27.99	1.0250	34.1	31.4	89
400.05	28	0.0025	69.7	43.6	89
400.05	28	0.0025	69.7	43.6	89
400.05	28	0.0025	69.7	43.6	89
400.05	28	0.0048	69.5	43.5	89
400.05	28	0.0103	69.0	43.3	89
400.05	28	0.0103	69.0	43.3	89
400.05	28	0.0247	67.8	42.7	89
400.05	28.01	0.0247	67.7	42.7	89
400.05	28.01	0.0247	67.6	42.7	89
350	20	0.2383	29.0	30.9	90
350	20	1.2415	26.5	26.6	90
350	20	2.6209	25.0	24.5	90
350	20	4.1626	24.1	23.2	90
350	20	5.8971	23.5	22.2	90
350	30	0.2383	27.5	29.6	90
350	30	1.2415	25.6	26.1	90
350	30	2.6209	24.4	24.2	90
350	30	4.1626	23.5	23.0	90
350	30	5.8971	22.9	22.1	90

## Appendix C Measured $\Delta_{dil}H$ values and Those Predicted Using the RIV Model for NaCl Solutions

$T$ (°C)	$P$ (MPa)	$m_i$ (mol/kg H <sub>2</sub> O)	$m_f$ (mol/kg H <sub>2</sub> O)	Measured (J/mol NaCl)	RIV (J/mol NaCl)	Reference
349.9	20.41	5.18	3.7780	-10100	-17156	91
349.9	20.45	5.18	1.6060	-37700	-41246	91
349.9	20.48	5.18	2.4520	-23900	-31464	91
349.9	20.48	1	0.7460	-9200	-6834.5	91
349.9	20.52	1	0.3290	-31700	-27607	91
349.9	20.52	1	0.2460	-38800	-34617	91
349.9	20.55	0.1	0.0250	-29100	-12509	91
349.9	20.55	0.1	0.0250	-29400	-12509	91
349.9	20.59	5.18	1.1940	-46900	-47375	91
349.9	20.59	0.1	0.0330	-25300	-10952	91
349.9	21.07	1	0.1640	-47300	-40862	91
349.9	21.07	0.1	0.0160	-37600	-13339	91
349.9	21.17	1	0.4950	-20900	-16122	91
349.9	21.2	5.18	0.7890	-58600	-55226	91
349.9	40.41	1	0.4950	-10800	-978.92	91
349.9	40.53	5.18	2.4480	-15900	-24965	91
349.9	40.66	5.18	0.7870	-36600	-30112	91
349.9	40.96	1	0.4950	-10700	-789.66	91
349.9	41.4	5.18	2.4480	-15600	-24841	91
402.2	41.72	5.18	3.7750	-13100	-38662	91
402.2	41.72	5.18	1.1910	-60200	-97009	91
402.2	41.72	1	0.2460	-52500	-50795	91
402.2	41.72	1	0.1640	-66200	-60566	91
402.2	41.72	0.1	0.0160	-58900	-13364	91
402.2	41.72	0.2	0.1000	-23400	-13220	91
402.2	41.72	0.2	0.0500	-43900	-20885	91
350	17.6	0.5	0.4500	-3000	-3706.3	92
350	17.6	0.5	0.3990	-7000	-7949.2	92
350	17.6	0.5	0.3490	-11000	-12650	92
350	17.6	0.5	0.2990	-15800	-17994	92
350	17.6	0.5	0.2490	-21100	-24123	92
350	17.6	0.5	0.1990	-27800	-31217	92
350	17.6	0.5	0.1490	-36000	-39523	92

<b><i>T</i> (°C)</b>	<b><i>P</i> (MPa)</b>	<b><i>m<sub>i</sub></i> (mol/kg H<sub>2</sub>O)</b>	<b><i>m<sub>f</sub></i> (mol/kg H<sub>2</sub>O)</b>	<b>Measured (J/mol NaCl)</b>	<b>RIV (J/mol NaCl)</b>	<b>Reference</b>
350	17.6	0.5	0.1	-46400	-45200	92
350	17.6	0.5	0.4500	-3100	-3706.3	93
350	17.6	0.5	0.3990	-6900	-7949.2	93
350	17.6	0.5	0.3490	-10800	-12650	93
350	17.6	0.5	0.2990	-15600	-17994	93
350	17.6	0.5	0.2490	-21200	-24123	93
350	17.6	0.5	0.2490	-21300	-24123	93
350	17.6	0.5	0.1990	-27900	-31217	93
350	17.6	0.5	0.1490	-36000	-39523	93
350	17.6	0.5	0.1000	-46200	-49163	93
370	24.7	0.1	0.0900	-4100	-2626.8	93
370	24.7	0.1	0.0800	-8700	-5344.8	93
370	24.7	0.1	0.0700	-13900	-8159.5	93
370	24.7	0.1	0.0600	-19600	-11077	93
370	24.7	0.1	0.0500	-26700	-14102	93
370	24.7	0.1	0.0400	-34600	-17242	93
370	24.7	0.1	0.0300	-45000	-20505	93
370	24.7	0.1	0.0200	-59300	-23898	93
370	24.7	0.1	0.0100	-80700	-27429	93
370	24.7	0.3	0.2700	-3100	-4713.3	93
370	24.7	0.3	0.2400	-7300	-9638.2	93
370	24.7	0.3	0.2100	-12200	-14968	93
370	24.7	0.3	0.1800	-17900	-20757	93
370	24.7	0.3	0.1500	-25000	-27073	93
370	24.7	0.3	0.1200	-32400	-33994	93
370	24.7	0.3	0.0900	-41400	-41618	93
370	24.7	0.3	0.0600	-51000	-50068	93
370	24.7	0.3	0.0300	-64300	-59496	93
380	24.7	0.1	0.0900	-13400	-4610	93
380	24.7	0.1	0.0800	-28100	-9413.4	93
380	24.7	0.1	0.0700	-47700	-14424	93
380	24.7	0.1	0.0600	-70300	-19658	93
380	24.7	0.1	0.0500	-98800	-25130	93
380	24.7	0.1	0.0400	-127000	-30861	93
380	24.7	0.1	0.0300	-162400	-36871	93
380	24.7	0.1	0.0200	-207800	-43184	93
380	24.7	0.1	0.0100	-264300	-49827	93
380	24.7	0.3	0.2700	-10000	-7621.6	93
380	24.7	0.3	0.2400	-23300	-15657	93
380	24.7	0.3	0.2100	-38400	-24439	93
380	24.7	0.3	0.1800	-55900	-34088	93
380	24.7	0.3	0.1500	-78100	-44749	93
380	24.7	0.3	0.0900	-136400	-69910	93

$T$ (°C)	$P$ (MPa)	$m_i$ (mol/kg H <sub>2</sub> O)	$m_f$ (mol/kg H <sub>2</sub> O)	Measured (J/mol NaCl)	RIV (J/mol NaCl)	Reference
380	24.7	0.3	0.0600	-175800	-84957	93
380	32	0.5	0.1000	-59700	-45977	93
350	17.6	0.5	0.1000	-46600	-49163	2
350	17.6	0.5	0.0500	-62000	-61006	2
350	17.5	0.5	0.4010	-3000	-7928.7	This study
350	17.5	0.5	0.3000	-13500	-18151	This study
350	17.5	0.5	0.2500	-16700	-24335	This study
350	17.5	0.5	0.2000	-22000	-31494	This study
350	17.5	0.5	0.1500	-32300	-39878	This study
350	17.5	0.5	0.1000	-41100	-49830	This study
350	17.5	0.5	0.0500	-55800	-61840	This study
350	28	2.09	1.8830	-2100	-1578.6	This study
350	28	2.09	1.6740	-4400	-3161.6	This study
350	28	2.09	0.6280	-34300	-14374	This study
350	28	2.09	0.5020	-30500	-17004	This study
350	28	2.09	0.4180	-26800	-19153	This study
350	28	2.09	0.3350	-29200	-21691	This study
350	28	2.09	0.2510	-34200	-24809	This study
350	28	2.09	0.2510	-33600	-24809	This study
350	28	2.09	0.2090	-29100	-26627	This study
350	28	2.09	0.1260	-30600	-30870	This study
350	28	1	0.9000	-2200	-1171.3	This study
350	28	1	0.5000	-11300	-7958.5	This study
350	28	1	0.3000	-33000	-13822	This study
350	28	1	0.2000	-32800	-17951	This study
350	28	1	0.2000	-28900	-17951	This study
350	28	1	0.1000	-39300	-23320	This study
350	28	0.5	0.4010	-2900	-2608	This study
350	28	0.5	0.3000	-6800	-5887.2	This study
350	28	0.5	0.2500	-7900	-7822.6	This study
350	28	0.5	0.2000	-11600	-10016	This study
350	28	0.5	0.1500	-15100	-12516	This study
350	28	0.5	0.1000	-18900	-15384	This study
350	28	0.5	0.0500	-19500	-18699	This study
350	28	0.5	0.0500	-26000	-18699	This study
360	20	0.5	0.4010	-10000	-10487	This study
360	20	0.5	0.3510	-16100	-16692	This study
360	20	0.5	0.3000	-22900	-23862	This study
360	20	0.5	0.2500	-31900	-31898	This study
360	20	0.5	0.1500	-50600	-51995	This study
360	20	0.5	0.1000	-74400	-64830	This study
360	20	0.5	0.0500	-97600	-80332	This study
360	23	0.5	0.4010	-6200	-7759.3	This study

<b><i>T</i> (°C)</b>	<b><i>P</i> (MPa)</b>	<b><i>m<sub>i</sub></i> (mol/kg H<sub>2</sub>O)</b>	<b><i>m<sub>f</sub></i> (mol/kg H<sub>2</sub>O)</b>	<b>Measured (J/mol NaCl)</b>	<b>RIV (J/mol NaCl)</b>	<b>Reference</b>
360	23	0.5	0.3000	-15300	-17483	This study
360	23	0.5	0.2000	-31600	-29769	This study
360	23	0.5	0.2000	-10000	-29769	This study
360	23	0.5	0.1750	-16100	-33390	This study
360	23	0.5	0.1000	-45200	-46010	This study
360	23	0.5	0.0500	-58800	-56284	This study
360	26	0.5	0.4010	-6000	-5863.4	This study
360	26	0.5	0.4010	-3800	-5863.4	This study
360	26	0.5	0.3510	-7000	-9257.3	This study
360	26	0.5	0.3000	-10000	-13109	This study
360	26	0.5	0.2500	-17100	-17339	This study
360	26	0.5	0.2500	-16000	-17339	This study
360	26	0.5	0.2000	-19900	-22103	This study
360	26	0.5	0.1500	-24800	-27511	This study
360	26	0.5	0.1000	-32400	-33704	This study
360	26	0.5	0.0500	-44900	-40870	This study
360	28	0.5	0.3510	-7500	-7721.3	This study
360	28	0.5	0.3000	-9000	-10909	This study
360	28	0.5	0.3000	-12700	-10909	This study
360	28	0.5	0.2500	-13800	-14393	This study
360	28	0.5	0.2000	-16400	-18295	This study
360	28	0.5	0.1500	-21800	-22698	This study
360	28	0.5	0.1500	-23300	-22698	This study
360	28	0.5	0.1000	-27500	-27703	This study
360	28	0.5	0.0500	-35800	-33444	This study
360	28	0.5	0.0500	-39200	-33444	This study
370	26	0.5	0.3000	-20400	-20949	This study
370	26	0.5	0.3000	-19000	-20949	This study
370	26	0.5	0.2500	-31000	-27748	This study
370	26	0.5	0.2000	-44100	-35442	This study
370	26	0.5	0.2000	-37400	-35442	This study
370	26	0.5	0.1500	-45800	-44230	This study
370	26	0.5	0.1500	-52800	-44230	This study
370	26	0.5	0.1500	-38300	-44230	This study
370	26	0.5	0.1500	-36900	-44230	This study
370	26	0.5	0.1000	-59400	-54380	This study
370	26	0.5	0.0500	-52400	-66256	This study
370	28	0.5	0.3510	-9000	-12327	This study
370	28	0.5	0.3000	-13300	-17418	This study
370	28	0.5	0.2500	-21800	-22987	This study
370	28	0.5	0.2500	-23600	-22987	This study
370	28	0.5	0.2000	-35700	-29237	This study
370	28	0.5	0.1500	-32100	-36308	This study

<b><i>T</i> (°C)</b>	<b><i>P</i> (MPa)</b>	<b><i>m<sub>i</sub></i> (mol/kg H<sub>2</sub>O)</b>	<b><i>m<sub>f</sub></i> (mol/kg H<sub>2</sub>O)</b>	<b>Measured (J/mol NaCl)</b>	<b>RIV (J/mol NaCl)</b>	<b>Reference</b>
370	28	0.5	0.1500	-43500	-36308	This study
370	28	0.5	0.1000	-38500	-44383	This study
370	28	0.5	0.0500	-53100	-53703	This study
375	24	0.01	0.0050	-48800	-2800.9	This study
375	24	0.01	0.0050	-62800	-2800.9	This study
375	24	0.01	0.0040	-69000	-3369.6	This study
375	24	0.01	0.0040	-78900	-3369.6	This study
375	24	0.01	0.0030	-99700	-3941.3	This study
375	24	0.05	0.0300	-10100	-9624	This study
375	24	0.05	0.0250	-12300	-12169	This study
375	24	0.05	0.0250	-12300	-12169	This study
375	24	0.05	0.0200	-22400	-14774	This study
375	24	0.05	0.0200	-15800	-14774	This study
375	24	0.05	0.0150	-21900	-17442	This study
375	28	0.5	0.4010	-8300	-9637	This study
375	28	0.5	0.3510	-13300	-15201	This study
375	28	0.5	0.3000	-18800	-21507	This study
375	28	0.5	0.2500	-41200	-28426	This study
375	28	0.5	0.2000	-38400	-36220	This study
375	28	0.5	0.1500	-45800	-45077	This study
375	28	0.5	0.1000	-52800	-55248	This study
375	28	0.5	0.0500	-77200	-67070	This study
375	32	0.5	0.4010	-6600	-6894.7	This study
375	32	0.5	0.3510	-9100	-10816	This study
375	32	0.5	0.3000	-13300	-15210	This study
375	32	0.5	0.2500	-17600	-19966	This study
375	32	0.5	0.2000	-26100	-25244	This study
375	32	0.5	0.1000	-38400	-37776	This study
375	32	0.5	0.0500	-49200	-45306	This study
380	32	0.5	0.4010	17700	-8326.2	This study
380	32	0.5	0.2500	-26600	-24187	This study



## Appendix D Measured $\Delta_{dil}H$ values and Those Predicted Using the RIV Model for LiCl Solutions

$T$ (°C)	$P$ (MPa)	$m_i$ (mol/kg H <sub>2</sub> O)	$m_f$ (mol/kg H <sub>2</sub> O)	Measured (J/mol NaCl)	RIV (J/mol NaCl)	Reference
350	17.6	0.25	0.2249	-3010	-3142.15	94
350	17.6	0.25	0.1998	-5920	-6542.04	94
350	17.6	0.25	0.1748	-10050	-10216.4	94
350	17.6	0.25	0.1497	-13240	-14234.4	94
350	17.6	0.25	0.1247	-18800	-18609.2	94
350	17.6	0.25	0.0997	-23280	-23411.8	94
350	17.6	0.25	0.0748	-29730	-28686.5	94
350	17.6	0.25	0.0498	-38770	-34557	94
350	17.6	0.25	0.0249	-48430	-41076.5	94
350	17.6	0.5	0.4496	-3200	-3414.85	94
350	17.6	0.5	0.3993	-6900	-7233.46	94
350	17.6	0.5	0.349	-10950	-11546.8	94
350	17.6	0.5	0.2989	-15620	-16442.7	94
350	17.6	0.5	0.2488	-20920	-22075.1	94
350	17.6	0.5	0.1989	-27270	-28599.3	94
350	17.6	0.5	0.149	-35100	-36281.6	94
350	17.6	0.5	0.0993	-45620	-45422.8	94
350	17.6	0.5	0.0496	-60930	-56536.8	94



## Appendix E Measured $\Delta_{dil}H$ values for Sodium Acetate Solutions

Applying the RIV model to sodium acetate solutions would be a logical next step because sodium acetate solutions have more than one aqueous reaction. This would provide a test of the effectiveness of the RIV model in modeling solutions with multiple aqueous reactions. There are no  $\Delta_{dil}H$  values for aqueous sodium acetate solutions near the critical point of water reported in the literature. Values for  $\Delta_{dil}H$  are important in applying the RIV model because aqueous reactions are strongly tied to enthalpic changes. The following  $\Delta_{dil}H$  values were collected to aid in applying the RIV model to aqueous sodium acetate solution as a part of future work.

$T$ (°C)	$P$ (MPa)	$m_i$ (mol/kg H <sub>2</sub> O)	$m_f$ (mol/kg H <sub>2</sub> O)	Measured (J/mol CH <sub>3</sub> CO <sub>2</sub> Na)
350	28	0.50	0.25	-4338.38
350	28	0.50	0.2	-7076.23
350	28	0.50	0.3	-4997.1
350	28	0.50	0.1	-15497.3
350	28	0.50	0.4	-1664.71
350	28	0.50	0.15	-9556.11
350	28	0.50	0.35	-1438.97
350	28	0.50	0.05	-19354.2
350	28	0.50	0.25	-5845.17
350	28	0.50	0.05	-19529.9
350	26	0.50	0.25	-6007.73
350	26	0.50	0.2	-15910.5
350	26	0.50	0.05	-26367
350	26	0.50	0.1	-25103
350	26	0.50	0.15	-18260.1
350	26	0.50	0.35	-6407.62
350	26	0.50	0.4	-2016.35
350	26	0.50	0.25	-10990

<i>T</i> (°C)	<i>P</i> (MPa)	<i>m<sub>i</sub></i> (mol/kg H <sub>2</sub> O)	<i>m<sub>f</sub></i> (mol/kg H <sub>2</sub> O)	Measured (J/mol CH <sub>3</sub> CO <sub>2</sub> Na)
350	26	0.50	0.05	-24329.9
350	26	0.50	0.1	-20324.3
350	26	0.50	0.25	-9048.67
350	24	0.50	0.25	-10476.4
350	24	0.50	0.05	-34102.9
350	24	0.50	0.1	-22845.1
350	24	0.50	0.15	-18879.9
350	24	0.50	0.2	-14853.2
350	24	0.50	0.3	-7686.4
350	24	0.50	0.35	-5163.85
350	24	0.50	0.4	-3265.31
350	24	0.50	0.2	-4459.26
350	24	0.50	0.25	-3887.14
350	24	0.50	0.3	-5061.78
350	24	0.50	0.25	-9355.64
350	24	0.50	0.05	-22960.7
350	24	0.50	0.05	-26996.6
350	24	0.50	0.1	-10953.9
350	24	0.50	0.15	-22866.8
360	28	0.50	0.25	-7406.37
360	28	0.50	0.05	-19229.7
360	28	0.50	0.15	-9287.74
360	28	0.50	0.35	-4300.09
360	28	0.50	0.1	-17898.1
360	28	0.50	0.2	-11658.9
360	28	0.50	0.3	-6964
360	28	1.00	0.5	-14673.8
360	28	1.00	0.1	-35011.4
360	26	0.50	0.25	-11039.5
360	26	0.50	0.05	-23220.9
360	26	0.50	0.1	-21769.2
360	26	0.50	0.15	-8189.39
360	26	0.50	0.2	-11798.9
360	26	0.50	0.3	-6250.74
360	26	0.50	0.25	-10758.1
360	26	0.50	0.35	-4499.56
360	24	0.50	0.25	-12721.1
360	24	0.50	0.05	-24852.4
360	24	0.50	0.15	-20478.9
360	24	0.50	0.1	-18944.4
360	24	0.50	0.2	-17568.5
360	24	0.50	0.3	-8860.62
360	24	0.50	0.35	-5431.35
360	24	0.50	0.4	-3814.43

<b><math>T</math> (°C)</b>	<b><math>P</math> (MPa)</b>	<b><math>m_i</math> (mol/kg H<sub>2</sub>O)</b>	<b><math>m_f</math> (mol/kg H<sub>2</sub>O)</b>	<b>Measured (J/mol CH<sub>3</sub>CO<sub>2</sub>Na)</b>
360	24	0.50	0.1	-32960.1
360	24	0.50	0.05	-20248.2
360	24	0.50	0.1	-27019.5



## **Appendix F RIV Model Fortran Code**

Code is located on attached compact disc.